8-2015

Ecology and Morphology of the Late Miocene Musk Deer, *Longirostromeryx wellsi* (Artiodactyla: Moschidae: Blastomerycinae)

Katheryn Y. C. Chen
University of Nebraska-Lincoln, katheryn.chen@huskers.unl.edu

ECOLOGY AND MORPHOLOGY OF THE LATE MIOCENE MUSK DEER, *LONGIROSTROMERYX WELLSI* (ARTIODACTYLA: MOSCHIDAE: BLASTOMERYCINAE)

by

Katheryn Y. C. Chen

A THESIS

Presented to the Faculty of

The Graduate College at the University of Nebraska

In Partial Fulfillment of Requirements

For the Degree of Master of Science

Major: Earth and Atmospheric Sciences

Under the Supervision of Professor Ross Secord

Lincoln, Nebraska

August, 2015

ECOLOGY AND MORPHOLOGY OF THE LATE MIOCENE MUSK DEER, *LONGIROSTROMERYX WELLSI* (ARTIODACTYLA: MOSCHIDAE: BLASTOMERYCINAE)

Katheryn Y. C. Chen, M.S.

University of Nebraska, 2015

Advisor: Ross Secord

Longirostromeryx wellsi, one of the latest surviving members of the extinct clade Blastomerycinae (Artiodactyla: Moschidae), possesses highly derived craniodental morphology that deviates from typical musk deer form. Previous work suggests that the unique anatomy of *L. wellsi* represents adaptations for occupying open savannas. To test this hypothesis I conduct principal components analysis on five postcranial bones of *L. wellsi,* comparing them to that of several extant ruminant artiodactyls, which are divided among seven habitat categories. These elements are also compared with the postcrania of other blastomerycines. These analyses indicate that *L. wellsi* anatomy is most similar to that of other blastomerycines, extant musk deer, and artiodactyls that occupy heavy woodland-bushland environments, antithetical to the traditional view that *L. wellsi* was adapted for open habitats. Slight differences among fossil blastomerycines suggest that early to middle Miocene species were better adapted to densely vegetated habitats than

later blastomerycines. Of the late Miocene taxa, *Parablastomeryx*, typically considered the more primitive form, may have been better suited to open environments than the more derived *Longirostromeryx*.

The most complete known specimen of *Longirostromeryx wellsi*, UNSM 125572, is described here. Some features, primarily of the forelimb and proximal hindlimb, show that *L. wellsi* was not a specialized runner, supporting the closed habitat hypothesis, though other features are indicative of cursorial modification. I propose that these conflicting features represent modification for a unique feeding specialization, appropriate for bushland environments. Overall, this study elaborates the complex ecological story of *L. wellsi*, including habitat and morphological similarities to other ruminants, with consequences for the evolutionary history of Blastomerycinae as well as paleoenvironmental interpretations of the late Miocene Great Plains.

ACKNOWLEDGEMENTS

I would like to acknowledge my primary advisor, Dr. Ross Secord, as well as my committee members, Dr. Jason Head and Dr. Patricia Freeman; I am grateful for their guidance and constructive contributions to this research. I would especially like to thank Dr. Kovarovic for generously making available modern artiodactyl measurements used in a previous study. I thank the following: Drs. Mike Voorhies, Christine Janice, Donald Prothero, as well as Tom Baldvins and Allison Bormet for their insightful discussions; Jennifer Britton and Sara ElShafie for travel assistance, and the latter for technical training in Avizo 3D software; Rick Otto, Greg Brown, and George Corner of the University of Nebraska State Museum (UNSM) for assistance with and preparation of specimens; technicians at the University of Nebraska Medical Center (UNMC) for CT scanning UNSM 125572; Pat Holroyd and Chris Conroy for access to collections at the University of California, Berkeley, Museum of Paleontology (UCMP) and Museum of Vertebrate Zoology, respectively; Judy Galkin and Eileen Westwig for access to collections at the American Museum of Natural History (AMNH); as well as Patricia Freeman, Thomas Labedz, and George Corner for access to the UNSM collections. I thank my mother, Jessica Chen, as well as Jeff Chen, David Powsner, Bekah Bagaco, Matt Peppers, Nicole Pierson, Shamar Chin, Bradi Nielsen, and Emily Campbell, Kathy French and the education staff at UNSM Morrill Hall for their encouragement throughout this process.

GRANT INFORMATION

The following sources provided funding for this research and related travel: the Hubbard Foundation for graduate support through the Hubbard Fellowship; Friends of the University of Nebraska State Museum for funding travel to the Society of Vertebrate Paleontology's 74th Annual Meeting; the Nebraska Geological Society and the American Association of Petroleum Geologists for the Yatkola-Edwards Award; the Doris O. and Samuel P. Welles Fund for travel to UCMP; a grant to Ross Secord from the National Science Foundation (EAR #1325612); and the Department of Earth and Atmospheric Sciences at the University of Nebraska for providing both graduate and travel support.

TABLE OF CONTENTS

CHAPTER 1: INTRODUCTION

The skeleton of any organism reflects the nature of its interactions with its environment. Researchers exploit this relationship between form and function using an approach known as ecomorphology or ecometrics (Polly et al., 2011). In this approach, measurable adaptive traits are correlated to corresponding ecological functions, which can be applied to instances where ecology is otherwise unknown or inaccessible, as in the fossil record (Van Valkenburgh, 1994). Morphology of the appendicular skeleton reflects adaptations for navigating across environments of varying complexity (Kappelman, 1988; Rose, 2006). Bone morphology therefore becomes a useful proxy for interpreting various aspects of ecology for organisms with no modern analogues (Van Valkenburgh, 1994; Eronen et al., 2010). Through measurements from long bones and phalanges, this study addresses paleohabitat preferences among members of an under-researched and extinct clade.

Blastomerycinae is an extinct clade of small hornless ruminants known from the Miocene epoch in North America. This clade is sometimes considered to be the only North American radiation of Moschidae, the extant clade comprised of musk deer (Webb and Taylor, 1980). This study focuses on one blastomerycine in particular—*Longirostromeryx wellsi*, a member of the most derived genus in Blastomerycinae.

Longirostromeryx wellsi is considered derived principally for its unique dentition and elongate rostrum (Janis, 2000; Webb, 1998, Prothero, 2008); Webb (1998) suggested that these unique features represent open habitat adaptations. *L. wellsi* further shows

isotopic signals indicative of feeding in open, savannah-like environments and is known from sites interpreted as such (Kita et al., 2014; Clementz et al., 2008; Voorhies and Thomasson, 1979), lending credence to Webb's (1998) interpretation. Consequentially, *L. wellsi* would have utilized an ecological niche completely different from any living moschid. *Moschus,* the only extant genus in Moschidae, shelters in montane woodlands, predominantly of eastern Asia (Sathyakumar, 1992). Unlike *L. wellsi*, early blastomerycines have been compared to members of *Moschus* and interpreted to share similar diet, habitat, and overall ecology (Janis, 2000).

The aim of this study is to assess habitat preference for *L. wellsi* and compare it to that of genus *Moschus* and early members of Blastomerycinae. I build upon research that was designed to evaluate paleoenvironments for the Pliocene of Laetoli, Tanzania, using an ecometric analysis of African bovid postcrania (Kovarovic, 2004; Kovarovic and Andrews, 2007, 2011). By expanding their scope of modern taxa and focusing on those of small to medium weight, these methods become more precise for small-bodied ruminants, which were abundant in the Cenozoic of North America. I use this model to interpret ecology specifically for *L. wellsi* and Blastomerycinae, though it holds the potential to be applied to many other groups.

This quantitative habitat assessment is supplemented by morphological interpretation of the most complete specimen of *Longirostromeryx wellsi* currently known. This specimen, UNSM 125572, was discovered at Ashfall Fossil Beds in northeastern Nebraska. A computed tomographic (CT) scan of UNSM 125572 reveals its anatomy, allowing for precise descriptions without disassembling the largely articulated

skeleton. The combination of a large-scale ecometric analysis and an in-depth study of a single representative specimen facilitates a comprehensive review of *L. wellsi* anatomy, providing insight into its unique adaptations, behaviors, and habitat preferences as well as its similarities to blastomerycines and modern moschids.

CHAPTER 2: BACKGROUND

2.1 Biochronology

Blastomerycinae is a clade exclusive to the Miocene of North America; I therefore refer to time-units, North American Land Mammal ages (NALMA), from within this epoch. NALMAs are biochronologic units described on the basis of first and last appearances as well as co-occurrences of characteristic fossils mammals (Lindsay, 2003; Tedford et al., 2004; Wood et al., 1941). NALMAs relevant to this study are outlined below based on dates given in Tedford et al. (2004): Arikareean (late Oligocene-earliest Miocene; ~30–19 Ma), Hemingfordian (early Miocene; ~19–16 Ma), Barstovian (middle Miocene; ~16–12.5 Ma), Clarendonian (late middle Miocene; ~12.5–9 Ma), and Hemphillian (late Miocene, earliest Pliocene; ~9–5 Ma). The fossils in this study represent taxa from the Hemingfordian, Barstovian, and Clarendonian, though blastomerycines span the entire Miocene, from the late Arikareean to the late Hemphillian.

2.2 Miocene Environments

Vegetation structure on the Great Plains of North America during the time of *Longirostromeryx wellsi* has important bearing on the interpretation of its ecology. Over the span of the Cenozoic, the North American interior progressed from a generally wooded environment to a more open and arid landscape; moreover, most authors agree that a substantial opening of the landscape occurred sometime during the Miocene epoch

(Axelrod, 1985; Webb 1977; Strömberg, 2004, 2011). Grasslands clearly prevailed as C_4 grasses expanded in the latest Miocene (~6.6 Ma) and into the Pliocene (Passey et al., 2002, Fox and Koch, 2004; Strömberg and McInerney, 2011; Kita et al., 2014; Edwards et al., 2010; McInerney, 2011); however, degree and timing of change in vegetation structure on the Great Plains during the early, mid, and early late Miocene is widely debated.

Evidence from phytoliths suggests that woody and herbaceous plants dominated the Nebraska landscape from the late Eocene through early Oligocene (Strömberg, 2004). The environment became more varied starting in the Oligocene, resulting in a greater presence of open habitats, such as savanna-woodlands, during the early Miocene (Strömberg, 2004; Strömberg and McInerney, 2011). Phytolith assemblages and several studies using stable carbon isotopes (Edwards et al., 2010; Passey et al., 2002; Fox and Koch, 2004; McInerney, 2011) indicate that open landscapes became more widespread and continuous around the Miocene-Pliocene boundary when C_4 grasses spread throughout the plains (Strömberg and McInerney, 2011; Strömberg, 2011).

Other lines of evidence place the spread of C_3 grasslands at a much earlier date. Kita et al. (2014) examined the changing landscape in Nebraska using stable isotopes, finding that the late Miocene was largely dominated by open habitats (grassland and savanna-woodland) no later than the late Clarendonian (Kita et al., 2014). Pollen and floral macrofossils suggest that open-habitat grasses appeared in North America near the Eocene-Oligocene transition, and became widespread in the Great Plains during the middle to late Miocene (Strömberg, 2011). Paleosols suggests that open-habitat grasses

existed in the early Oligocene, becoming dominant in the early Miocene (20 Ma) (Retallack, 2007; Strömberg, 2011).

Browsing ungulates were abundant among early Miocene communities; their success was likely due to the level of primary productivity in their habitats (Janis et al., 2000, 2002, 2004). Because basal blastomerycines have been interpreted as browsers occupying closed environments (Janis, 2000), it is therefore reasonable to assume that an opening of the landscape would have been damaging for this clade. In fact, the demise of blastomerycines follows the decline of browsers, which Janis et al. (2000) attributed to the progressive opening of landscapes and decline in primary productivity (Janis et al., 2002, 2004).

Blastomerycinae is a lineage that evolved during a time when the North American interior was generally wooded, and survived to the time of C_4 grassland expansion. If the latest-surviving blastomerycines, *Longirostromeryx* and *Parablastomeryx*, show a preference for open environments, this would indicate an adaptive strategy responding to increases in aridity and changes in vegetation structure. If their preference is for closed habitats and is similar to the early blastomerycines, it may indicate that neither *Longirostromeryx* nor *Parablastomeryx* were sufficiently adapted to such low primary productivity, and they could not survive the loss of habitat, or other such drastic changes that occurred at the end of the Miocene epoch.

2.3 Systematics

Cope described the first blastomerycine when he named the species *Blastomeryx gemmifer* (Cope, 1877). However, subfamily Blastomerycinae was not described until 1937 when Childs Frick compiled previously described taxa along with several new species in his monographic study of horned ruminants (1937). He included the following genera or subgenera, though these are largely treated as genera in later works (Webb, 1998; Prothero, 2008): *Problastomeryx*, *Pseudoblastomeryx*, *Parablastomeryx*, *Pseudoparablastomeryx*, *Blastomeryx*, *Machaeromeryx*, and *Longirostromeryx* (Frick, 1937). *Pseudoparablastomeryx* has since been removed from Blastomerycinae and placed in Leptomerycidae (Taylor and Webb, 1976). Frick's taxa are considered overly split and his diagnoses are not well defined (Prothero and Liter, 2008); however, his was the first major overview of the clade and is still one of the only texts to outline all of Blastomerycinae. Prothero (2008) published the first revision of blastomerycine systematics since Frick (1937); his study distinguished blastomerycine taxa primarily using the ratio of premolar to molar row, which greatly consolidated the number of recognized species.

The amount of work on blastomerycine phylogeny is so limited that the intricacies of their generic, sub-family, and even family relationships are poorly understood. Blastomerycine interrelationships were largely untouched until 1998 when S. David Webb reviewed the clade for his chapter on hornless ruminants; to date, he has published the only interpretation on the relationship among blastomerycine genera (replicated in Figure 1) (Webb, 1998, pp. 468).

Webb and Taylor (1980) were the first to formally propose the relationship between the Blastomerycinae and Moschidae, the Old World musk deer; this designation was based on cranial, dental, and postcranial synapomorphies. Since this alliance was proposed, studies focusing on blastomerycines have largely followed this convention (Janis and Scott, 1987; Janis, 2000; Prothero, 2008; McKenna and Bell, 1997; Gentry et al., 1999). Recent studies on early Eurasian moschids have, however, suggested that the characters uniting Moschidae and Blastomerycinae are present in tragulids and ancient bovids, and are therefore too primitive to be useful in family-level phylogenetic analyses (Vislobokova and Lavrov, 2009). Some morphological analyses (Vislobokova and Lavrov, 2009; Sánchez et al., 2010) use most parsimonious trees of cranial, dental, mandibular and postcranial characters to argue that blastomerycines do not fall within Moschidae (Sánchez et al., 2010). Sánchez et al. (2010) support monophyly of Bovidae, *Moschus*, *Hispanomeryx, Micromeryx, Sperrgebietomeryx,* and *Namibiomeryx*—to the exclusion of *Dremotherium* and *Blastomeryx*.

Even if blastomerycines are shown to belong in Moschidae, there are some discrepancies regarding the relationships of Moschidae, Cervidae, and Bovidae. Based on morphological and molecular evidence, some have considered Moschidae to fall within or sister to Cervidae (Janis and Scott, 1987; Bibi, 2014; Fernández and Vrba, 2005; Su et al., 1999; Gentry et al., 1999). Others studies have found moschids to be the sister taxon to all higher ruminants (Webb and Taylor, 1980; Bibi, 2014). More recent studies support the monophyly of Moschidae and Bovidae, to the exclusion of Cervidae,

based on morphological characters as well as molecular evidence (Bibi, 2013, 2014; Vislobokova and Lavrov, 2009; Sánchez et al., 2010; Hassanin and Douzery, 2003).

Complexities of phylogeny among blastomerycines, Old World moschids, and other ruminants, demonstrate the necessity of a taxon-free approach in interpreting paleoecology. While recognizing the relationship between Blastomerycinae and *Moschus* is somewhat dubious, I compare these two groups because of their morphological similarities as well as the historical assumption of monophyly.

The blastomerycines measured for this study include the following genera: *Parablastomeryx, Problastomeryx, Pseudoblastomeryx, Blastomeryx,* and *Longirostromeryx*. *Parablastomeryx gregorii* is the type species of the genus *Parablastomeryx.* This species is known only from the late Clarendonian of Nebraska, though other members of this genus are also known from the early Hemingfordian of Florida and early Barstovian of Nevada (Fig. 1). *Parablastomeryx* contains the largest-bodied species of blastomerycine and is considered to be more primitive than other blastomerycines (Janis, 2000). It possesses brachydont molars, large premolars, and a short diastema.

Problastomeryx primus is the only species in its genus recognized by Prothero (2008). It ranges from the late Arikareean to the Barstovian (Fig. 1) in South Dakota, Texas, Idaho, Nebraska, and Saskatchewan (Prothero, 2008). *Pr. primus* is a large blastomerycine with longer and more robust limbs and a premolar row at least 70% as long as the molar row (Prothero, 2008). *Pseudoblastomeryx advena* is the type and only species of its genus; it is known from the latest Arikareean through early Hemingfordian

(Fig. 1) in South Dakota, Nebraska, and California (Prothero, 2008). *Ps. advena* is smaller than *Pr. primus*, and also retains an unreduced premolar row.

Blastomeryx gemmifer is the type species of *Blastomeryx* and is the only species in this genus recognized by Prothero (2008). *B. gemmifer* is known from the late Arikareean to early Clarendonian (Fig. 1) of Nebraska, South Dakota, Colorado, Saskatchewan, Montana, New Mexico, Oregon, Nevada, and Texas. They are medium-sized blastomerycines with slightly reduced premolars (Prothero, 2008).

Blastomeryx wellsi was first described by Matthew in 1904, based on a fragmentary ramus larger than that of *Blastomeryx gemmifer* with reduced premolars. This became the type specimen of Frick's (1937) newly erected taxon, *Longirostromeryx wellsi*. Genus *Longirostromeryx* is identified as a medium to small blastomerycine with long rostra, long diastema, a 25–40 mm molar row, a 13–19 mm premolar row, hypsodont molars, and a greatly reduced or absent p2 (Prothero, 2008; Frick, 1937).

While Frick (1937) erected seven species of *Longirostromeryx*, Prothero (2008) recognized only two—*L. wellsi* and *L. clarendonensis*. Prothero (2008) synonymized several *Longirostromeryx* specimens into one taxon, *L. wellsi*, which is the type species for its genus. *L. wellsi* spans nearly eight million years (Prothero, 2008) and is known from the late Barstovian of Texas, the late Barstovian to late Hemphillian of New Mexico, and the early Clarendonian to late Hemphillian of Nebraska and South Dakota (Fig. 1). *L. clarendonensis* appears later, is more derived, and is known only from the early Clarendonian of Texas (Prothero, 2008; Webb, 1998; Frick, 1937).

Longirostromeryx wellsi is the larger species, with molar rows ~30–40 mm, premolar rows ~ 14–20 mm, and a shorter diastema than *L. clarendonensis* (Prothero, 2008). *L. wellsi* shows a temporal trend towards increasingly specialized features, with time: reduction of the premolar row, reduction of the p2, elongation of the diastema, increased hypsodonty of the molars, and decrease in size (Webb, 1998). These features are even more pronounced in *L. clarendonensis*. Compared to *L. wellsi, L. clarendonensis* has a smaller body size, increased hypsodonty, reduced premolars, a typically absent p2, and more elongate diastema (Prothero, 2008; Frick, 1937).

2.4 Blastomerycine Ecology

Extant musk deer are solitary, crepuscular animals that are known from eastern and central Asia (Sathyakumar, 1992; Nyambayar et al., 2008). They generally occupy habitats at altitudes well above 2500 meters, frequenting lower elevation forest and scrub environments during the day and higher altitude meadows at night (Sathyakumar, 1992; Green, 1985). Observational studies highlight their preference for warmer slopes at moderate inclines and their dependence on cover from shrubs (Green, 1985; Sathyakumar, 1992). They are typically found in habitats of dense larch, birch, or shrub, as well as other mixed forest, high altitude habitats (Sathyakumar, 1992; Nyambayar et al., 2008). Musk deer are known to navigate rocky environments to escape predators and can run exceptionally fast, though only for short distances (Nyambayar et al., 2008). Though they seem to transition between landscapes of varying vegetation structure, overall, the habitat of these animals is characterized by their dependence on shelter.

Moschus moschiferous is capable of climbing inclined trunks more than three meters above the ground in order to reach its food source (Nyambayar et al., 2008). Though their diets vary regionally and seasonally, moschids show a preference for low fiber foods, and have been known to consume lichen, forbs, and woody plant leaves (Nyambayar et al., 2008; Green, 1985, 1987; Sathyakumar, 1992).

The ecology of extant musk deer may inform our understanding of extinct artiodactyls classically considered to be moschids. Eurasian moschids in particular have been evaluated in terms of their similarity to modern musk deer. The earliest known member of genus *Moschus*, *Moschus grandaevus*, lived in the late Miocene (~7 Ma) of China and Siberia (Vislobokova and Lavrov, 2009). Based on morphological similarities, *M. grandaevus* was compared to *Moschus moschiferous*, though flora indicates the former inhabited drier environments and consumed a more generalized diet of herbaceous plants, relying less on lichens (Vislobokova and Lavrov, 2009). Microwear analyses on moschids from the site of La Milloque, France, suggested that these late Oligocene musk deer utilized two different feeding strategies: *Dremotherium quercyi* was a small browser feeding on leaves, while *Dremotherium guthi* and *Bedenomeryx milloquensis* were large-bodied grazers (Novello et al., 2010).

Based on observations of their dental morphology, early blastomerycines are presumed to occupy a niche similar to that of modern moschids or tragulids (Webb, 1998; Janis, 2000). They are hypothesized to act as solitary forest-edge foragers that practiced territorial behavior including intraspecific combat (Webb, 1998; Janis, 2000). Preliminary microwear analyses of the Barstovian-Clarendonian *Blastomeryx* and

Clarendonian *Longirostromeryx* suggest that both genera consumed browse, though the range in scratch counts for the former suggests that *Blastomeryx* had a more varied diet than *Longirostromeryx* (Carr and Pagnac, 2011).

Janis (2000) observed the extreme differences in dentition, size, and skeletal morphology of the Clarendonian blastomerycines, suggesting that *Parablastomeryx* and *Longirostromeryx* utilized two different ecological strategies. *Parablastomeryx* was considered the more primitive form, retaining somewhat low-crowned teeth, which is reminiscent of forest-browsing taxa (Janis, 2000). Genus *Longirostromeryx* was presumed to be the more derived form, better adapted to drier, more open, mixed-feeding habitats than the contemporaneous *Parablastomeryx* (Janis, 2000; Webb, 1998). This assumption about *Longirostromeryx* was based on the level of hypsodonty in cheek teeth as well as the elongate rostra they exhibit. Prothero (2008) noted that the geographical range of *Longirostromeryx* is not entirely consistent with the interpretation that this genus was suited to dry, open, or arid areas as they are not found in the fossiliferous regions in Nevada, Oregon, or California, which would have also been arid during the Clarendonian and Hemphillian.

2.5 Ecometrics

To assess behaviors and habitat preferences for long extinct clades, it is best to use a taxon-free approach like those in ecometrics. Ecometrics, sometimes known as ecomorphology, utilizes the relationship between ecological function and plastic morphological characters, measurable across a broad sample of organisms. The

characters in these studies necessarily reflect adaptation to an environment. The aim of my study is to establish the relationship between habitat and linear measurements of postcranial bones in modern artiodactyls, in order to apply that function to blastomerycines.

Morphology has been used to assess many aspects of ecology in fossil organisms. The field of mammalian paleoecology, in particular, has used this approach to interpret dietary behavior (Damuth and Janis, 2011; Janis et al., 2000, 2002, 2004; Mihlbachler and Solounias, 2006; Mihlbachler et al., 2011), locomotor function (Garland and Janis, 1993; Kappelman, 1988; Samuels and Van Valkenburg, 2008; Gingrich, 2005; Elissamburu and Vizcaíno, 2004; Croft and Anderson, 2008; Christiansen, 2002; Schmidt and Fischer, 2009), and habitat preference (Kovarovic, 2004; Kovarovic and Andrews 2007, 2011).

A large proportion of mammalian ecometric analyses employed for paleohabitat reconstruction center on Bovidae (DeGusta and Vrba, 2003; 2005; Kappelman, 1988; Kappelman et al., 1997; Klein et al., 2010; Kovarovic and Andrews, 2007, 2011; Plummer and Bishop, 1994; Plummer et al., 2008; Scott, 1985; Weinand, 2007). Ecological and anatomical diversity of modern bovids results in robust analyses that are useful paleoenvironmental proxies for hominid fossil sites. However, identifying traits that represent an even broader taxonomic group will increase the utility of this method for reconstructing ecological niche and interpreting paleoenvironment.

Ruminant artiodactyls occupying open habitats tend to have proportionally longer legs than those occupying closed habitats as long limbs promote greater stride length and

speed (Scott, 1985). Long limbs in ruminants may be selected for to reduce the cost of transportation, perhaps as a result of increasing home range size for greater foraging (Janis and Wilhelm, 1993); indeed, body size is closely tied to the distance a mammal travels in its territory (Jetz et al., 2004; Swihart et al., 1988; Lindstedt et al., 1986). A more popular interpretation is that ungulate limb length evolved for speed (Christiansen, 2002; Scott, 1985).

Cursoriality is tied to habitat because its evolution is dictated by the need to run across large, open landscapes (Scott, 1985). Herbivorous ungulates occupying open areas are vulnerable to fast predators and must be able to flee in order to survive. Skeletal modifications for extreme cursoriality by way of increased stride length and rate include: joints allowing for exclusively parasagittal limb movement, elongate and gracile distal limbs, proximally concentrated muscle masses, reduced bony crests and processes for muscle attachments, reduced ulnae and fibulae, loss of lateral toes, and some fusion in the carpals (Rose, 2006).

For distance running, joint stability becomes an important factor and selection favors those with joints oriented for unidirectional fore and aft movement (Kappelman, 1988); lateral or twisting movements are selected against because they increase the risk of injury. In contrast, ungulates adapted to closed canopy habitats show a greater degree of joint maneuverability that allows them to navigate easily around large vegetative obstacles (Kappelman, 1988). These adaptations to navigate spatially different habitats are necessarily reflected in skeletal morphology; variations in skeletal elements that

reflect these abilities should therefore indicate the habitat to which the animal is adapted (Samuels and Van Valkenburg, 2008).

Body size further plays a role in open versus closed-habitat adaptations. Grassland ungulates evince greater size and longer limbs relative to body size than do their forest-dwelling counterparts; forest-dwellers must rely on reduced size both for the ability to rapidly hide and for nutritional efficiency (Christiansen, 2002). Proxies of body size, limb length, and limb slenderness should therefore indicate preferred habitat, to some degree. With a well-established dataset of these and other metrics in modern artiodactyls, it becomes possible to connect anatomy to environment and therefore interpret the anatomy in a single fossil taxon to infer its ability to navigate certain habitats.

The type and amount of vegetative cover on a landscape are crucial components that define habitat types. Early studies on ungulate paleoecology (Kappelman, 1988, 1991; Plummer and Bishop, 1994; Reed, 1998) defined habitats using three categories based on amount of vegetative cover: open, intermediate, and closed habitat. More recent studies (DeGusta and Vrba, 2003, 2005; Kappelman, 1997; Plummer et al., 2008; Weinand, 2007) have favored a four-habitat scheme: plains, light cover, heavy cover, and forest. These four categories are considered to be broad enough to use for fossil assemblages that have some spatial and temporal averaging, but specific enough to separate patterns of adaptive traits (DeGusta and Vrba, 2003). Still more discriminating studies (Kovarovic, 2004; Kovarovic and Andrews, 2007) have divided habitats into highly specific categories defined by percent canopy cover, vegetation type, vegetation

height, and to some degree, altitude. Kovarovic (2004), and Kovarovic and Andrews (2007), utilized these parameters to create seven habitat categories; because this scheme carries the greatest potential for specificity and explanatory power, it is used in this study of blastomerycine paleohabitat. The habitat divisions are outlined later in this paper (Section 3.3).

A variety of postcranial metrics have been implemented in ecometric studies of ungulates, including measurements of the distal and proximal femur (Kappelman, 1988), the tibial plateau and calcaneum (Curran, 2012; Kovarovic and Andrews, 2007), astragali (DeGusta and Vrba, 2003; Plummer et al., 2008; Weinand, 2007), metapodials (Klein et al., 2010; Scott and Maga, 2005), and phalanges (DeGusta and Vrba 2005a; 2005b). Kappelman (1988, 1991) and Kappelman et al. (1997) demonstrated that eight metric characters of bovid femora could predict habitat type with 81–85% accuracy using four habitat categories. Kappelman (1988) showed that ungulates adapted to savanna habitats possessed laterally extended femoral heads to limit abduction and rotation at the hip, and elliptical femoral condyles to increase the moment arm of extensor muscles across the knee. Spheroidal femoral heads are more typical of forest bovids for greater maneuverability (Kappelman 1988). Kappelman's approach shows that complete femora are successful for interpreting varying locomotor abilities and therefore habitats.

Plummer and Bishop (1994) used 19 metric characteristics of metapodials to predict habitat type with 62–89% accuracy using three habitat categories. DeGusta and Vrba (2005) measured characteristics of proximal, intermediate, and distal phalanges that correctly predicted habitat preference for four habitat categories with success of 71.0%,

70.6%, and 71.3%, respectively. Comprehensive studies by Kovarovic (2004) and Kovarovic and Andrews (2007) consider a number of skeletal elements from the distal limbs of ruminants to assess habitat. Using discriminant function analyses, they found that certain elements were better at predicting certain habitats; the overall best predictors across habitat groups included humeri, femora, metatarsals, and radii (Kovarovic and Andrews, 2007).

Further studies have assessed various relationships between two or more bony elements as indicators of degrees of locomotion and other environmental proxies. Christiansen (2002) used multivariate analyses to assess covariation of running speeds with a number of skeletal parameters; he concluded that most osteological adaptations for cursoriality represent a decrease in energetic cost for locomotion rather than running speed. Croft and Anderson (2007) utilized multivariate analyses to compare limb lengths, widths, and ratios. Schmidt and Fischer (2009) also conducted a broad study of limb proportions using 189 extant mammalian species. They found that intra-limb proportions in the first and the third elements of each limb (typically scapula: radio-ulna and femur: metatarsal) correlated significantly with locomotor mode and running ability. These types of studies are, however, only relevant to paleontological research where complete skeletons are known.

This study utilizes an ecometric approach of using limb elements that reflect locomotor ability as indicators of habitat preference for small ruminant artiodactyls. The approach of this study is largely built upon the foundations of research from Kovarovic (2004), as well as Kovarovic and Andrews (2007, 2011), using their measurement

scheme as well as habitat scheme; I, however, expand the scope of modern taxa to better account for the variety of morphologies within Ruminantia. Overall, this approach should result in more precise interpretations of habitat in Blastomerycinae, and in particular, *Longirostromeryx wellsi*.

CHAPTER 3: MATERIALS AND METHODS

3.1 Approach

In order to assess blastomerycine ecology, a relationship between bone morphology and habitat and must first be demonstrated. I examine the relationship of these two variables using linear measurements of limb elements from a sample of modern taxa for which species identification and habitat preference are known. I use principal components analysis (PCA) of limb elements to identify variation in bone shape across the sample, and non-parametric analyses of variance to determine the relationship between habitat preference and PCA values. Given the diversity of taxa in this study, the relationship between bone shape and habitat are assumed to indicate adaptation to moving through certain habitat types and are not assumed to be the result of phylogenetic conservatism. Using only the elements that successfully separate modern taxa by habitat, these methods are applied to fossils of several blastomerycines in order to interpret paleohabitat.

3.2 Data Sample

Both fossil and modern specimens in this study come from the University of Nebraska State Museum (UNSM) in Lincoln, Nebraska, and the American Museum of Natural History (AMNH), in New York, New York. Additionally, two modern specimens from the Museum of Vertebrate Zoology (MVZ) in Berkeley, California, are included. These data are supplemented by data from modern artiodactyls originally used

in Kovarovic (2004). Dr. Kovarovic contributed these data, which she collected from four museums: the Natural History Museum in London (NHM), the Powell-Cotton Museum in Kent (PC), the Smithsonian Institution National Museum of Natural History in Washington, D.C. (USNM), and AMNH.

Because the fossil material for this study represents an extinct clade of small ruminant artiodactyls, this study must make comparisons based on data from an analogous modern group. This study utilizes a sample of ecologically diverse taxa within crown Ruminantia, specifically sampling Moschidae, Bovidae, Cervidae, Tragulidae, and Antilocapridae. These taxa represent inhabitants of a wide range of African, Asian, European and North American habitats. Modern specimens collected in their native habitats were preferred over domesticated or zoo specimens.

Blastomerycines were small artiodactyls, weighing between 5 and 18 kg (Janis, 2000). This study therefore utilizes small modern specimens where the average weight of its species is less than 100 kg. I determined average weight through a literature review of the following sources: Kovarovic and Andrews (2007), Nowak (1999), and the University of Michigan's Animal Diversity Web (Myers et al., 2015). Furthermore, both modern and fossil specimens in this study were determined to be adults based on dental eruption and fusion of limb bone epiphyses. The sample of modern specimens includes 163 individuals, which represents 56 species and 34 genera. Number of specimens per taxon ranged from n=1 to n=11. Information on all modern specimens used in this study is listed in Appendix B and all fossil specimens in Appendix C.

3.3 Habitat Assignment

This approach requires that modern taxa be assigned to habitat categories that reasonably reflect the variability in locomotor adaptations. Each taxon is assigned to one of seven habitat categories based on the scheme outlined in Kovarovic (2004) and Kovarovic and Andrews (2007). Those seven categories are as follows: grassland, wooded-bushed grassland, light woodland-bushland, heavy woodland-bushland, forest, montane heavy cover, and montane light cover. Percent canopy cover and height of vegetative cover are the most important variables used to define these habitat categories. Definitions for each category are described below and are based on definitions given in Kovarovic and Andrews (2007).

The "grassland" category encompasses all open plains and true grasslands, as well as treeless environments including tundra, steppe, and desert. Grasses, typically less than one meter high, abound in true grasslands; woody vegetation covers less than 2% of the ground.

"Wooded-bushed grassland" can be locally well-developed habitats or areas between woodland and riverine or floodplains. Grasses dominate the ground vegetation and may grow to three meters high. There is some contribution of herbaceous and woody growth, and open canopy vegetation are scattered or grouped throughout the habitat, with 3–40% cover. This category also includes semi-desert habitats, which are found in more arid climates and contain dwarfed, thorny shrubs and trees less than two meters tall, as well as seasonally fluctuating grasses and herbs.

"Light" and "heavy woodland-bushland" categories combine woodland and bushland habitat types and are differentiated by amount of canopy cover. "Light woodland-bushland" has 40–60% canopy cover, comprised of short trees and bushes. Grasses represent a more important part of the ground cover in light woodland-bushland than in heavy woodland-bushland. "Heavy woodland-bushland" is denser with 61–75% canopy cover, comprised of tall trees and shrubs. Mixed woodland, bushland, and dense thickets prevail in this habitat category.

"Forest" habitats have 76–100% canopy cover with interlocking crowns and generally multiple stories. Where low-level ground cover is present, it is predominately herbs and shrubs, as opposed to grasses.

The final two categories uniquely incorporate the vertical dimension. "Montane light cover" and "montane heavy cover" describe habitats encompassing a broad range of vegetative cover at higher altitudes of mountainous regions. "Light cover" indicates habitats are open or lightly covered by woody vegetation and includes habitats above the tree line. "Heavy cover" describes denser woodland or forest habitats at high altitudes.

Although not every ruminant limits itself to such a narrow category, each taxon is nevertheless assigned to a single, "best-fit" habitat in order to make ecological analyses viable. Though this approach is an over-simplification of true animal behavior, it does provide the greatest potential for describing precise habitats and environments. Habitat assignments are derived from Kovarovic and Andrews (2007), supplemented by information from Nowak (1999) and the University of Michigan's Animal Diversity Web (Myers et al., 2015). Habitat assignments are listed by species in Table 1.

3.4 Element Selection and Measurement

In her 2004 study, Kovarovic used discriminant function analyses (DFAs) on linear measurements of largely bovid post-crania to determine which elements most reliably predict habitat. Kovarovic (2004) and Kovarovic and Andrews (2007) found that several bones are useful as habitat proxies. The elements with the overall highest percent of correct classification are as follows: humerus (68.0%), femur (66.7%), metatarsal (66.5%), radius (58.0%), proximal phalanges (57.1%), and distal phalanges (55.8%) (Kovarovic and Andrews, 2007). Further support for the ecometric utility of these elements comes from earlier studies conducted solely on bovids (DeGusta and Vrba, 2005; Kappelman, 1988; Plummer and Bishop, 1994).

Based on their abilities to correctly assign habitat in DFA, I utilize measurements from the humerus, femur, metatarsal, radius, and proximal phalanges in this study. The distal humerus is also included as it is much more common in fossil collections than are complete humeri. Kovarovic and Andrews (2007) found the distal humerus reports 48.8% overall correct classification, which is high enough to indicate biological meaning.

The single-element measurement protocol utilized in this study is based on that of Kovarovic (2004). Although this protocol includes a number of standard measurements (e.g., greatest length, functional length), it further utilizes a number of novel measurements devised originally for use in Kovarovic's 2004 study (Degusta and Vrba, 2003; Kovarovic, 2004; Kovarovic and Andrews, 2007; Von Driesch, 1976).

Descriptions of measurements and measurement codes are listed in Table 2; figures are available in Appendix A.

These measurements were taken with digital calipers (except one case where they were digitally measured from a 3D scan of a specimen) and recorded to at least one tenth of a millimeter. A subset of specimens was measured multiple times. There are no great variations among measurements of the same anatomy; therefore it is concluded that intraobserver error is minimal. Some of the data are, however, contributed by Dr. Kovarovic. There are no cases where both authors measured the same specimen, so interobserver error cannot be empirically assessed; however, both authors measured specimens of the same species. Measurements of these specimens show similar lengths and proportions, suggesting that the measuring scheme from Kovarovic (2004) describes reliable and repeatable dimensions.

The specimens in this study represent a wide range of body size (Table 1), from 2.25 kg (*Neotragus pygmaeus*) to 99 kg (*Damaliscus hunteri*). Principal components analysis of the untransformed data describes a pattern influenced almost entirely by greatest length. The greatest length measurements are not normally distributed for the majority of elements; therefore measurements are transformed using the natural logarithm in order to represent geometric normality (Gingerich, 2000). Subsequent analyses and discussion of analyses refer to the natural log-transformed measurements.

While single element analyses are typically the most applicable to fragmentary fossil specimens, more holistic measurement schemes are ideal as they more accurately reflect the proportions and abilities of an animal. There are a few exceptionally

preserved blastomerycine skeletons, which enables me to utilize several basic anatomical proportions to assess habitat. Based on the principle that animals adapted for running across open plains will evince long and slender distal limbs compared to their proximal limbs (Kappelman, 1988; Rose, 2006), I use length width ratios of several long bones. Furthermore, several functional indices are used including the brachial, humero-femoral, and femero-metatarsal index (Garland and Janis, 1993; Elissamburu and Vizcaíno, 2004; Croft and Anderson, 2007). Intermemberal and crural indices were also evaluated; however, a Kruskal-Wallis test of variance showed that there were no significant differences among habitat groups using these ratios. Ratios used in this study are derived from some of the measurements used in the single limb analyses; descriptions of the ratios are listed in Table 3.

Only two complete (or nearly complete) skeletons of fossil taxa were measured for this study; they are UNSM 125572, a representative of *Longirostromeryx wellsi*, and AMNH F:AM 31360, a representative of *Parablastomeryx gregorii*. These are the only specimens consistently used across all (except one) of the single limb analyses and in the ratio analyses. Fossil specimens representing any species of blastomerycine and any of the relevant elements (humerus, radius, femur, metatarsal and phalanges) were measured using the same measuring scheme as was used on the modern specimens. Fossil specimens are identified to the species level where possible, however, due to the fact that many of these specimens are isolated postcrania, some are identified to the generic level. For this reason as well as aforementioned complications regarding species nomenclature,

this study groups fossils by genera for all analyses. All linear measurements of the fossils are recorded in Appendix D.

3.5 Statistical Analyses of Modern Samples

There are several options for analyzing datasets that contain multiple variables; this study focuses on principal components analysis (PCA), an ordination technique. PCA is a dimension reducing method that transforms large and complex datasets into more manageable groups of information. Dimension reducing techniques are valuable to ecometric studies that must compare multiple variables of complex morphologies in fossil and extant specimens (Van Valkenburgh et al., 2003; Croft and Anderson, 2007; Gingrich, 2003, 2005).

PCAs are able to interpret patterns in a dataset that contains multiple variables by identifying paths through the data that describe the greatest amount of variance; these are expressed in terms of principal components. Habitat groups, phylogenetic groups, or any other division of the data may be independently applied to these PCA results. The ability for PC values to describe habitat is subsequently tested using analyses of variance. This approach further holds the potential for future studies using these data to describe variance among locomotor groups, size groups, or even using values from another ecologically relevant proxy.

To test the capability of this method to discriminate habitat preferences among taxa, I initially utilize PCA on linear metrics of post-cranial elements for modern taxa only. Eight datasets are compiled using the Ln-transformed measurements for thirteen

linear metrics of the humerus, five of the distal humerus, eight of the radius, thirteen of the femur, thirteen of the metatarsal, nine of fore- and hind-foot proximal phalanges, five of the distal phalanges, and eight ratios of the appendicular skeleton. These data are averaged to produce one set of measurements per species. The dataset for the humerus comprises of measurements from 51 modern taxa, the radius and femur both use 53 taxa, the metatarsal uses 50 taxa, the proximal phalanges use 41, distal phalanges use 26, and the ratio dataset uses 48 modern taxa. These data are transformed into principal components using the paleontological statistics freeware, PAST, version 3, which was the program used to compute all subsequent statistical analyses (Hammer et al., 2001).

To test for statistically significant differences among habitat groups, analyses of variance are applied to their PC scores. Kruskal-Wallis tests are non-parametric tests of variance that assess the values for any number of groups, determining the likelihood that those groups sample the same population. It tests the null hypothesis that the median values of two or more groups are equal. Kruskal-Wallis tests indicate that the PC values for linear metrics of the humerus, distal humerus, radius, femur, metatarsal, proximal phalanges, as well as the ratio scheme for modern taxa, all express significant differences among at least some of the habitat groups (Table 4). This result indicates that these elements are suitable for interpreting habitat preference in blastomerycines.

The Mann-Whitney U test is a post-hoc test that further refines the resolution of the Kruskal-Wallis test. The Mann-Whitney U test assesses only two samples at a time, and can therefore describe the differences between medians for any two habitat-groups. *p*-values from these tests indicate the probability that randomly sampling a value from

one group could place it in another. Statistically significant *p*-values, those less than 0.05, reject the null hypothesis that two groups sample the same population. Mann-Whitney tests are performed on data for which the Kruskal-Wallis test indicates significant differences among sample medians. The results of these Mann-Whitney tests indicate that PC scores of these data do reliably separate habitat for some habitat groups.

A supplementary method is used to judge the utility of PCA as an approach to differentiate habitat amongst these data; the mean PC values, known as centroids, are calculated for each habitat group and plotted with two standard errors. In most cases, components 1 and 2 are used, as they describe the most and second most amount of variance in the dataset; however, component 3 is sometimes favored over component 2 when it successfully differentiates key habitat groups in a Mann-Whitney U test. The PCA centroids show that some groups tend to cluster together, however, several habitat groups will clearly separate from the rest. Based on these results, PCA of some post-cranial elements can confidently be used to identify habitat. These methods and these data are therefore applied to fossil taxa in an effort to interpret aspects of their paleoecology.

Summaries and loadings for all principal component analyses for modern specimens are available in Appendix E, along with scatter plots, centroid values, and results of the Mann-Whitney U tests.

3.6 Statistical Analyses of Fossil Samples

Fossil specimens are analyzed using methods similar to those described in section 3.5. Fossil humeri are added to a database of modern humeri, Ln transformed, reduced to principal components, and assessed using Kruskal-Wallis and Mann-Whitney U tests. This process is repeated for the distal humerus, radius, femur, metatarsal, and ratios. It is also used on the proximal phalanges, however, these cannot be accurately assigned to the forefoot or hindfoot for fossil specimens; therefore, fossils phalanges are assessed twice, once with proximal phalanges from the forefeet of modern specimens, and once with those of the hindfeet.

In these analyses, measurements are not averaged by species. Kovarovic and Andrews (2007) found that despite the imbalance in their dataset, overrepresented taxa did not swamp out biological signals in their DFA. Furthermore, it is not appropriate to compare individual fossils to species averaged values; therefore, measurements from all individuals are included in the PCAs. Scores are compared using Kruskal-Wallis and Mann-Whitney U tests for the following groups: grassland, wooded-bushed grassland, light woodland-bushland, heavy woodland-bushland, forest, montane light cover, montane heavy cover, *Longirostromeryx* spp. from the Clarendonian, *Parablastomeryx gregorii* from the Clarendonian, *Blastomeryx* spp. from the Clarendonian, *Blastomeryx* spp. from the Barstovian, and the Hemingfordian blastomerycines—*Problastomeryx primus*, *Pseudoblastomeryx advena,* and *Blastomeryx* sp.

Mann-Whitney tests show PC 1 and 2 are generally best at distinguishing groups. These components are therefore plotted in scatterplots along with the centroids of each group. Centroids represent the unweighted mean of PC values for species in each habitat

group. For modern groups, PC scores of individuals are averaged to create one datum per species; these species-averaged values are then averaged per group to designate the centroid. For fossil groups, PC scores for all specimens are averaged to create the centroid. These are mapped on to the PCA scatterplots along with standard error, which represent the accuracy of those centroids.

To determine the influence of phylogeny on these results, PC scores of bovids are compared to that of cervids. Antilocaprids, moschids, and tragulids are excluded due to their small sample sizes. There are fewer cervids in this study than bovids; however, these taxa represent an array of habitat preferences. The cervids in this study include: *Odocoileus virginianus*, *Elaphodus cephalophus*, *Pudu puda*, *Pudu mephistophiles*, *Muntiacus reevsi*, and *Dama dama*. Mann-Whitney U tests compare the PC scores for bovids versus cervids and the *p*-value represents the validity of the null hypothesis that these two groups sample the same population.

Body size may also influence results. To assess the relationship between body size and PCA values, the natural logarithm of the body is regressed against components 1 and 2 for all modern specimens in this study. Linear regressions are fitted to these data using Microsoft Excel. The correlation coefficient (r) represents the strength of the relationship between body size and PC values.

CHAPTER 4: RESULTS

Summaries and loadings for all principal component analyses of fossil and modern specimens are available in Appendix F, along with centroid values.

4.1 Humerus

PCA of the humerus is comprised of data from the following: three *Longirostromeryx* spp. from the Clarendonian, one *Parablastomeryx gregorii* from the Clarendonian, and 145 modern artiodactyls. This PCA produced thirteen principal components. The eigenvalue, a measure of the variance of variables for a given component, is 1.430 for PC 1, which explains 96.3% of the variance among these data. Component loadings represent the correlation coefficients between variables and components; loadings for PC 1 show positive correlation among all thirteen measurements. The equal loading of variables in component 1 indicates that all variables, in this case linear measurements, are related to each other. PC 2 has an eigenvalue of 0.015 and explains 1.0% variance; loadings of PC 2 describe a positive relationship of H1, H2, and H4, which are negatively correlated with H5 and H11 (codes defined in Table 2).

The Kruskal-Wallis one-way analysis of variance reports H-values and *p*-values that indicate significant difference among sample medians for PCs 1 and 2 (Table 5). The Mann-Whitney U test further indicates significant differences in PC scores among many of the groups (Table 6). Due to the limited sample of fossil specimens, the Mann-

Whitney test is less capable of confidently comparing these with other groups; nevertheless, the test rejects the null hypothesis that *Longirostromeryx* spp. represent the same distribution as light woodland-bushland taxa and montane light cover taxa for PC 1, as well as wooded-bushed grassland, light woodland-bushland, and forest taxa for PC 2. These components are not capable of rejecting the null hypothesis that *Longirostromeryx* spp. is from the same distribution as heavy woodland-bushland or montane heavy cover taxa, using the first two principal components.

Based on the results of the Kruskal-Wallis test, PC 1 and 2 are selected for the scatterplot, which shows the distribution of these two components for all specimens in the humeral dataset (Fig. 2). These are overlain by the centroid values, derived from the mean PC values of taxa from each habitat group. Figure 2 shows that the three *Longirostromeryx* spp. specimens express similar PC 1 scores, yet exhibit a remarkably variable distribution of PC 2, giving the centroid of that component a wide margin of error. Two standard errors of the *Longirostromeryx* spp. centroid overlap the range of two standard errors of the heavy woodland-bushland and forest groups. This graph additionally shows that the centroid for *Longirostromeryx* spp. is most closely associated with four specimens from the montane heavy cover group; these points represent four *Moschus moschiferous* specimens, the only modern musk deer in this study. If blastomerycines and moschids are monophyletic, this result would suggest that humeral anatomy is conserved within the group. Though *P. gregorii* is represented by a single taxon, its principal components place it within range of the montane heavy cover and

heavy woodland-bushland centroids, further supporting the notion that humeral anatomy was conserved within the family.

4.2 Distal Humerus

PCA of the distal humerus is comprised of data from eight *Longirostromeryx* spp. from the Clarendonian, one *Parablastomeryx gregorii* from the Clarendonian, one *Blastomeryx* spp. from the Clarendonian, one *Problastomeryx primus* from the Hemingfordian, and 145 modern artiodactyls. This PCA produced five principal components. PC 1 has an eigenvalue of 0.557 and explains 97.3% of the variance among these data; loadings show positive correlation among all measurements, which influence PC 1 nearly equally. PC 2 has an eigenvalue of 0.007 and explains 1.3% variance; loadings of PC 2 describe an inverse relationship between H11 and H12 (Table 2).

The Kruskal-Wallis analysis shows significant differences among sample medians for both PC 1 and 2 (Table 5), as does the Mann-Whitney U test (Table 7). The Mann-Whitney U test rejects the null hypothesis that PC 1 of *Longirostromeryx* spp. represents the same distribution as grassland, wooded-bushed grassland, light woodland-bushland, and montane light cover taxa; it is not able to reject the null hypothesis that *Longirostromeryx* specimens represent the same PC 1 distributions as taxa from forest or heavy woodland-bushland environments. PC 2 is not able to differentiate between *Longirostromeryx* spp. and other groups. Due to the limited sample of *Blastomeryx* spp., *Pr. primus,* and *P. gregorii* specimens, the Mann-Whitney U test is less capable of confidently comparing these with other groups.

PC 1 and 2 are selected for the scatterplot (Fig. 3) based on the results of the Kruskal-Wallis tests. All fossil specimens plot within a narrow range of PC 1 values, but within a wide range of PC 2 values. *Longirostromeryx* spp. shows generally lower PC 2 scores than do other blastomerycine groups; however, each other blastomerycine group is represented by single points. All of the fossil taxa show affinities with heavy woodland-bushland and forest groups, though they also cluster near data representing *M. moschiferous*.

4.3 Radius

PCA of the radius is comprised of data from eight *Longirostromeryx* spp. from the Clarendonian, one *Parablastomeryx gregorii* from the Clarendonian, one *Blastomeryx* spp. from the Clarendonian, one *Blastomeryx* spp. from the Barstovian, and 151 modern artiodactyls. This PCA has eight principal components. PC 1 has an eigenvalue of 1.003 and explains 96.9% of the variance among these data; loadings show positive correlation among all measurements, which influence PC 1 nearly equally. PC 2 has an eigenvalue of 0.012 and explains 1.2% variance; loadings of PC 2 are influenced greatly by R1 (Table 2).

Both the Kruskal-Wallis analysis (Table 5) and the Mann-Whitney U test (Table 8) show significant differences among sample medians for PC 1 and 2 values. Once again, the sample size of *Longirostromeryx* spp. makes it possible to compare to other habitat groups, while the limited sample of other blastomerycines are less statistically significant. The Mann-Whitney test of both PC 1 and 2 rejects the null hypothesis that

Longirostromeryx spp. represents the same distribution as wooded-bushed grassland or montane light. Its PC 1 values are significantly different from that of grassland and light woodland-bushland taxa, whereas PC 2 values show differences with forest and montane heavy taxa. The only group of modern taxa for which the Mann-Whitney test cannot reject the null hypothesis is the heavy woodland-bushland group.

PC 1 and 2 are selected for the scatterplot (Fig. 4). This scatterplot shows *Longirostromeryx* spp. only within range of the heavy woodland-bushland centroid. Like the previous plots, blastomerycines fall within the same quadrant as *M. moschiferous*. The fossil specimens show PC 2 values higher than most of the modern specimens. Once again, other blastomerycine groups each contain single data points. Both Barstovian and Clarendonian representatives of the genus *Blastomeryx* are closely allied with *Longirostromeryx* spp. and are more closely affiliated with the heavy woodland-bushland group, even though they do not fall within two standard errors of any modern group's centroid. *P. gregorii* is similarly allied with *Longirostromeryx* spp.; however, it is placed closer to wooded-bushed grassland and light woodland-bushland groups.

4.4 Femur

PCA of the femur is comprised of data from four *Longirostromeryx* spp. from the Clarendonian, one *Parablastomeryx gregorii* from the Clarendonian, one *Problastomeryx primus* from the Hemingfordian, and 152 modern artiodactyls. The PCA has produced thirteen principal components. PC 1 has an eigenvalue of 1.269 and explains 95.8% of the variance; loadings show positive correlation among all measurements, which

influence PC 1 nearly equally. PC 2 has an eigenvalue of 0.023 and explains 1.7% variance; loadings of PC 2 describe a positive correlation of F3, F6, and F13, which are negatively correlated with F11 (Table 2).

The Kruskal-Wallis analysis shows significant differences among sample medians for both components (Table 5), however this signal is stronger in PC 2 than in PC 1. The Mann-Whitney U test of these components further indicates significant differences in PC scores among several groups (Table 9). This test rejects the null hypothesis that *Longirostromeryx* spp. represents the same distribution of PC 1 values as grassland, light woodland-bushland, and montane light cover taxa. It rejects the null hypothesis that *Longirostromeryx* spp. comes from the same population as all categories except the montane heavy categories. The only category for which the null hypothesis was not rejected in both PC 1 and 2 was montane heavy. These components are not capable of rejecting the null hypothesis regarding the relationships of other blastomerycines, due to their small sample sizes.

PC 1 and 2 are selected for the scatterplot (Fig. 5). *Moschus moschiferous* exhibits extremely high PC 2 values, which are slightly higher than any of the blastomerycines; however, their PC 1 values are nearly identical to *Longirostromeryx* spp. and *Pr. primus*. All fossil taxa show close affiliations with the montane heavy category, though *Longirostromeryx* spp. and *Pr. primus* are within range of the heavy woodland-bushland category and *P. gregorii* are more near the quadrant containing montane light taxa.

4.5 Metatarsal

PCA of the metatarsal is comprised of data from seven *Longirostromeryx* spp. from the Clarendonian, one *Parablastomeryx gregorii* from the Clarendonian, five *Blastomeryx* spp. from the Clarendonian, three *Blastomeryx* spp. from the Barstovian, from the Hemingfordian, one *Problastomeryx primus,* one *Blastomeryx gemmifer*, and two *Pseudoblastomeryx advena*, and 151 modern artiodactyls. This PCA has produced thirteen principal components. PC 1 has an eigenvalue of 1.200 and explains 85.2% of the variance; loadings show positive correlation among all measurements, which influence PC 1 nearly equally. PC 2 has an eigenvalue of 0.121 and explains 8.6% variance; loadings of PC 2 describe an inverse relationship between MT11 versus MT1 and MT2 (Table 2).

The Kruskal-Wallis analysis for the first two components (Table 5) shows that the metatarsal is the most effective element in this study for distinguishing groups. The success of this may be, in part, related to the greater evenness of modern samples as well as the relatively large fossil sample. The Mann-Whitney U test of these components further shows significant differences among median PC scores of many groups (Table 10). The Mann-Whitney U test shows that *Longirostromeryx* spp. has a significantly different distribution from both montane categories for both PC 1 and PC 2. It furthermore has a significantly different distribution from wooded-bushed grassland and light woodland-bushland taxa for PC 1. These results are exactly the same for *Blastomeryx* spp. from the Clarendonian, similar to the results for *Blastomeryx* spp. from the Barstovian (though the null hypothesis cannot be rejected for montane heavy

affiliations using PC 1), as well as the Hemingfordian blastomerycines (which also show significant differences from wooded-bushed grassland and light woodland-bushland categories). Because there is only one *P. gregorii* specimen, the Mann-Whitney test cannot effectively separate this from any other group.

PC 1 and 2 are selected for the scatterplot (Fig. 6). The centroid of *Longirostromeryx* spp. is very closely associated with that of the heavy woodland-bushland group. All fossil specimens fall within the heavy woodland-bushland range. All blastomerycines but one have centroids that fall within the range of forest taxa. *P. gregorii* is much closer to the centroids for light woodland-bushland and wooded-bushed grassland groups. *Blastomeryx*, *Problastomeryx, Pseudoblastomeryx* specimens are closely associated with to each other, indicating their metatarsal morphology is conserved over time.

4.6 Forefoot Proximal Phalanx

PCA of the forefoot proximal phalanx is comprised of data from five *Longirostromeryx* spp. from the Clarendonian, two *Parablastomeryx gregorii* from the Clarendonian, four *Blastomeryx* spp. from the Clarendonian, two *Blastomeryx* spp. from the Barstovian, six Hemingfordian blastomerycines, and 111 modern artiodactyls. This produced nine principal components. PC 1 has an eigenvalue of 1.066 and explains 91.8% of the variance among these data; loadings show positive correlation among all measurements, which influence PC 1 nearly equally. PC 2 has an eigenvalue of 0.046

and explains 3.9% variance; the negative association of Pa1 and Pa5b with most other factors largely influences the loadings of PC 2 (Table 2).

Both the Kruskal-Wallis analysis (Table 5) and the Mann-Whitney U test (Table 11) show significant differences among sample medians for PC 1 and 2 values. *Longirostromeryx* spp. shows significantly different PC 1 distributions from the wooded-bushed grassland, light woodland-bushland, and montane light taxa; it shows significantly different PC 2 distributions from wooded-bushed grassland, light woodland-bushland, heavy woodland-bushland, and montane heavy taxa. The Mann-Whitney test cannot reject the null hypothesis that *Longirostromeryx* spp. comes from the same distribution as forest or grassland taxa based on combined PC 1 and 2 values. Based on the limited sample of grassland specimens, the Mann-Whitney U test is not able to distinguish this group from others very well; limited sample of grassland taxa may influence the results seen in fossil taxa. Clarendonian *Blastomeryx* spp. evinces similar results as *Longirostromeryx* spp. with only the additional difference between PC 2 values compared to the montane light category. Hemingfordian taxa and Clarendonian *Blastomeryx* spp. phalanges are the only fossil groups that show significant difference from one another; this is true for both components. The Hemingfordian group shows significant differences to PC values for most modern groups, though the null hypothesis cannot be rejected based on PC 1 and 2 of this sample compared to forest and grassland dwelling taxa. The sample of *Blastomeryx* spp. from the Barstovian is less clearly separated from other groups, only separating from light woodland-bushland in PC 1 and wooded-bushed grassland and heavy woodland-bushland with component 2; the scope of

results is likely due to the small sample size. *P. gregorii* also has a small sample size and is only distinguished from forest taxa using PC 1.

PC 1 and 2 are selected for the scatterplot (Fig. 7) based on the results of the Kruskal-Wallis test. This figure shows that none of the fossils cluster near the centroid of the grassland habitat, suggesting that limited sample size prevents the Mann-Whitney test from identifying differences between the fossil and grassland taxa. Clarendonian *Longirostromeryx* spp. and *Blastomeryx* spp. as well as Barstovian *Blastomeryx* spp. cluster near each other, indicating morphological similarities in their proximal phalanges. These also plot near PC values from *M. moschiferous*. The Hemingfordian specimens are distinct from other fossils and easily fall within the range of forest taxa. The Barstovian and Clarendonian taxa show more positive PC 1 values, but also plot within range of the forest or montane heavy groups. *P. gregorii* shows even higher PC 1 values and appears to be best fit with the light woodland-bushland, or possibly the wooded-bushed grassland group.

The results of analyses for either fore or hindfoot phalanges should be considered in conjunction with one another as the fossil specimens represent a mixture of fore and hindfoot elements. When one is considered without the other, this may lead to faulty interpretations.

4.7 Hindfoot Proximal Phalanx

PCA of the hindfoot proximal phalanx is comprised of the same fossil data outlined in section 4.6, as well as measurements from 113 modern artiodactyl phalanges.

This PCA has produced nine principal components. PC 1 has an eigenvalue of 0.821 and explains 91.4% of the variance; loadings show positive correlation among all measurements, which influence PC 1 nearly equally. PC 2 has an eigenvalue of 0.040 and explains 4.5% variance; loadings of PC 2 describe a relationship between Pa3 and Pa3b, which are negatively associated with Pa5b (Table 2).

Both the Kruskal-Wallis analysis (Table 5) and the Mann-Whitney U test (Table 12) show significant differences among sample medians for PC 1 and 2 values. Tests of PC 1 do not reject the null hypothesis that any of the fossil taxa occupied heavy woodland-bushland, forest, or grassland environments. Similar to the case with forefoot proximal phalanges, the low sample size of grassland taxa in this analysis are likely the cause for the latter result. The Mann-Whitney of PC 1 rejects the null hypothesis that *Longirostromeryx* spp. comes from the same distribution as wooded-bushed grassland, light woodland-bushland and montane light taxa; this result is the same for *Blastomeryx* spp. from the Clarendonian. PC 1 only rejects wooded-bushed grassland as a match for Barstovian *Blastomeryx* spp., which may be due to its small sample size. This test does not reject the hypothesis that the Hemingfordian specimens sample grassland, heavy woodland-bushland, or forest distributions. This test on PC 2 rejects the hypothesis that the fossils represent the same populations as almost all of the modern groups, with the exception of grassland categories and some montane categories (in Clarendonian and Barstovian *Blastomeryx* spp., and *P. gregorii*). The only fossil groups distinguished from one another are the Hemingfordian taxa and the Clarendonian *Longirostromeryx* spp.

PC 1 and 2 are selected for the scatterplot (Fig. 8). The distribution of taxa confirms results from the Mann-Whitney test: all fossil taxa are more closely related to each other than they are to modern groups. These data further show that the Hemingfordian taxa have a more negative PC 1 value and that *P. gregorii* has a more positive PC 1 value than the other Barstovian and Clarendonian blastomerycines in this study. These also cluster near the modern taxon, *M. moschiferous*. This figure describes either a non-analogue system, extreme phalangeal adaptations, or reflects problems using this method that may be comparing mostly fossil forefoot phalanges to modern hindfoot phalanges.

4.8 Ratios

PCA of several key ratios is comprised of data from one *Longirostromeryx wellsi* from the Clarendonian, one *Parablastomeryx gregorii* from the Clarendonian, and 129 modern artiodactyls. This PCA has produced five principal components. PC 1 has an eigenvalue of 9.543 and explains 69.6% of the variance among these data; loadings show a high correlation coefficient of the metatarsal length:width ratio (described in Table 3). PC 2 has an eigenvalue of 3.083 and explains 22.5% variance; loadings of PC 2 describe a positive relationship in length:width ratios of the humerus, radius, and femur. PC 3 also describes a substantial amount of variance among these data (eigenvalue of 0.714; 5.2% variance); however, the comparatively small difference among percent variance explained by the first several components suggests that the suite of features used here are not capable of making such powerful distinctions among samples as the single element

analyses. This is likely due to the lack of close association among these ratios. This result suggests that sampled taxa do not exhibit systematic changes in the sampled proportions and that these variations are likely described by a far more complex relationship. Nevertheless, the results of the ratio analyses are capable of distinguishing some amount of variation, as seen in both the Kruskal-Wallis (Table 5) and the Mann-Whitney U test (Table 13), which show significant differences among sample medians; however, the limited number of fossil specimens in this study renders this method incapable of analytically assessing the differences between the fossil and modern groups.

PC 1 and 2 are selected for use in the scatterplot (Fig. 9) based on the results of the Kruskal-Wallis tests. *L. wellsi* and *P. gregorii* appear to have unusual body proportions, separating from most modern taxa. Specimens with similar PC 1 and PC 2 values to these fossil taxa include: *Neotragus batesi*, *Madoqua kirkii*, *Cephalophus monticola*, and *Moschus moschiferous*. These are heavy-woodland bushland, forest, and montane heavy cover taxa—essentially artiodactyls that are largely required to navigate spatially complex habitats.

4.9 Phylogeny and Body Size

When PC 1 values of cervids are compared with those of bovids, a Mann-Whitney U test cannot reject the null hypothesis that these come from the same population (Table 14); this is true for all elements in this study, which indicates that PC 1 is not driven by phylogenetic differences between these groups. This test on PC 2 values largely rejects

the null hypothesis, indicating that this component is sometimes driven by phylogenetic relationships (Table 14).

Dimensions of limb elements are a good reflection of body size because these bones are responsible for supporting the animal's weight. Figure 10 represents the influence of body size on the first two principal components of the radius for all modern taxa in this study. The result $r = 0.95$ shows that PC 1 of the radius is highly correlated with body size (Fig. 10a). The relationship between PC 1 and body size proves to be even greater than the relationship between bone length and body size; a regression of Ln body size versus Ln of measurement R1 showed $r = 0.90$. However, both PC 1 and R1 are more successful indicators of size than PC 2. With a correlation coefficient of 0.01, PC 2 of the radius is clearly not correlated to body size (Fig. 10b). All other elements used in this study follow this trend where PC 1 reflects size and PC 2 does not—though neither component for the ratio analysis correlates to size (Table 15). These results show that despite the attempt to mute the influence of size on this study, size is the strongest factor separating these ruminants by habitat.

Scaling relationships can be used to predict body mass in living and fossil ruminants (Scott, 1983). Scott (1990) used linear measurements, similar to the ones in this study, and found that non-length dimensions of long bones or length of proximal bones correlated to body size. PCAs use all measurements so are better able to account for holistic shape than single measurements. In this study, PC 1 is so highly correlated to body size that those values are used here to assess size of fossil taxa. The PC values that are most closely tied to size are the humerus, distal humerus, radius and femur (Table

15). Based on the regression of these four elements, *Blastomeryx* spp. and *Problastomeryx primus* fall within the 9–13 kg size range, *Longirostromeryx* spp. falls within the 12–17 kg range, and *Parablastomeryx gregorii* is somewhere between 18–26 kg (Table 16). This is consistent with the findings of Scott (1990), who interpreted *Blastomeryx* spp. to be between 11–15 kg, using ruminant-based regressions.

CHAPTER 5: ECOLOGICAL DISCUSSION

5.1 Ecology of *Longirostromeryx wellsi*

Webb (1998) hypothesized that *Longirostromeryx,* the latest and most derived genus of Blastomerycinae, displays characters that indicate adaptation to more open environments. Janis (2000) suggested that the morphology of *Longirostromeryx* represents a deviation from the forest-edge browsing form of earlier blastomerycines and indicates that an open-habitat, mixed-feeding ecology is likely. While *L. wellsi* possesses several postcranial features that could support this interpretation—fused cannon bones, the absence of lateral digits, a reduced fibula, and an elongate distal limb—my quantitative assessment of this taxon has produced different results. Most of the Mann-Whitney U tests comparing PC scores of the *Longirostromeryx* Clarendonian group to modern artiodactyls strongly reject the null hypothesis that these fossils fall within wooded-bushed grassland, light woodland-bushland, and montane light cover categories.

The null hypothesis is rejected for several tests between *Longirostromeryx* spp. and the grassland group, however this is not the case for all elements. Based on the distribution of centroids on the scatterplots (Figs. 2–9), it appears that there are no examples where *Longirostromeryx* spp. falls within the range of the grassland centroid; therefore, the inability of the Mann-Whitney tests to distinguish among these groups is interpreted as artifacts of inadequate sample sizes, rather than indicators of morphological similarity. These results indicate that members of *Longirostromeryx*, which almost entirely represent the species *L. wellsi*, were not adapted for living in open environments.

Only three of the discussed Mann-Whitney U tests are able to reject the null hypothesis that *Longirostromeryx* spp. morphologically resembles taxa adapted for living in heavy woodland-bushland habitats; this is rejected for PC 2 of the femur, PC 2 of the forefoot proximal phalanx, and PC 2 of the hindfoot proximal phalanx (Tables 9, 11, 12). The centroid of this habitat group is furthermore, most commonly associated with *Longirostromeryx* spp. PC data on all scatterplots. Based on these results, it appears that *Longirostromeryx wellsi* is adapted for traversing the heavily vegetated and spatially complex environments that comprise the heavy woodland-bushland category. In this study, these are defined as areas with dense vegetation of tall trees and shrubs that create about 61–75% canopy cover.

The Mann-Whitney U tests vary by element in associating *Longirostromeryx* spp. specimens with the forest and montane heavy cover groups; therefore these environments may also influence the species' limb adaptations. Forest and heavy-woodland bushland groups are related as they both represent environments with heavy vegetative cover, especially trees. The montane heavy cover category represents heavy woodland-bushland and forest-like environments that occur at high altitudes. It is reasonable to expect that taxa adapted for any of these three habitat categories would evince similar limb morphologies to each other. Postcranial features shared among *L. wellsi* and taxa occupying closed habitats that support this interpretation include lack of fusion between the radius and ulna, minimal fusion in the carpals, slender limbs, and somewhat long muscle anchors. Furthermore, the association between other blastomerycines and closed

habitat artiodactyls suggests that these adaptations are primitive within the clade, and conserved through most of its members.

5.2 Blastomerycines and Moschids

This study incorporates data from *Moschus*, the presumed closest living relative of *Longirostromeryx wellsi.* Almost all of the PCAs placed blastomerycines near to the modern musk deer *M. moschiferous*. This similarity between components of *Moschus* and *Longirostromeryx* spp. suggest either that phylogeny was heavily swamping the data, or that these genera were similarly adapted for closed environments. Phylogeny, however, is not likely a problem for these data as *L. wellsi* is a highly derived end member of Blastomerycinae and *M. moschiferous* is an extant representative of the Old World musk deer, putting millions of years of evolution between them.

By assessing the difference in PC values between two major groups of this study, it becomes clear which components are controlled by phylogeny and which are not. PC 1, the principal component explaining the most variance among data, is not noticeably influenced by phylogeny; however, Mann-Whitney U tests cannot, for the most part, reject the null hypothesis for PC 2. Significant differences between the medians of PC 2 values for cervids versus bovids, indicates that this component represents differences that appear to separate by family. Differences between these groups may represent differences in inherited traits, though they still likely reflect functional differences, given that cervids utilize longer hindlimb suspensions in galloping than bovids and tend to inhabit generally more closed environments than bovids (Scott, 1987).

Similarity between PC 1 values for blastomerycines and extant moschids is therefore interpreted as analogous niche utilization. The proximity of PC 2 values further agrees with the interpretation of blastomerycines as extinct members of clade Moschidae; however, this is not a true test of phylogeny. If blastomerycines are closely related to moschids, ecology and morphology are apparently conserved in the group. This may indicate a similar condition in their last common ancestor, though further data would be needed to test this hypothesis. Based principally on PC 1 scores, which are independent of phylogeny, *Moschus moschiferous* and the blastomerycines in this study seemed to have utilized similar habitats. Whether or not blastomerycines are moschids, results of this study indicate that the postcranial skeletal morphology of *Moschus* is very similar to that of *Longirostromeryx wellsi* and the other tested blastomerycines, with the exception of *Parablastomeryx gregorii*.

5.3 Differences Among Blastomerycinae

This research not only tests the hypothesis that *Longirostromeryx wellsi* possesses open habitat adaptations, but also compares the condition of *L. wellsi* to that of other blastomerycines. Several authors have suggested that blastomerycines evince forest-dwelling adaptations, with the exception of the genus *Longirostromeryx* (Webb, 1998; Janis, 2000: Prothero, 2008). If results support this hypothesis, it would suggest that the clade's departure from a primitive browsing condition was an adaptive response to floral changes in the Miocene (Janis et al. 2002). However, the results indicate

Longirostromeryx spp. may have been better adapted to forested environments than were some contemporaneous blastomerycines.

Although data from other blastomerycines are few, several PCA scatterplots as well as quantitative results from the Mann-Whitney tests on proximal phalanges and the metatarsal describe a consistent pattern. *Blastomeryx* spp. from both Clarendonian and Barstovian NALMAs are closely associated with values from *Longirostromeryx* spp., indicating morphological similarities between these groups. Therefore, *Blastomeryx* is interpreted to be similarly adapted to heavy woodland-bushland habitats in the Barstovian and Clarendonian.

The only statistically significant difference among fossil groups is in PC 1 and PC 2 of the forefoot proximal phalanx (Fig. 13, Table 11); here the Hemingfordian taxa significantly differ from the Clarendonian *Longirostromeryx* spp. Based on the limited data, it appears that Hemingfordian taxa show greater affinities for forested environments than do later specimens of the same clade. This supports the interpretation of early blastomerycines as forest dwelling taxa (Janis, 2000) and supports the hypothesis that some later blastomerycines adapted to more mixed or open environments, possibly in response to the increase of open habitats and reduction of closed habitats (Janis et al., 2000). However, additional data scaled to a finer resolution would be needed to verify this interpretation.

Janis (2000) suggested that *Parablastomeryx,* the largest of the blastomerycines, represents a late-surviving forest-adapted blastomerycine, and compared its ecological strategy to that of contemporaneous dromomerycids. In this study the genus is

represented by only one skeleton of *Parablastomeryx gregorii*. Because it is represented by such scant data, analyses of variance are not able to describe the relationship of this taxon to modern species; however, PC values for this specimen do appear to differ from the other blastomerycines in this study. PC values of *Parablastomeryx gregorii* tend to be closer to the light woodland-bushland and wooded-bushed grassland centroid than are the other blastomerycines; this result may relate to its larger size (Table 16), which likely signals an expanded home range for this taxon (Jetz et al., 2004, Lindstedt et al., 1986; Swihart et al., 1988; Janis and Wilhelm, 1993). Its position in PCA scatterplots (Figs. 2–7) indicates that the limbs of *Parablastomeryx gregorii* are better adapted to open environments than that of *Longirostromeryx wellsi*.

5.4 Environmental Interpretation

While these results largely describe habitat preference among members of Blastomerycinae, they also impact paleoenvironmental interpretations for sites where their fossils are found. *Longirostromeryx wellsi* in particular is known from several specimens from the early Clarendonian Ashfall Fossil Beds in northeastern Nebraska. Evidence from environmental proxies suggests Ashfall was a dry savannah dominated by C_3 grasses during the late Miocene (Voorhies and Thomasson, 1979; Kita et al., 2014).

Stable isotopes from fauna at Ashfall Fossil Beds, an early Clarendonian site containing *L. wellsi,* are consistent with a semi-arid environment (Kita et al., 2014). Even stable isotopic values from *L. wellsi* ($\delta^{13}C$ -8.3 ± 0.6, Clementz et al., 2008) are consistent with feeding on a water-stressed C_3 vegetation in (Kita et al., 2014). However,

if *L. wellsi* had a diet of lichen (Teeri, 1981), much like *Moschus moschiferous*, or fruit, flowers, or bark (Codron et al. 2005), this may explain deceptively high carbon isotope values in this taxon.

Longirostromeryx wellsi is a small ruminant artiodactyl that would not have been successful in completely open environments. The presence of blastomerycines at this site supports the interpretation that the landscape was likely mosaic with some grasses and some woodlands (Fox and Koch, 2004; Kita et al., 2014; Voorhies 1971; Thomasson, 2005; Voorhies and Thomasson, 1979; Webb, 1977). It is likely that *L. wellsi* took to shelter in more restricted areas of denser vegetation, potentially bushes or small trees.

The persistence of taxa adapted to closed environments in the Clarendonian supports the interpretation that mixed and patchy environments persisted in North America through much of the Miocene (Strömberg, 2011). Based on evidence from phytoliths, true grasslands were not abundant (~50%) in North America until ~5.5 Ma (Strömberg and McInerney, 2011; Strömberg, 2011; McInerney, 2011); these interpretations are supported by multiple other proxies that place the extreme expansion of grasslands in the North American interior around the latest Miocene to Pliocene (Kita et al, 2014; Fox and Koch, 2004; Passey et al., 2002; Edwards et al., 2010). The demise of Blastomerycinae at the end of the Hemphillian coincides with the decline of browsers and the spread of C_4 grasslands (Janis et al., 2002; Passey et al., 2002). This decline, likely caused by loss of habitat, is the most probable explanation for their extinction (Janis et al., 2002).

Overall the story of Blastomerycinae told by these data indicates that early members of this clade were likely forest-dwelling taxa, much like modern musk deer that occupy montane woodlands. By the Barstovian or Clarendonian, this clade experienced slight modifications allowing them to occupy more mixed woody environments. Of the two latest surviving genera in this clade, *Parablastomeryx* shows greater adaptation to semi-open environments than does *Longirostromeryx*; however, both genera are extinct by the latest Hemphillian, likely due to loss of habitat or the change in environmental conditions that coincided with the expansion of open habitats and the spread of C_4 grasslands (Passey et al., 2002; Janis et al., 2002).

CHAPTER 6: *LONGIROSTROMERYX WELLSI* CASE STUDY

6.1 Introduction

A Clarendonian faunal community, including a large number of ungulates, has been uncovered from a volcanic ash deposit at Ashfall Fossil Beds State Historical Park in northeastern Nebraska. The exceptionally preserved biocenosis at the Ashfall locality is particularly useful for paleoecological analyses, including paleohabitat reconstruction. Among those preserved in the ash are some of the best-known skeletons of *Longirostromeryx wellsi*. The most complete specimen of this species, UNSM 125572, preserves most of its anatomy in partial articulation: cranium, mandible, hyoid, 7 cervical vertebrae, 6 thoracic vertebrae, 4 lumbar vertebrae, 11 caudal vertebrae, sacrum, right half of innominate, all four articulated limbs, sternum, and nearly half of the ribs. Thanks to the CT scan of UNSM 125572, this specimen can be assessed without disturbance. Its morphology reveals indicators of locomotor and dietary behavior as well as those features that make it unique among blastomerycines.

6.2 Geologic Context

UNSM 125572 (Fig. 11) comes from a lagerstätte faunal assemblage at the Poison Ivy quarry, now known as Ashfall Fossil Beds State Historical Park, in Antelope County, Nebraska. The fauna is medial Clarendonian in age, and its substrate corresponds to the 11.93 Ma Ibex Hollow tuff (Tedford et al., 2004; Tucker et al., 2014). Fossils of reptiles, birds, and mammals were preserved in three dimensions at this site due to rapid burial by

an aeolian ash originating at the Bruneau-Jarbidge eruptive center in Idaho (Perkins et al., 1998). The deposit is up to three meters thick and sits near the base within the Cap Rock Member of the Ash Hollow Formation (Skinner et al., 1968).

Over twenty taxa are preserved within the ash bed, though many other fossils, including amphibians, fish, plants, and mammals sit within a silty sandstone just below the ash (Tucker et al., 2014). The silty sand and overlying ash appear to fill a depression, interpreted to be a standing body of water based on diatoms, aquatic animals, and symmetrically rippled bedding planes (Voorhies and Thomasson, 1979; Tucker et al., 2014). Specimens are stratigraphically separated by size with the smallest on the bottom, slightly larger animals just above, and the largest mammals on the top, indicating that species perished in at least three different times. Over a hundred skeletons of the rhinoceros, *Teleoceras major,* comprise the uppermost layer in this depression, which indicates that they outlived the underlying taxa; this is further supported by well-developed hypertrophic osteopathy in specimens of *T. major* and the other large ungulates, indicating a prolonged period of inhaling ash (Tucker et al., 2014). Just below *Teleoceras* are several species of equids and camelids. Smaller taxa, including *Longirostromeryx wellsi,* come from the lowest part of the ash deposit, indicating that *L. wellsi* was among the first to perish from ash inhalation.

One of the greatest discoveries at Ashfall Fossil Beds was not of fauna, but of flora. Silicified anthoecia (husks) of grasses, *Berriochloa* spp., were found within the mouths and ribs of the rhinoceros, *Teleoceras major* (Voorhies and Thomasson, 1979). The presence of these grasses and these grazers indicates that *Berriochloa* made up at

least some portion of the *Teleoceras* diet and that they were present on the medial Clarendonian landscape of Nebraska. *Berriochloa* anthoecia indicate more open and arid environments, which agrees with the recent isotopic work (Kita et al., 2014) that points to Ashfall as a savannah-like environment, comprised partly of water-stressed C_3 vegetation or a component of C_4 vegetation.

6.3 CT Scan

The completeness and level of articulation of UNSM 125572 make it the most important specimen of *Longirostromeryx wellsi* currently known. The preservation of this specimen enriches our understanding of *L. wellsi* anatomy and allows for investigation into its taphonomy. To preserve this information, this specimen was kept in its original matrix and CT scanned. UNSM 125572 was scanned at the University of Nebraska Medical Center in Omaha, NE using a standard medical algorithm. Images were taken for every 0.625mm. The medical CT files were extracted using OsiriX freeware, then manually segmented and measured in Avizo 8.0. Descriptions are based on a combination of the physical specimen (Fig. 11) and its digital rendering (Fig. 12).

6.4 Cranium and Dentition

In 1904, Matthew named *Blastomeryx wellsi* based on a partial ramus, including p3–m3, which was larger than that of *Blastomeryx gemmifer* with smaller premolars and slightly taller crowns (Matthew, 1904, 1908). Frick (1937) assigned this to the genus *Longirostromeryx,* describing additional craniodental material. Because the cranium and

dentition of *L. wellsi* have been described, descriptions of these components here are brief. I focus on postcrania, which have not been described for this species.

The cranium and mandible (Fig. 13) are largely intact, though the CT scan reveals that the mandible is somewhat fractured and laterally compressed; nevertheless, the angle of its symphysis, as well as the width of the skull, indicates the jaw is long and narrow. The diastema between the lower p2 and the anterior teeth is about 62 mm long (Table 17), a length that is 30% greater than the row of cheek teeth (p2 – m3). The braincase is likewise narrow, with a slight nuchal crest and even slighter sagittal crest. The CT scan reveals a thin hyoid preserved in place, though poor resolution prevents precise view of its morphology. The skull lacks the characteristic saber-like canines, indicating that UNSM 125573 was a female. Fused epiphyses, and fully erupted and somewhat worn cheek teeth indicate that she is an adult.

6.5 Axial Skeleton

The majority of the vertebral column is preserved in this specimen. Its neck is complete and articulated through the sixth thoracic vertebra (Fig. 14). Some of the anterior ribs, as well as the manubrium of the sternum, are articulated along the neck. The xiphoid process and four segments of the sternal body are in articulation and are preserved near the ribs and forelimbs. Less than 50% of the ribcage is present. Nine consecutive ribs are preserved in relative position to one another, and several others are scattered nearby. The first rib is 59 mm long, but the longest rib preserved is 130 mm (Table 17).

All seven cervical vertebrae are present and in articulation (Fig. 14). The axis, the longest vertebra in the skeleton, is 75% longer than the atlas. *Parablastomeryx gregorii* (F:AM 31360), the contemporaneous blastomerycine that was nearly twice the weight of *L. wellsi*, has an atlas length of 36 mm and an axis length of 46 mm; UNSM 125572, by comparison, has a 28 mm atlas and 50 mm axis (Table 17). The extant *Moschus moschiferous* may be closer in body size to *L. wellsi*; while the size of UNSM 125572's atlas is comparable to that of *M. moschiferous* (29 mm length), its axis is slightly longer than that of *M. moschiferous* (43 mm). Based on length of the second through seventh cervical vertebra (Table 17), interpretation of *L. wellsi* as a long-necked moschid is valid. Spinous processes on cervical vertebra 2 through 7 are so low that they project noticeably above the cranial articular process only in C6.

The six most anterior thoracic vertebrae are present and in articulation. The anterior articular facet of the seventh thoracic vertebra is also present, though the remainder of that bone is not discernable anywhere else; this break may indicate scavenging at the shoulder of UNSM 125572. Spinous processes are nearly complete in only T4 and T5.

The posterior half of the specimen (Fig. 15) is oriented in the opposite direction from the anterior skeleton, indicating that these elements were disarticulated before burial. Four lumbar vertebrae, the sacrum, and all caudal vertebrae are present and articulated. The four most posterior lumbar vertebrae are presumably L3–L6. These vertebrae display low spinous processes and long transverse processes that curve anteriorly, making a 70° angle from the body; this is especially pronounced in the two

posterior-most vertebrae. The vertebrae have bodies similar in length (Table 17), though the body of L6 is about 60% wider than that of L3.

UNSM 125572 has a slender sacrum, relative to *Moschus moschiferous*, that is in articulation with the right ilium. Posterior to the sacral ala, the sacrum holds a fairly constant width through the body, and expands slightly at the sacral apex. Articulated with the sacrum are twelve caudal vertebrae. Distance from the base of the sacrum to the distal end of the posterior-most vertebra is 149 mm. Neural spines and prominent transverse processes are present in the five anterior-most vertebrae, after which the vertebrae become much smaller and more slender.

6.6 Forelimb

UNSM 125572 possesses a long and gracile forelimb with elongate distal elements (Fig. 16); a brachial index of 111.5 (Table 18) indicates a much longer radius than humerus. For this specimen, the distal limb is much better preserved than the proximal limb. The scapula is not preserved, except for a fragment of the distal end (visible in the CT scan), including the gleniod fossa and coracoid process. The scapular fragment is located in the matrix near the pelvis and sacrum. The lack of complete scapulae, as well as the fracture pattern (Haynes, 1983) of the fragmentary scapula, the humeri, and the 7th thoracic vertebra indicates that this individual was scavenged, potentially by one of the canids at Ashfall. Complete scapulae from other specimens of *L. wellsi* at Ashfall have narrow necks and wide, straight dorsal borders that curve slightly at the corners.

Both humeri are fractured at the shaft. They lack the proximal portion, though the distal portions are intact and in articulation with the radius and ulna. Based on the similarity in size of distal humeri in UNSM 125572 and UNSM 27831, the latter is used to supplement information for the former. The greatest functional length (H2) of the humerus in UNSM 27831 is 113.3 mm. The origin of the deltoid crest tends to be subtle and the greater tubercle extends less than 10 mm beyond the head. UNSM 27831 has a wide head and a shaft that tapers distally. In UNSM 125572 and other *L. wellsi* humeri, the width of the trochlea is similar to the width of the distal end. The olecranon fossa tends to be transversely narrow but anterior-posteriorly long.

The radius and ulna of UNSM 125572 are not fused; the gap between them is as great as 4.5 mm, suggesting that the interosseous membrane was functional and that *L. wellsi* had somewhat mobile forelimbs. However, the shaft of the ulna is quite thin, indicating that only the radius was weight bearing. An olecranon-ulnar index of 23.1 (Table 18) indicates a moderate size olecranon, similar to *Moschus moschiferous* (~ 21) but greater than *Parablastomeryx gregorii* (16.9). The radius is anterior-posteriorly flattened. Despite this being the predominant weight bearing bone in the forearm, it is more slender than that of the average ruminant artiodactyl.

The carpals are preserved in this specimen; however, due to their tight articulation and the low resolution of the scan, the digital rendering of the carpals does not accurately reflect their morphology. The metacarpal is one complete cannon bone with no evidence of lateral digits. The metacarpal is about 10 mm shorter than the metatarsal (Table 17). The proximal end has a noticeably greater breadth than depth. The epicondyles are

parallel to each other and are close together, separated by only a few millimeters. Digits 3 and 4 are long and articulate with the metacarpal. Four round sesamoids sit on the palmar side of the metacarpal-phalangeal joint. These sesamoids resemble those of *Antilocapra* more than those of *Odocoileus* and other deer possessing lateral digits. This further supports that lateral digits were never present on fore limbs of UNSM 125572.

6.7 Hindlimb

The hindlimb of UNSM 125572 is clearly longer than the forelimb (Fig. 11). With an intermembral index of 74 (Table 18), *L. wellsi* limb proportions fall near the average for generalized mammals (Howell, 1944). Femorometatarsal index for UNSM 125572 is 93, which is well above that of generalized mammals, though not as extreme as the gerenuk or gazelle. The elongate distal limb is suggestive of cursorial adaptations and more proximally located muscle attachments.

The right half of the pelvis is completely intact while the left side preserves only disarticulated fragments of the ilium, ischium, and pubis (Fig. 15). Pelvic length is comparable to that of ruminants of similar body size. The pelvis resembles that of *Moschus moschiferous*, with an elongate foramen obturatum and a prominent ischial spine. The interior of the acetabulum is approximately 19 by 15 mm, and still holds the head of the right femur.

Both femora are present and complete in the specimen, and are in articulation with their respective patella and tibia. The femur is proportionally more slender than is average in ruminants, and more gracile than expected for a ruminant with such long distal

limbs. The femoral head is narrow and leads into an obtuse neck. The greater trochanter is prominent, though it projects less than 10 mm above the head. It is connected to the posteriomedially projecting lesser trochanter through a concave crest. At the distal end, the medial and lateral condyles are of a similar breadth; however, the depth of the medial side is noticeably smaller than on the lateral side. This is particularly apparent when examining the differing height of the patellar ridges. This condition of condylar unevenness is more extreme than in *Moschus moschiferous*, though less than in *Litocranius walleri*, the gerenuk.

The tibia is long, particularly compared to the femur, though with a crural index of 119 (Table 18), it is within a normal range for small ruminants. The tibia possesses a proximal articular surface resembling an isosceles triangle. Similar to *Moschus moschiferous*, the tibia of *L. wellsi* has a prominent tibial tuberosity and anterior crest. The cross section of the shaft rounds out in the distal half of the tibia. Only a vestige of the fibula remains; it is slender and is approximately 30% the length of the tibia. The talar facet of the tibia is rectangular in shape. Both tibiae articulate with astragali, though only the right side retains the calcaneum.

The proximal astragalus is deeply trochleated and is situated tightly within the grooves of the distal tibia (Fig. 17). It appears similar to *Moschus moschiferous* with the lateral border being slightly greater than the medial border (Table 17). The calcaneum of *L. wellsi* is similar in size and proportions to that of *M. moschiferous*, though the calcaneal tuberosity is somewhat more pointed in the posterior aspect. The posterior portion of the calcaneum is long, extending 30.8 mm from the talar articular surface to

the most posterior point—this represents 85% of the calcaneum. Proximal to the metatarsal is a large cubonavicular and a diminutive medial cuneiform. The relationship between these two bones resembles that of most other small ruminants such as tragulids or *Muntiacus*.

The proximal end of the metatarsal is fairly square with breadth approximating depth. The metatarsal is long and straight with a prominent anterior groove. Like the metacarpal, the metatarsal bears no evidence of lateral digits. Similar to the metacarpal, it distally articulates with long phalanges and round sesamoids. The hindfoot phalanges are slightly larger than the forefoot phalanges (Table 17). The proximal phalanx is nearly 75% longer than the intermediate phalanx. The intermediate phalanx is slightly shorter than the distal phalanx.

CHAPTER 7: ANATOMICAL DISCUSSION AND CONCLUSIONS

Childs Frick (1937) first noted the extreme specializations in the cranium and dentition of *Longirostromeryx wellsi* that made it an easily recognizable member of its clade; postcrania, however, have been largely neglected. UNSM 125572 is the most complete skeleton of *L. wellsi* and this study is the first to describe the complete postcranial anatomy of this species. Furthermore, the quantitative assessment of *L. wellsi* postcrania provides a better understanding of its habitat, size, phylogeny, and overall morphological affinities to other ruminants.

Principal components analyses on five bones, the humerus, radius, femur, metatarsal, and proximal phalanges, indicates that these are effective habitat proxies for small-bodied ruminants. Furthermore, PC 1 is highly correlated with body size and PC 2 with family-level identification. In almost all of the analyses, blastomerycines plots near the modern musk deer, *Moschus moschiferous*, suggesting that their anatomy is highly similar and that *Moschus* is a reasonable modern analogue for blastomerycines. While this is not a test of phylogeny, these results may support the interpretation that blastomerycine are monophyletic with Moschidae (Webb and Taylor, 1980; Webb 1998; Janis and Scott, 1987; Janis, 2000; Prothero, 2008; McKenna and Bell, 1997; Gentry et al., 1999).

PCA results align the blastomerycine fossils with modern ruminants from heavy woodland-bushland environments, suggesting that this was their preferred habitat. Heavy woodland-bushland is defined as an environment where grass is a minor component and

predominantly small trees and bushes create 40–60% canopy cover. This interpretation of *L. wellsi* as a *Moschus*-like, heavy woodland-bushland, browsing musk deer is antithetical to the interpretation of *L. wellsi* as an open habitat end member of Blastomerycinae (Webb, 1998; Prothero, 2008; Janis, 2000).

If North America was becoming more open and dry as *L. wellsi* evolved, this species probably experienced some open landscapes. Despite this, *L. wellsi*, a small musk deer with morphology similar to earlier blastomerycines, was best suited to wooded habitats, as indicated by PCA and morphological interpretation. As small ruminants without armor, it is not likely that these were highly gregarious animals; they would most likely have operated in small troops. As presumably solitary ruminants, it is highly unlikely that *L. wellsi* inhabited grasslands or areas providing little protection, as they would have been particularly vulnerable prey.

Longirostromeryx wellsi displays an unusual suite of features that further muddle the interpretation of its behavior. It possesses reduced premolars, yet its molars are more hypsodont than that of earlier blastomerycines or even contemporaneous blastomerycines (*Parablastomeryx gregorii*). Unlike *Moschus moschiferous*, it has no lateral digits, however, the radius and ulna remain unfused, allowing for forearm mobility. The elongate distal limbs and lack of lateral digits suggest adaptations towards hyper-cursoriality; however, if the *L. wellsi* body plan were designed for speed, we should expect to see a much shorter olecranon, as in *Parablastomeryx gregorii*, and musculature moved to the proximal limb.

A possible solution for this seemingly non-compatible combination of features is the behaviors of the browsing bovid *Litocranius walleri*, the gerenuk. Though the molars of *L. wellsi* are mesodont, and more hypsodont than other blastomerycines (Webb, 1998), microwear analyses suggest it was a browser with a specialist diet (Carr and Pagnac, 2011). The elongate and narrow rostrum, characteristic of *L. wellsi* suggests unique feeding behavior. This trait may have been useful for feeding on difficult to reach plants, much like the gerenuk, which uses its long tongue and pointed muzzle to pluck foliage from among a blockade of thorns (Kingdon, 1982). Similar to *L. walleri, L. wellsi* possesses a long neck that would have been useful for reaching exceptionally high sources of food, browsing over the tops of bushes.

Litocranius walleri further uses a bipedal stance to lengthen its reach, allowing it to exploit foliage in small trees and from bushes up to two meters above the ground (Kingdon, 1982). Though *L. wellsi* possesses a slender sacrum, its asymmetrical femoral condyles and rigid lower limb could have aided in assuming a bipedal stance to reach a higher, more restricted food source. *L. walleri* has long hind limbs that lengthen its reach. *L. wellsi* too has femora much longer than expected, though not as long as its distal limbs; this long distal limb may have served to boost the animal up for a greater range of food. Though the utilization of a bipedal feeding stance is difficult to test, and a long neck would have helped it reach valuable food regardless of its posture. The comparison between *L. wellsi* and *L. walleri* requires more exploration, yet it is one hypothesis that may explain the unusual suite of feature seen in *Longirostromeryx wellsi*.

The anatomical description of this specimen shows that *L. wellsi* possessed a combination of features not seen in extant ruminants. The forearm indicates that mobility was important to their lifestyle—or at least that running was not. The hindlimb, which is long and without lateral toes, seems adapted for cursoriality, though feeding posture rather than running may have driven the selection of these features. The elongation of the neck and snout appear advantageous for consuming difficult to reach sources of food.

While *Longirostromeryx wellsi* does display some anatomical differences from extant musk deer that indicate greater adaptability to more mixed environments, both postcranial anatomy and rigorous ecometric assessment of *L. wellsi* reject the hypothesis that it was an open-habitat ruminant. These analyses indicate *L. wellsi* was suited for navigating spatially complex habitats such as woodland and bushland. The results of this study therefore necessitate a reevaluation of Clarendonian and Barstovian paleoenvironments, as *L. wellsi*, a successful and long-lived taxon, would have required woodland habitats capable of sheltering it throughout its range, across the Great Plains.

LITERATURE CITED

Axelrod, D. I. 1985. Rise of the grassland biome, central North America. Botanical Review 51:163–201.

Bibi, F. 2013. A multi-calibrated mitochondrial phylogeny of extant Bovidae (Artiodactyla, Ruminantia) and the importance of the fossil record to systematics. BMC Evolutionary Biology 13:166.

Bibi, F. 2014. Assembling the ruminant tree: combining morphology, molecules, extant taxa, and fossils. Zitteliana B 32:197–211.

Carr, J., and D. Pagnac. 2011. Why the long face? Dental microwear comparison of *Longirostromeryx* and *Blastomeryx* (Artiodactyla, Moschidae). Journal of Vertebrate Paleontology 31(2, Supplement):84–84.

Christiansen, P. 2002. Locomotion in terrestrial mammals: the influence of body mass, limb length and bone proportions on speed. Zoological Journal of the Linnean Society 136:685–714.

Clementz, M.T., P. A. Holroyd, and P. L. Koch. 2008. Identifying aquatic habits of herbivorous mammals through stable isotope analysis. Palaios 23:574–585.

Codron, J., D. Codron, J. A. Lee-Thorp, M. Sponheimer, W. J. Bond, D. de Ruiter, and R. Grant. 2005. Taxonomic, anatomical, and spatio-temporal variations in the stable carbon and nitrogen isotopic compositions of plants from an African savanna. Journal of Archaeological Science, 32:1757–1772.

Cope, E. D. 1877. Report upon the extinct Vertebrata obtained in New Mexico by parties of the expedition of 1874. Wheeler Survey 4:1–370.

Croft, D. A., and L. C. Anderson. 2008. Locomotion in the extinct notoungulate Protypotherium. Palaeontologia Electronica 11:1–20.

Curran, S. C. 2012. Expanding ecomorphological methods: geometric morphometric analysis of Cervidae post-crania. Journal of Archaeological Science 39:1172–1182.

Damuth, J., and C. M. Janis. 2011. On the relationship between hypsodonty and feeding ecology in ungulate mammals, and its utility in palaeoecology. Biological Reviews 86:733–758.

DeGusta, D., and E. Vrba. 2003. A method for inferring paleohabitats from the functional morphology of bovid astragali. Journal of Archaeological Science 30:1009–1022.

DeGusta, D., and E. Vrba. 2005a. Methods for inferring paleohabitats from the functional morphology of bovid phalanges. Journal of Archaeological Science 32:1099–1113.

DeGusta, D., and E. Vrba. 2005b. Methods for inferring paleohabitats from descrete traits of the bovid postcranial skeleton. Journal of Archaeological Science 32:1115–1123.

Edwards, E. J., C. P. Osborne, C. A. Strömberg, and S. A. Smith. 2010. The origins of C_4 grasslands: integrating evolutionary and ecosystem science. Science 328:587–591.

Elias, M. K. 1942. Tertiary prairie grasses and other herbs from the High Plains. Geological Society of America Special Papers 41:7–171.

Elissamburu, A. and S. F. Vizcaíno. 2004. Limb proportions and adaptations in caviomorph rodents (Rodentia: Caviomorpha). Journal of Zoology 262:145–159.

Eronen, J. T., D. Polly, M. Fred, J. Damuth, D. C. Frank, V. Mosbrugger, C. Scheidegger, N. C. Stenseth, and M. Fortelius. 2010. Ecometrics: The traits that bind the past and present together. Integrative Zoology 5:88–101.

Fernández, M. H., and E. S. Vrba. 2005. A complete estimate of the phylogenetic relationships in Ruminantia: a dated species-level supertree of the extant ruminants. Biological Reviews 80:269–302.

Fox, D. L., and P. L. Koch. 2004. Carbon and oxygen isotopic variability in Neogene paleosol carbonates: constraints on the evolution of the C_4-grasslands of the Great Plains, USA. Palaeogeography, Palaeoclimatology, Palaeoecology 207:305–329.

Frick, C. 1937. Horned Ruminants of North America. Bulletin of the American Museum of Natural History 69:1–669.

Garland, T., Jr., and C. M. Janis. 1993. Does metatarsal/ femur ratio predict maximal running speed in cursorial mammals? Journal of Zoology 229:133–151.

Gentry, A. W., G. E. Rössner, and E. P. J. Heizmann. 1999. Suborder Ruminantia. Miocene Land Mammals of Europe 23:225–253.

Gingerich, P. D. 2000. Arithmetic or geometric normality of biological variation: an empirical test of theory. Journal of Theoretical Biology 204:201–221.

Gingerich, P. D. 2003. Land-to-sea transition in early whales: evolution of Eocene Archaeoceti (Cetacea) in relation to skeletal proportions and locomotion of living semiaquatic mammals. Paleobiology 29:429–454.

Gingerich, P. D. 2005. Aquatic adaptation and swimming mode inferred from skeletal proportions in the Miocene desmostylian *Desmostylus*. Journal of Mammalian Evolution 12:183–194.

Green, M. J. B. 1985. Aspects of the ecology of the Himalayan musk deer. Ph.D. dissertation, University of Cambridge, Cambridge, United Kingdom, 292 pp.

Green, M. J. B. 1987. Diet composition and quality in Himalayan musk deer based on fecal analysis. Journal of Wildlife Management 51:880–892.

Hammer, Ø., D. A. T. Harper, P. D. Ryan. 2001. PAST: Paleontological statistics software package for education and data analysis. Palaeontologia Electronica 4:9 pp. Available at http://palaeo-electronica.org/2001_1/past/issue1_01.htm.

Hassanin, A., and E. J. Douzery. 2003. Molecular and morphological phylogenies of Ruminantia and the alternative position of the Moschidae. Systematic Biology 52:206–228.

Haynes, G. 1983. A guide for differentiating mammalian carnivore taxa responsible for gnaw damage to herbivore limb bones. Paleobiology 9:164–172.

Howell, A. B. 1944. Speed in Animals: Their Specialization for Running and Leaping. University of Chicago Press, Chicago, Illinois, 270 pp.

Janis, C. M. 2000. The Endemic Ruminants of the Neogene of North Amrerica; pp. 26–37 in E. S. Vrba, and G. B. Schaller (eds.), Antelopes, Deer and Relatives: Fossil Record, Behavioral Ecology, Systematics, and Conservation. Yale University Press, New Haven, Connecticut.

Janis, C. M., and K. M. Scott. 1987. The interrelationships of higher ruminant families: with special emphasis on the members of the Cervoidea. American Museum Novitates 2893:1–85.

Janis, C. M., and P. B. Wilhelm. 1993. Were there mammalian pursuit predators in the Tertiary? Dances with wolf avatars. Journal of Mammalian Evolution 1:103–125.

Janis, C. M., J. Damuth, and J. M. Theodor. 2000. Miocene ungulates and terrestrial primary productivity: Where have all the browsers gone? Proceedings of the National Academy of Sciences USA 97:237–61.

Janis, C. M., J. Damuth, and J. M. Theodor. 2002. The origins and evolution of the North American grassland biome: the story from the hoofed mammals. Palaeogeography, Palaeoclimatology, Palaeoecology 177:183–198.

Janis, C. M., J. Damuth, and J. M. Theodor. 2004. The species richness of Miocene browsers, and implications for habitat type and primary productivity in the North American grassland biome. Palaeogeography, Palaeoclimatology, Palaeoecology 207:371–398.

Jetz, W., C. Carbone, J. Fulford, and J. H. Brown. 2004. The scaling of animal space use. Science 306:266–268.

Kappelman, J. 1988. Morphology and locomotor adaptations of the bovid femur in relation to habitat. Journal of Morphology 198:119–130.

Kappelman, J. 1991. The paleoenvironment of *Kenyapithecus* at Fort Ternan. Journal of Human Evolution 20:95–129.

Kappelman, J., T. Plummer, L. Bishop, A. Duncan, and S. Appleton. 1997. Bovids as indicators of Plio-Pleistocene paleoenvironments in East Africa. Journal of Human Evolution 32:229–256.

Kingdon, J. 1982. Gerenuk; pp. 427–437 in J. Kingdon, East African Mammals: An Atlas of Evolution in Africa Volume 3, Part D. University of Chicago Press, Chicago, Illinois.

Kita, Z. A., R. Secord, and G. S. Boardman. 2014. A new stable isotope record of Neogene paleoenvironments and mammalian paleoecologies in the western Great Plains during the expansion of C_4 grasslands. Palaeogeography, Palaeoclimatology, Palaeoecology 399:160–172.

Klein, R. G., R. G. Francisus, and T. E. Steele. 2010. Morphometric identification of bovid metapodials to genus and implications for taxon-free habitat reconstruction. Journal of Archaeological Science 37:389–401.

Kovarovic, K. 2004. Bovids as paleoenvironmental indicators: A paleoecological analysis of bovid postcranial remains from Laetoli, Tanzania. Ph.D. dissertation, University College London, London, England, 559 pp.

Kovarovic, K., and P. Andrews. 2007. Bovid postcranial ecomorphological survey of the Laetoli paleoenvironment. Journal of Human Evolution 52:663–680.

Kovarovic, K., and P. Andrews. 2011. Environmental change within the Laetoli fossiliferous sequence: vegetation catenas and bovid ecomorphology; pp. 367–380 in T.

Harrison (ed.), Paleontology and Geology of Laetoli: Human Evolution in Context. Volume 1: Geology, Geochronology, Paleoecology and Paleoenvironment. Springer Science and Business Media, New York, New York.

Lindsay, E. H. 2003. Chronostratigraphy, biochronology, datum events, land mammal ages, stage of evolution, and appearance event ordination. Bulletin of the American Museum of Natural History 279:212–230.

Lindstedt, S. L., B. J. Miller, and S. W. Buskirk. 1986. Home range, time, and body size in mammals. Ecology 67:413–418.

Matthew, W. D. 1904. A complete skeleton of *Merycodus*. Bulletin of the American Museum of Natural History 20:103–130.

Matthew, W. D. 1908. Osteology of *Blastomeryx* and phylogeny of the American Cervidae. Bulletin of the American Museum of Natural History 23:535–562.

McInerney, F. A., C. A. Strömberg, and J. W. White. 2011. The Neogene transition from C_3 to C_4 grasslands in North America: stable carbon isotope ratios of fossil phytoliths. Paleobiology 37:23–49.

McKenna, M. C., and S. K. Bell. 1997. Classification of mammals above the species level. Columbia University Press, New York, New York. 640 pp.

Mihlbachler, M. C., and N. Solounias. 2006. Coevolution of tooth crown height and diet in oreodonts (Merycoidodontidae, Artiodactyla) examined with phylogenetically independent contrasts. Journal of Mammalian Evolution 13:11–36.

Mihlbachler, M. C., F. Rivals, N. Solounias, N., and G. M. Semprebon. 2011. Dietary change and evolution of horses in North America. Science 331:1178–1181.

Myers, P., R. Espinosa, C. S. Parr, T. Jones, G. S. Hammond, and T. A. Dewey. 2015. The Animal Diversity Web. Available at http://animaldiversity.org. Accessed February 16, 2015.

Nyambayar, B., H. Mix, and K. Tsytsulina. 2008. *Moschus moschiferus*. The IUCN Red List of Threatened Species, Version 2014.3. Available at www.iucnredlist.org. Accessed February 16, 2015.

Novello, A., C. Blondel, and M. Brunet. 2010. Feeding behavior and ecology of the Late Oligocene Moschidae (Mammalia, Ruminantia) from La Milloque (France): evidence from dental microwear analysis. Comptes Rendus Palevol 9:471–478.

Nowak, R. M. 1999. Walker's Mammals of the World, Volume 2. 6th edition. Johns Hopkins University Press, Baltimore, Maryland. pp 837–2015.

Passey B. H., T. E. Cerling, M. E. Perkins, M. R. Voorhies, J. M. Harris, S. T. Tucker. 2002. Environmental change in the Great Plains: an isotopic record from fossil horses. Journal of Geology 110:123–40.

Perkins, M. E., F. H. Brown, W. P. Nash, S. K. Williams, and W. McIntosh. 1998. Sequence, age, and source of silicic fallout tuffs in middle to late Miocene basins of the northern Basin and Range province. Geological Society of America Bulletin 110:344–360.

Plummer, T. W., and L. C. Bishop. 1994. Hominid paleoecology at Olduvai Gorge, Tanzania as indicated by antelope remains. Journal of Human Evolution 27:47–75.

Plummer, T. W., L. C. Bishop, and F. Hertel. 2008. Habitat preference of extant African bovids based on astragalus morphology: operationalizing ecomorphology for palaeoenvironmental reconstruction. Journal of Archaeological Science 35:3016–3027.

Polly, P. D., J. T. Eronen, M. Fred, G. P. Dietl, V. Mosbrugger, C. Scheidegger, D. C. Frank, J. Damuth, N. C. Stenseth, and M. Fortelius. 2011. History matters: ecometrics and integrative climate change biology. Proceedings of the Royal Society of London B: Biological Sciences 278:1131–1140.

Prothero, D. R. 2008. Systematics of the musk deer (Artiodactyla: Moschidae: Blastomerycinae) from the Miocene of North America. New Mexico Museum of Natural History and Science Bulletin 44:207–225.

Prothero, D. R., and M. R. Liter. 2008. Systematics of the dromomerycines (Artiodactyla: Palaeomerycidae) from the Miocene and Pliocene of North America. New Mexico Museum of Natural History and Science Bulletin 44:273–298.

Reed, K. E. 1998. Using large mammal communities to examine ecological and taxonomic structure and predict vegetation in extant and extinct assemblages. Paleobiology 24:384–408.

Retallack, G. J. 2007. Cenozoic paleoclimate on land in North America. Journal of Geology 115:271–94.

Rose, K. 2006. The Beginning of the Age of Mammals. Johns Hopkins University Press, Baltimore, Maryland, 428 pp.

Samuels, J. X., and B. Van Valkenburg. 2008. Skeletal indicators of locomotor adaptations in living and extinct rodents. Journal of Morphology 269:1387–1411.

Sánchez, I. M., M. S. Domingo, and J. Morales. 2010. The genus *Hispanomeryx* (Mammalia, Ruminantia, Moschidae) and its bearing on musk deer phylogeny and systematics. Palaeontology 53:1023–1047.

Sathyakumar, S. 1992. The Musk Deer. Sanctuary Asia 12(5):52–57.

Schmidt, M., and M. S. Fischer. 2009. Morphological integration in mammalian limb proportions: dissociation between function and development. Evolution 63:749–766.

Scott, K. M. 1983. Prediction of body weight of fossil Artiodactyla. Zoological Journal of the Linnean Society 77:199–215.

Scott, K. M. 1985. Allometric trends and locomotor adaptations in the Bovidae. Bulletin of the American Museum of Natural History 197:197–288.

Scott, K. M. 1990. Postcranial dimensions of ungulates as predictors of body mass; pp. 301–335 in J. Damuth and B. J. MacFadden (eds.), Body Size in Mammalian Paleobiology: Estimation and Biological Implications. Cambridge University Press, New York, New York.

Scott, R. S., and M. Maga. 2005. Paleoecology of the *Akkasdagi hipparions* (Mammalia, Equidae), late Miocene of Turkey. Geodiversitas 27:809–830.

Semprebon, G., C. M. Janis, and N. Solounias. 2004. The diets of the Dromomerycidae (Mammalia: Artiodactyla) and their response to Miocene vegetational change. Journal of Vertebrate Paleontology 24:427–444.

Skinner, M. F., S. M. Skinner, and R. J. Gooris. 1968. Cenozoic rocks and faunas of Turtle Butte, south-central South Dakota. Bulletin of the American Museum of Natural History 138:1–379.

Strömberg, C. A. E. 2004. Using phytolith assemblages to reconstruct the origin and spread of grass-dominated habitats in the great plains of North America during the late Eocene to early Miocene. Palaeogeography, Palaeoclimatology, Palaeoecology 207:239–275.

Strömberg, C. A. E. 2011. Evolution of grasses and grassland ecosystems. Annual Review of Earth and Planetary Sciences 39:517–544.

Strömberg, C. A. E., and F. A. McInerney. 2011. The Neogene transition from C_3 to C_4 grasslands in North America: assemblage analysis of fossil phytoliths. Paleobiology 37:50–71.

Su, B., Y. X. Wang, H. Lan, W. Wang, and Y. Zhang. 1999. Phylogenetic study of complete cytochrome *b* genes in musk deer (genus *Moschus*) using museum samples. Molecular Phylogenetics and Evolution 12:241–249.

Swihart, R. K., N. A. Slade, and B. J. Bergstrom. 1988. Relating body size to the rate of home range use in mammals. Ecology 69: 393–399.

Taylor, B. E., and S. D. Webb. 1976. Miocene Leptomerycidae (Artiodactyla, Ruminantia) and their relationships. American Museum Novitates 2596:1–22.

Tedford, T. H., L. B. Albright III, A. D. Barnosky, I. Ferrusquia-Villafranca, R. M. Hunt Jr., J. E. Storer, E. E. Swisher III, M. R. Voorhies, S. D. Webb, and D. P. Whistler. 2004. Mammalian biochronology of the Arikareean through Hemphillian interval (late Oligocene through early Pliocene epochs); pp. 169–231 in M. O. Woodburne (ed.), Late Cretaceous and Cenozoic Mammals of North America: Biostratigraphy and Geochronology. Columbia University Press, New York, New York.

Teeri, J. A. 1981. Stable carbon isotope analysis of mosses and lichens growing in xeric and moist habitats. Bryologist 84:82–84.

Thomasson, J. R. 2005. *Berriochloa gabeli* and *Berriochloa huletti* (Gramineae: Stipeae), two new grass species from the late Miocene Ash Hollow Formation of Nebraska and Kansas. Journal of Paleontology 79:185–199.

Tucker, S. T., R. E. Otto, R. M. Joeckel, and M. R. Voorhies. 2014. The geology and paleontology of Ashfall Fossil Beds, a late Miocene (Clarendonian) mass-death assemblage, Antelope County and adjacent Knox County, Nebraska, USA. Field Guides 36:1–22.

Van Valkenburgh, B. 1994. Ecomorphological analysis of fossil vertebrates and their paleocommunities; pp. 140–166 in P. C. Wainwright and S. M. Reilly (eds.), Ecological Morphology: Integrative Organismal Biology. University of Chicago Press, Chicago, Illinois.

Van Valkenburgh, B., T. Sacco, and X. Wang. 2003. Pack hunting in Miocene borophagine dogs; evidence from craniodental morphology and body size. Bulletin of the American Museum of Natural History 279:147–162.

Vislobokova, I. A. and A. V. Lavrov. 2009. The earliest musk deer of the genus *Moschus* and their significance in clarifying of evolution and relationships of the family Moschidae. Paleontological Journal 43:326–338.

Von Den Driesch, A. 1976. A guide to the measurement of animal bones from archaeological sites. Peabody Museum Bulletins 1:1–148.

Voorhies, M. R. 1971. Paleoclimatic significance of crocodilian remains from the Ogallala Group (Upper Tertiary) in northeastern Nebraska. Journal of Paleontology 45:119–121.

Voorhies, M. R., and J. R. Thomasson. 1979. Fossil grass anthoecia within Miocene rhinoceros skeletons: diet in an extinct species. Science 206:331–333.

Webb, S. D. 1977. A history of savanna vertebrates in the New World. Part I: North America. Annual Review of Ecology and Systematics 8:355–380.

Webb, S. D. 1998. Hornless ruminants; pp. 463–476 in C. M. Janis (ed.), Evolution of Tertiary Mammals of North America: Vol. 1 Terrestrial Carnivores, Ungulates, and Ungulate-like Mammals. Cambridge University Press, Cambridge, Massachusetts.

Webb, S. D., and B. E. Taylor. 1980. The phylogeny of hornless ruminants and a description of the cranium of *Archaeomeryx*. Bulletin of the American Museum of Natural History 167:121–157.

Weinand, D. C. 2007. A study of parametric versus non-parametric methods for predicting paleohabitat from Southeast Asian bovid astragali. Journal of Archaeological Science 34:1774–1783.

Wood, H. E., R. W. Chaney, J. Clark, E. H. Colbert, G. L. Jepsen, J. B. Reeside, and C. Stock. 1941. Nomenclature and correlation of the North American continental Tertiary. Geological Society of America Bulletin 52:1–48.

TABLES

Table 1. Modern specimens by habitat assignment, species, number of specimens, and average weight (kg)

Species by habitat	Average Weight	n=	Species by habitat	Average weight	n=
Grassland			**Heavy Woodland-Bushland**		
Addax nasomaculatus	97.5	2	*Madoqua kirkii*	5.5	5
Damaliscus dorcas	67.5	1	*Madoqua saltiana*	3.25	5
Procapra picticaudata	27.5	3	*Neotragus batesi*	3.75	4
			Neotragus moschatus	5	6
Wooded-Bushed Grassland			*Neotragus pygmaeus*	2.25	1
Antilocapra americana	53	2	*Philantomba maxwellii*	7.5	1
Antilope cervicapra	35	2	*Tragelaphus scriptus*	52	11
Damaliscus hunteri	99	3	*Tragelaphus spekii*	85	4
Gazella rufifrons	25	2	*Tragulus nigricans*	4.5	1
Gazella soemmerringi	42	2			
Gazella spekei	20	2	**Forest**		
Gazella subgutturosa	25.5	6	*Cephalophus dorsalis*	21	6
Gazella thomsonii	22.5	4	*Cephalophus leucogaster*	17.5	5
Kobus kob	90.5	5	*Cephalophus monticola*	6.25	5
Kobus leche	95	1	*Cephalophus nigrifrons*	16	6
Madoqua guentheri	4.6	2	*Hyemoschus aquaticus*	10.85	5
Ourebia ourebi	17	5	*Pudu puda*	12	1
Raphicerus campestris	11.5	6	*Tragulus javanicus*	4.35	1
Redunca fulvorufula	28.5	5			
			Montane Light Cover		
Light Woodland-Bushland			*Capra sibirica*	82.5	4
Aepyceros melampus	60	7	*Oreamnos americanus*	93	2
Dama dama	70	1	*Ovis canadensis*	98	2
Gazella cuvieri	25	2	*Ovis vignei*	61.5	3
Gazella granti	57.5	4	*Pseudois nayaur*	52.5	3
Litocranius walleri	40	7	*Rupicapra rupicapra*	37	4
Odocoileus virginianus	90	4			
Oreotragus oreotragus	13	4	**Montane Heavy Cover**		
Raphicerus sharpei	9	3	*Elaphodus cephalophus*	33.5	6

Redunca redunca	50	5	*Moschus moschiferus*	14.5	5
Sylvicapra grimmia	16.75	7	*Muntiacus reevsi*	13.5	1
			Naemorhedus crispus	82.5	2
			Naemorhedus goral	28.5	6
			Naemorhedus swinhoei	95	1
			Pudu mephistophiles	9.6	2

Table 2. Definitions of measurements and measurement codes, reproduced from Kovarovic (2004). Measurements are illustrated in Appendix A.

Code	Definition
Humerus	
H1	Greatest length of the humerus
H2	Functional length of the humerus
H4	Measure of the most distal point of the deltoid crest to the tip of the greater tuberosity
H5	Width of the humeral head
H6	Anterior-posterior diameter of the proximal end
H7	Transverse diameter of the proximal end
H8*	Width of the trochlea and capitulum
H9*	Anterior-posterior diameter of the distal end
H10*	Transverse diameter of the distal end
H11*	Width of the trochlea in posterior view
H12*	Length of trochlea in posterior view
H13	Anterior-posterior mid-shalt diameter
H14	Transverse mid-shaft diameter
	* Indicates distal humerus measurements
Radius	
R1	Greatest length of the radius
R2	Anterior-poster diameter of the proximal end
R3	Transverse diameter of the proximal end
R4	Transverse width of the articular surface of the proximal end
R5	Anterior-posterior diameter of the distal end

R6	Transverse diameter of the distal end
R7	Anterior-poster mid-shaft diameter
R8	Transverse mid-shaft diameter

Femur

F2	Functional length of femur
F3	Anterior-posterior diameter of the proximal end
F4	Transverse diameter of the proximal end
F5	Measure of the distance between the tip of the greater trochanter and the tip of the lesser trochanter
F6	Measure of the distance between the tip of the lesser trochanter and the tip of the head
F7	Anterior-posterior diameter of the femoral head
F8	Transverse diameter of the femoral head
F9	Anterior-posterior diameter of the distal end
F10	Transverse diameter of the distal end
F11	Measure of the width of the anterior trochlea
F12	Measure of the width of the interior trochlea
F13	Anterior-posterior mid-shaft diameter
F14	Transverse mid-shaft diameter

Metatarsal

MT1	Greatest length of the metatarsal
MT2	Functional length of the metatarsal
MT3	Anterior-posterior diameter of the proximal end
MT4	Transverse diameter of the proximal end
MT5	Anterior-posterior diameter of the distal end
MT6	Transverse diameter of the distal end
MT7	Measure of the distance between the medial and lateral verticillus
MT8	Diameter of the lateral epicondyle
MT9	Transverse width of the lateral epicondyle
MT10	Measure of the distance between the medial and lateral epicondyle at the most proximal point
MT11	Measure of the distance between the medial and lateral epicondyle at the most distal point
MT12	Anterior-posterior mid-shaft diameter
MT13	Transverse mid-shaft diameter

Proximal Phalanx

Pa1	Greatest length of the proximal phalanx
Pa2	Transverse diameter of distal end
Pa3	Transverse width of the distal articular surface
Pa3b	Dorsal-palmar length of the distal articular surface
Pa4	Transverse width of the proximal end
Pa5	Transverse width of the proximal articular surface
Pa5b	Dorsal-palmar length of the proximal articular surface
Pa6	Dorsal-palmar mid-shaft diameter
Pa7	Transverse mid-shaft diameter

Calcaneum

C1	Greatest length of the calcaneum

Table 3. Descriptions of ratios based on linear measurements from Table 2

Code	Ratio
H2/H14	Humeral robustness
R1/R9	Radial robustness
F2/F14	Femoral robustness
MT1/MT13	Metatarsal robustness
MT1/F2	Femoro-metatarsal ratio
C1/MT1	Hindlimb mechanical advantage
R1/H2	Brachial ratio

Table 4. Kruskal-Wallis test for equal medians of the first three principal components of species-averaged data from modern specimens; there is a significant difference among sample medians where *p* (same) is < 0.05

Element, Component	H (chi^2)	H_c (tie corrected)	*p* (same)
Humerus, PC 1	18.71	18.71	0.005
Humerus, PC 2	25.69	25.69	<0.001
Humerus, PC 3	8.304	8.304	0.217

Distal Humerus, PC 1	19.94	19.94	0.003
Distal Humerus, PC 2	10.34	10.34	0.111
Distal Humerus, PC 3	17.00	17.00	0.009
Radius, PC 1	21.94	21.94	0.001
Radius, PC 2	14.97	14.97	0.021
Radius, PC 3	12.24	12.24	0.057
Femur, PC 1	20.23	20.23	0.003
Femur, PC 2	26.16	26.16	<0.001
Femur, PC 3	18.98	18.98	0.004
Metatarsal, PC 1	23.63	23.63	0.001
Metatarsal, PC 2	23.98	23.98	0.001
Metatarsal, PC 3	6.343	6.343	0.386
Proximal Phalanges, PC 1	19.85	19.85	0.003
Proximal Phalanges, PC 2	23.81	23.81	0.001
Proximal Phalanges, PC 3	7.71	7.71	0.260
Ratios PC 1	18.99	18.99	0.004
Ratios PC 2	20.37	20.37	0.002
Ratios PC 3	15.27	15.27	0.018

Table 5. Kruskal-Wallis test for equal medians showing principal components that show significant difference among sample medians (p [same] < 0.05) for PCAs that combined modern and fossil specimens

Element, Component	H (chi^2)	H_c (tie corrected)	p (same)
Humerus, PC 1	46.10	46.10	<0.001
Humerus, PC 2	84.97	84.97	<0.001
Distal Humerus, PC 1	53.58	53.58	<0.001
Distal Humerus, PC 2	39.24	39.24	<0.001
Radius, PC 1	58.63	58.63	<0.001
Radius, PC 2	51.52	51.52	<0.001
Femur, PC 1	46.48	46.48	<0.001
Femur, PC 2	85.85	85.85	<0.001
Metatarsal, PC 1	84.74	84.74	<0.001
Metatarsal, PC 2	76.06	76.06	<0.001
Forefoot Proximal Phalanx, PC 1	62.11	62.11	<0.001
Forefoot Proximal Phalanx, PC 2	76.15	76.15	<0.001
Hindfoot Proximal Phalanx, PC 1	61.30	61.30	<0.001

Hindfoot Proximal Phalanx, PC 2	77.45	77.45	<0.001
Ratios PC 1	56.25	56.25	<0.001
Ratios PC 2	45.00	45.00	<0.001

Table 6–13. Raw *p* values of a Mann-Whitney U test on the first principal components (upper right corner) and second principal components (lower left corner), where G= grassland, WBG= wooded-bushed grassland, LWB= light woodland-bushland, HWB= heavy woodland-bushland, F= forest, MTL= montane light cover, MTH= montane heavy cover, L (Cl)= *Longirostromeryx* spp. from the Clarendonian, P (Cl)= *Parablastomeryx gregoiri* from the Clarendonian, B (Cl)= *Blastomeryx* spp. from the Clarendonian, B (Ba)= *Blastomeryx* spp. from the Barstovian, Pr (H)= *Problastomeryx primus* from the Hemingfordian, Prs (H)= *Problastomeryx primus* and *Pseudoblastomeryx advena* from the Hemingfordian. Cells are shaded where $p < 0.05$, thus indicating the test rejects the null hypothesis that those two groups sample the same distribution.

Table 6. *p* values of a Mann-Whitney U test on PC 1 (upper right) and PC 2 (lower left) of the humerus.

	G	WBG	LWB	HWB	F	MTL	MTH	L (Cl)	P (Cl)
G		0.279	0.369	0.221	0.002	0.396	0.114	0.052	0.289
WBG	0.092		0.190	0.368	<0.001	0.001	0.430	0.105	0.793
LWB	0.391	<0.001		0.016	<0.001	0.002	0.037	0.017	0.488
HWB	0.004	<0.001	<0.001		0.110	<0.001	0.766	0.601	0.875
F	0.007	<0.001	<0.001	0.233		<0.001	0.002	0.774	0.119
MTL	0.005	<0.001	<0.001	0.606	0.018		<0.001	0.013	0.148
MTH	0.011	<0.001	<0.001	0.588	0.075	1		0.180	0.862
L (Cl)	0.052	0.006	0.010	0.138	0.017	0.213	0.251		0.371
P (Cl)	0.289	0.104	0.141	0.753	0.225	1	1	1	

Table 7. *p* values of a Mann-Whitney U test on PC 1 (upper right) and PC 2 (lower left) of the distal humerus.

	G	WBG	LWB	HWB	F	MTL	MTH	L (Cl)	P (Cl)	B (Cl)	Pr (H)
G		0.326	0.326	0.221	0.002	0.648	0.181	0.009	0.289	0.289	0.289
WBG	0.151		0.250	0.296	<0.001	0.006	0.355	0.003	0.431	0.227	0.128
LWB	0.014	0.001		0.011	<0.001	0.004	0.030	<0.001	0.436	0.166	0.100
HWB	0.003	<0.001	0.005		0.129	<0.001	0.807	0.367	0.875	0.753	0.753
F	0.039	0.008	0.908	0.023		<0.001	0.002	0.441	0.119	0.862	0.603
MTL	0.058	0.412	0.075	<0.001	0.121		<0.001	<0.001	0.148	0.148	0.148

MTH	0.017	0.002	0.518	0.093	0.640	0.023		0.059	0.862	0.386	0.119
L (Cl)	0.270	0.319	0.661	0.054	0.474	0.710	0.541		0.175	0.561	0.175
P (Cl)	0.289	0.156	0.299	0.753	0.386	0.148	0.488	0.561		1	1
B (Cl)	0.289	0.128	0.225	0.528	0.298	0.148	0.225	0.561	1		1
Pr (H)	0.289	0.156	0.544	1	0.386	0.148	1	0.561	1	1	

Table 8. *p* values of a Mann-Whitney U test on PC 1 (upper right) and PC 2 (lower left) of the radius.

	G	WBG	LWB	HWB	F	MTL	MTH	L (Cl)	P (Cl)	B (Cl)	B (Ba)
G		0.469	0.369	0.221	0.002	0.692	0.140	0.008	0.724	0.289	0.289
WBG	0.323		0.299	0.19	<0.001	0.002	0.105	0.003	0.715	0.101	0.171
LWB	0.464	0.909		0.009	<0.001	0.017	0.026	<0.001	0.544	0.141	0.166
HWB	0.684	0.128	0.173		0.074	<0.001	0.747	0.575	0.875	0.753	0.753
F	0.096	<0.001	<0.001	0.034		<0.001	0.001	0.347	0.117	0.934	0.804
MTL	0.101	<0.001	0.001	0.065	0.782		<0.001	<0.001	0.137	0.137	0.137
MTH	0.035	<0.001	<0.001	0.006	0.796	0.336		0.109	0.847	0.248	0.335
L (Cl)	0.075	0.021	0.116	0.092	<0.001	0.005	0.004		0.175	0.175	0.175
P (Cl)	0.289	0.171	0.260	0.431	0.117	0.137	0.177	0.847		1	1
B (Cl)	0.289	0.101	0.194	0.156	0.117	0.137	0.123	0.175	1		1
B (Ba)	0.289	0.101	0.194	0.207	0.117	0.137	0.123	0.175	1	1	

Table 9. *p* values of a Mann-Whitney U test on PC 1 (upper right) and PC 2 (lower left) of the femur.

	G	WBG	LWB	HWB	F	MTL	MTH	L (Cl)	P (Cl)	Pr (H)
G		0.573	0.286	0.189	0.002	0.744	0.131	0.030	0.724	0.289
WBG	0.120		0.592	0.181	<0.001	0.058	0.033	0.055	0.673	0.147
LWB	0.572	0.007		0.036	<0.001	0.055	0.001	0.025	0.603	0.166
HWB	0.500	0.007	0.238		0.186	0.019	0.623	0.804	0.940	0.821
F	0.040	<0.001	<0.001	0.036		<0.001	0.006	0.261	0.117	0.804
MTL	0.005	<0.001	<0.001	<0.001	0.014		<0.001	0.005	0.148	0.148
MTH	0.003	<0.001	<0.001	<0.001	<0.001	0.112		0.333	0.934	0.457
L (Cl)	0.030	0.002	0.002	0.006	0.022	0.170	0.670		0.289	0.289
P (Cl)	0.289	0.101	0.119	0.152	0.216	0.247	0.934	0.724		1
Pr (H)	0.289	0.101	0.119	0.152	0.216	0.385	0.804	0.724	1	

Table 10. *p* values of a Mann-Whitney U test on PC 1 (upper right) and PC 2 (lower left) of the metatarsal.

	G	WBG	LWB	HWB	F	MTL	MTH	L (Cl)	P (Cl)	B (Cl)	B (Ba)	Pr (H)
G		0.092	0.027	0.027	0.026	0.132	0.027	0.057	0.540	0.081	0.149	0.105
WBG	0.356		0.733	0.020	<0.001	0.007	0.027	<0.001	0.584	<0.001	0.005	0.001
LWB	0.104	<0.001		0.003	<0.001	0.037	0.009	<0.001	0.583	0.001	0.011	0.005
HWB	0.134	0.007	0.727		0.032	<0.001	0.683	0.452	0.862	0.434	0.503	0.311
F	0.955	0.139	0.003	0.018		<0.001	<0.001	0.422	0.117	0.865	0.616	0.908
MTL	0.177	<0.001	<0.001	<0.001	0.015		<0.001	<0.001	0.133	0.001	0.010	0.003
MTH	0.255	<0.001	<0.001	<0.001	0.034	0.478		0.018	1	0.013	0.069	0.026
L (Cl)	0.306	0.500	0.540	0.60	0.194	<0.001	<0.001		0.190	0.144	0.172	0.299
P (Cl)	0.540	0.715	0.291	0.488	0.934	0.133	0.119	1		0.242	0.371	0.289
B (Cl)	0.561	0.938	0.226	0.255	0.396	0.002	0.004	0.626	1		1	0.713
B (Ba)	0.773	1	0.207	0.339	0.681	0.010	0.010	1	1	0.766		0.112
Prs (H)	0.817	0.027	0.026	0.021	0.727	0.003	0.026	0.219	0.289	0.903	0.860	

Table 11. *p* values of a Mann-Whitney U test on PC 1 (upper right) and PC 2 (lower left) of the forefoot proximal phalanges.

	G	WBG	LWB	HWB	F	MTL	MTH	L (Cl)	P (Cl)	B (Cl)	B (Ba)	Pr (H)
G		0.134	0.025	0.034	0.027	0.695	0.039	0.081	0.245	0.105	0.245	0.067
WBG	0.134		0.475	0.179	<0.001	0.009	0.466	0.047	0.765	0.021	0.168	<0.001
LWB	0.105	0.534		0.007	<0.001	0.004	0.285	0.009	0.317	0.005	0.049	<0.001
HWB	0.203	0.701	0.426		0.097	<0.001	0.225	0.490	0.799	0.533	0.671	0.125
F	0.753	<0.001	<0.001	0.002		<0.001	0.001	0.127	0.027	0.640	0.571	0.243
MTL	0.896	<0.001	<0.001	<0.001	0.063		0.011	0.004	0.050	0.008	0.050	0.002
MTH	0.465	<0.001	<0.001	<0.001	0.039	0.541		0.308	0.842	0.227	0.55	0.001
L (Cl)	0.847	0.001	0.005	0.002	0.280	0.213	0.012		0.175	0.270	0.847	0.008
P (Cl)	0.699	0.082	0.120	0.107	0.753	0.090	0.028	0.081		0.105	0.245	0.067
B (Cl)	0.817	0.011	0.021	0.011	0.469	0.034	0.003	0.066	0.817		0.105	0.014
B(Ba)	0.699	0.027	0.058	0.034	0.488	0.514	0.207	0.333	0.245	0.247		0.617
Prs (H)	0.868	<0.001	0.002	<0.001	0.243	0.273	0.019	0.523	0.067	0.014	0.067	

Table 12. *p* values of a Mann-Whitney U test on PC 1 (upper right) and PC 2 (lower left) of the hindfoot proximal phalanges.

	G	WBG	LWB	HWB	F	MTL	MTH	L (Cl)	P (Cl)	B (Cl)	B (Ba)	Pr (H)
G		0.168	0.020	0.031	0.027	0.188	0.028	0.081	0.245	0.105	0.245	0.067

WBG	0.309		0.957	0.188	<0.001	0.119	0.326	0.002	0.208	0.002	0.027	<0.001
LWB	0.087	0.447		0.017	<0.001	0.113	0.110	0.006	0.298	0.003	0.056	<0.001
HWB	0.062	0.026	0.036		0.108	0.003	0.199	0.541	0.709	0.582	0.709	0.056
F	0.051	<0.001	0.002	0.459		<0.001	0.002	0.970	0.068	0.371	0.753	0.067
MTL	0.884	0.056	0.004	<0.001	0.001		0.031	0.006	0.057	0.011	0.057	0.003
MTH	0.842	0.008	<0.001	<0.001	<0.001	0.280		0.085	0.642	0.054	0.163	0.002
L (Cl)	0.081	<0.001	<0.001	0.001	<0.001	0.006	0.015		0.175	0.270	0.847	0.036
P (Cl)	0.245	0.027	0.020	0.031	0.027	0.057	0.097	0.561		0.105	0.245	0.067
B (Cl)	0.105	0.002	0.001	0.003	0.003	0.011	0.054	0.391	0.105		0.105	0.456
B(Ba)	0.245	0.027	0.020	0.031	0.027	0.057	0.054	0.333	0.245	0.247		0.067
Prs (H)	0.067	<0.001	<0.001	<0.001	<0.001	0.003	0.019	0.315	0.617	0.241	0.243	

Table 13. *p* values of a Mann-Whitney U test on PC 1 (upper right) and PC 2 (lower left) of key ratios (Table 3).

	G	WBG	LWB	HWB	F	MTL	MTH	L (Cl)	P (Cl)
G		0.460	0.201	0.740	0.210	0.240	0.097	0.540	0.540
WBG	0.559		0.190	0.058	<0.001	<0.001	<0.001	0.539	0.342
LWB	0.227	0.190		0.011	<0.001	<0.001	<0.001	0.961	0.347
HWB	0.054	<0.001	0.004		0.007	0.016	0.005	0.335	0.248
F	0.044	<0.001	0.001	0.597		0.942	0.814	0.115	0.115
MTL	0.151	0.380	0.987	0.076	0.034		0.749	0.175	0.175
MTH	0.039	<0.001	<0.001	0.203	0.207	0.006		0.177	0.177
L (Cl)	0.540	0.105	0.102	0.123	0.115	0.175	0.123		1
P (Cl)	0.540	0.105	0.151	0.335	0.207	0.175	0.441	1	

Table 14. *p* values from Mann-Whitney U tests comparing principal components of Cervidae versus Bovidae. Cells are shaded where $p < 0.05$, indicating the test rejects the null hypothesis that the PC values of cervids and bovids sample the same distribution.

Element	PC 1	PC 2
Humerus	0.865	0.054
Distal Humerus	0.905	0.003
Radius	0.741	<0.001
Femur	0.610	0.002
Metatarsal	0.418	0.046
Forefoot Proximal Phalanx	0.485	<0.001
Hindfoot Proximal Phalanx	0.841	<0.001
Ratios	0.028	0.018

Table 15. Equations, *r*, and r^2 values of linear regressions where y is the natural logarithim of species average body mass in kilograms (Table 1) and x is principal components 1 or 2 from each analysis. Cells are shaded where r > 0.8, thus indicating strong correlation between body size and principal components.

Element	x =	Regression	*r*	r^2
Humerus	PC 1	y = 0.7206x + 3.2568	0.96	0.92
	PC 2	y = 0.3377x + 3.2737	0.04	<0.01
Distal Humerus	PC 1	y = 1.1482x + 3.222	0.96	0.92
	PC 2	y = 0.6674x + 3.2723	0.06	<0.01
Radius	PC 1	y = 0.8433x + 3.2591	0.95	0.91
	PC 2	y = -0.1136x + 3.2992	0.01	<0.01
Femur	PC 1	y = 0.7581x + 3.243	0.95	0.89
	PC 2	y = 0.81x + 3.2666	0.13	0.02
Metatarsal	PC 1	y = 0.7405x + 3.2316	0.92	0.85
	PC 2	y = -0.049x + 3.3264	0.02	<0.01
Forefoot Proximal Phalanx	PC 1	y = 0.7697x + 3.1872	0.92	0.86
	PC 2	y = 0.4978x + 3.2947	0.13	0.02
Hindfoot Proximal Phalanx	PC 1	y = 0.9099x + 3.1348	0.92	0.85
	PC 2	y = 2.7043x + 3.4247	0.43	0.19
Ratios	PC 1	y = 0.0099x + 3.3083	0.04	<0.01
	PC 2	y = -0.3137x + 3.2891	0.61	0.37

Table 16. Estimated body size in kg of fossil blastomerycines based on linear regressions (Table 15). H= humerus, d H= distal humerus, R= radius, F= femur, Av.= mean estimate.

Specimen No.		Species	NALMA	Estimated Size (kg)				
				H	**d H**	**R**	**F**	**Av.**
AMNH	13822	*Problastomeryx primus*	Hemingfordian				12.7	12.7
F:AM	144683	*Problastomeryx primus*	Hemingfordian		9.0			9.0
F:AM	144681	*Blastomeryx gemmifer*	Barstovian			12.5		12.5
F:AM	54716	*Blastomeryx* sp.	Clarendonian			10.0		10.0
F:AM	54722	*Blastomeryx* sp.	Clarendonian		12.3			12.3
F:AM	54701a	*Longirostromeryx* sp.	Clarendonian		13.3			13.3
F:AM	54701b	*Longirostromeryx* sp.	Clarendonian		17.4			17.4
F:AM	54682	*Longirostromeryx* sp.	Clarendonian	13.7	11.8			12.7
F:AM	54684	*Longirostromeryx* sp.	Clarendonian			15.4		15.4

F:AM	54703	*Longirostromeryx* sp.	Clarendonian				17.4	17.4
F:AM	54706	*Longirostromeryx* sp.	Clarendonian	14.3	12.7			13.5
F:AM	54708	*Longirostromeryx* sp.	Clarendonian				16.3	16.3
F:AM	54684c	*Longirostromeryx* sp.	Clarendonian			14.4		14.4
F:AM	54684d	*Longirostromeryx* sp.	Clarendonian			14.7		14.7
F:AM	54703a	*Longirostromeryx* sp.	Clarendonian				15.5	15.5
F:AM	31729	*Longirostromeryx blicki*	Clarendonian			14.5		14.5
F:AM	54726	*L. clarendonensis*	Clarendonian		13.0			13.0
F:AM	54726b	*L. clarendonensis*	Clarendonian		12.6			12.6
UNSM	125572	*Longirostromeryx wellsi*	Clarendonian		11.6	14.6	15.8	14.0
UNSM	27831	*Longirostromeryx wellsi*	Clarendonian	13.1	13.7	15.0		13.9
UNSM	133126	*Longirostromeryx wellsi*	Clarendonian			15.4		15.4
UNSM	133127	*Longirostromeryx wellsi*	Clarendonian			15.4		15.4
F:AM	31360	*Parablastomeryx gregorii*	Clarendonian	20.3	18.3	25.3	24.4	22.1

Table 17. Measurements from UNSM 125572 (for measurement standards, see Von Driesch, 1976).

Bone, side	Dimension	Measurement (mm)
Cranium, left		
	Length of cheektooth row	43.2
	Length of molar row	28.1
	Length of premolar row	15.5
	Greatest inner length of orbit	32.1
	Greatest inner height of orbit	26.2
Mandible, left		
	Length from angle	154.3
	Length from condyle	155.7
	Gonion caudale length	42.0
	Length of horizontal ramus	122.5
	Middle height of vertical ramus	48.6
	Oral height of vertical ramus	72.8
	Length of cheektooth row	47.4
	Length of molar row	34.1
	Length of premolar row	13.3
	Length of diastema	62.0
Vertebrae		

	Greatest length, Cervical 1	28.4
	Breadth over wings, Cervical 1	33.5
	Length of corpus and dens, Cervical 2	49.8
	Breadth of cranial articular surface, Cervical 2	24.0
	Greatest length, Cervical 3	40
	Greatest length, Cervical 4	39
	Greatest length, Cervical 5	37
	Greatest length, Cervical 6	31
	Greatest length, Cervical 7	25
	Physiological length of the body, Lumbar 3	23
	Physiological length of the body, Lumbar 4	24
	Physiological length of the body, Lumbar 5	25
	Physiological length of the body, Lumbar 6	23
	Combined length of caudal vertebrae	149
Ribs		
	Greatest length, Rib 1	59
	Greatest length, longest rib	130
Sternum		
	Greatest length, manubrium	23.8
	Greatest length, xiphoid process	38.2
Sacrum		
	Physiological length	71.6
	Greatest length on the ventral side	79.6
	Greatest breadth	64.4
Scapula, right		
	Breadth of the glenoid cavity	12.5
	Length of the glenoid cavity	14.5
Humerus, left		
	Breadth of trochlea	19.3
Ulna, left		
	Greatest length	146
	Length of olecranon	25.6
Radius, left		
	Greatest length	126.3
	Breadth of proximal end	18.6
	Depth of proximal end	10.3
	Breadth of distal end	17.3
	Depth of distal end	13
	Breadth of mid-shaft	13.8
	Depth of mid-shaft	7.8
Metacarpal, left		
	Greatest length	126
	Breadth of proximal end	16

	Depth of proximal end	12
Proximal phalanx, left forefoot		
	Greatest length, digit 3	26.6
Intermediate phalanx, left forefoot		
	Greatest length, digit 3	17.1
Distal phalanx, left forefoot		
	Greatest length of sole, digit 4	18.2
Innominate, right		
	Greatest length of one half	151
	Length of symphysis	40
	Length of acetabulum on the rim	19
Femur, left		
	Greatest length	147.6
	Greatest length from head	142.3
	Breadth of proximal end	32
	Depth of head	15.2
	Breadth of distal end	27.2
	Depth of distal end	35.8
	Breadth of mid-shaft	11.7
	Depth of mid-shaft	13.8
Patella, left		
	Greatest length	19.7
	Greatest breadth	16.1
Tibia, left		
	Greatest length	176
	Breadth of proximal end	27.7
	Depth of proximal end	31
	Breadth of distal end	21.5
	Depth of distal end	14
Astragalus, left		
	Greatest length of lateral side	20.9
	Depth of lateral side	10.1
	Greatest length of medial side	20.0
Calcaneum, left		
	Greatest length	46.3
	Greatest breadth	15.3
Metatarsal, left		
	Greatest length	137.3
	Breadth of proximal end	15.7
	Depth of proximal end	16.5
Proximal phalanx, right hindfoot		
	Greatest length, digit 3	29.9
Intermediate phalanx, right hindfoot		

Greatest length, digit 3	17.3
Distal phalanx, right hindfoot	
Greatest length of sole, digit 3	19.6

Table 18. Indices of some dimensions of the UNSM 125572 *L. wellsi* skeleton. *Indicates data supplemented by UNSM 27831.

Index name	**Definition**	**Index value**
Intermembral index	(humerus + radius) x 100 / (femur + tibia)	74.0*
Brachial index	radius x 100 / humerus	111.5*
Crural index	tibia x 100 / femur	119.2
Tibioradial index	radius x 100 / tibia	71.8
Femorometatarsal index	metatarsal x 100 / femur	93.0
Olecranon-ulnar index	olecranon x 100 / (ulna – olecranon)	21.3
Femur robustness index	mid-shaft breadth x 100 / femur	7.9
Radial robustness index	mid-shaft breadth x 100 / radius	10.9

FIGURES

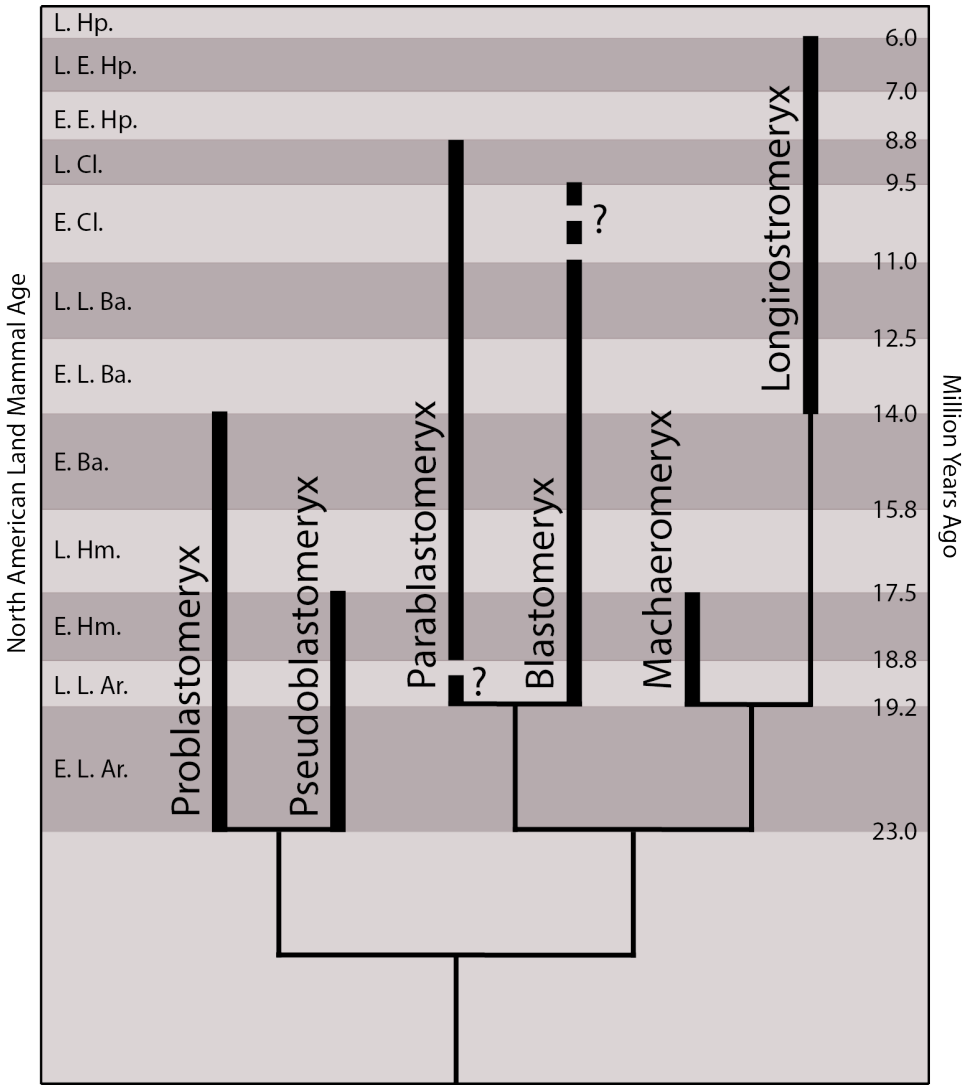

Figure 1. Range of blastomerycine genera indicated by thick bars; phylogenetic hypothesis, based on that of Webb (1998), indicated by thin lines; ranges in terns of North American Land Mammal Ages (NALMA) where E.= early, L.= late, Ar.= Arikareean, Hm.= Hemingfordian, Ba.= Barstovian, Cl.= Clarendonian, Hp.= Hemphillian; modified from Webb (1998).

Figure 2–9. Scatterplot representations of the principal component analyses on fossil and modern taxa, overlain by centroid values for each group (Appendix F). Error bars represent two standard errors of the centroid.

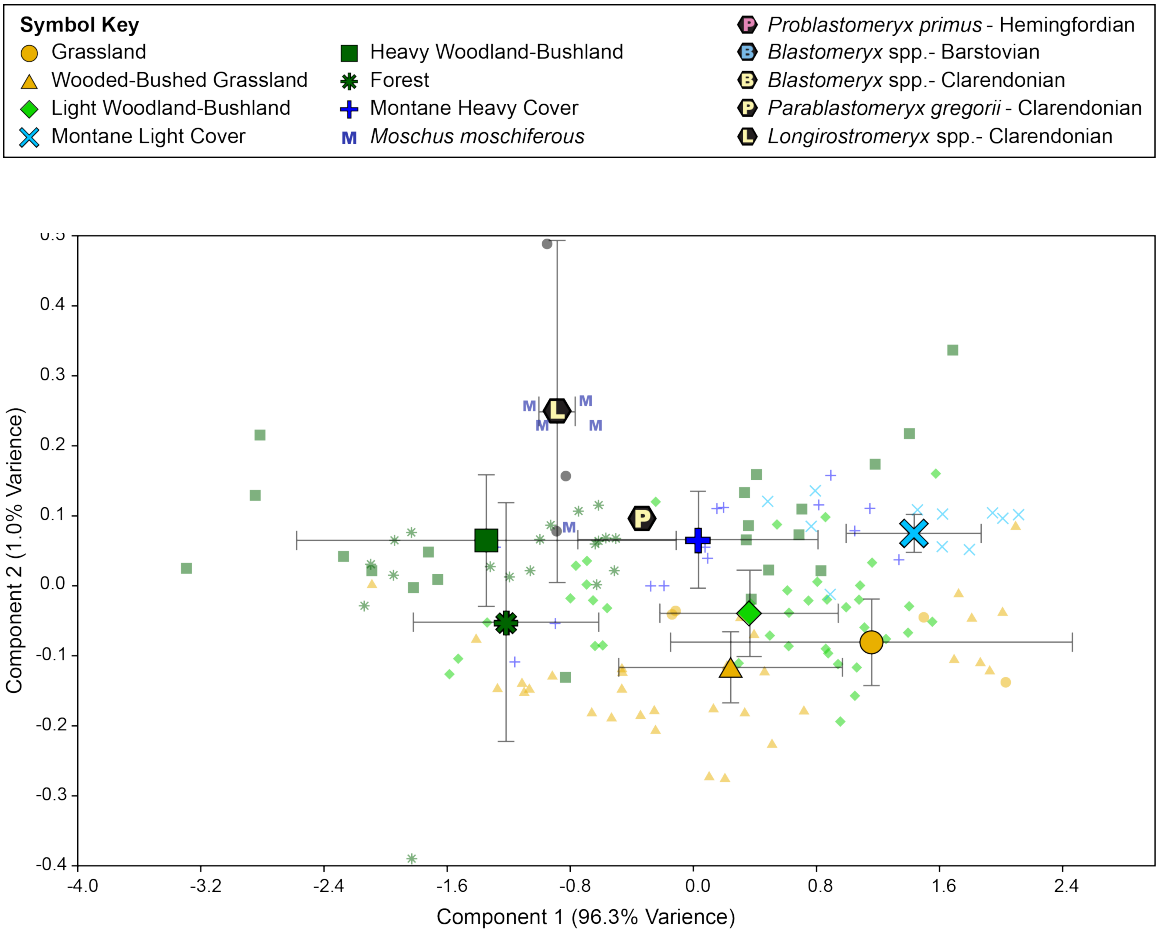

Figure 2. Components 1 and 2 of the humerus.

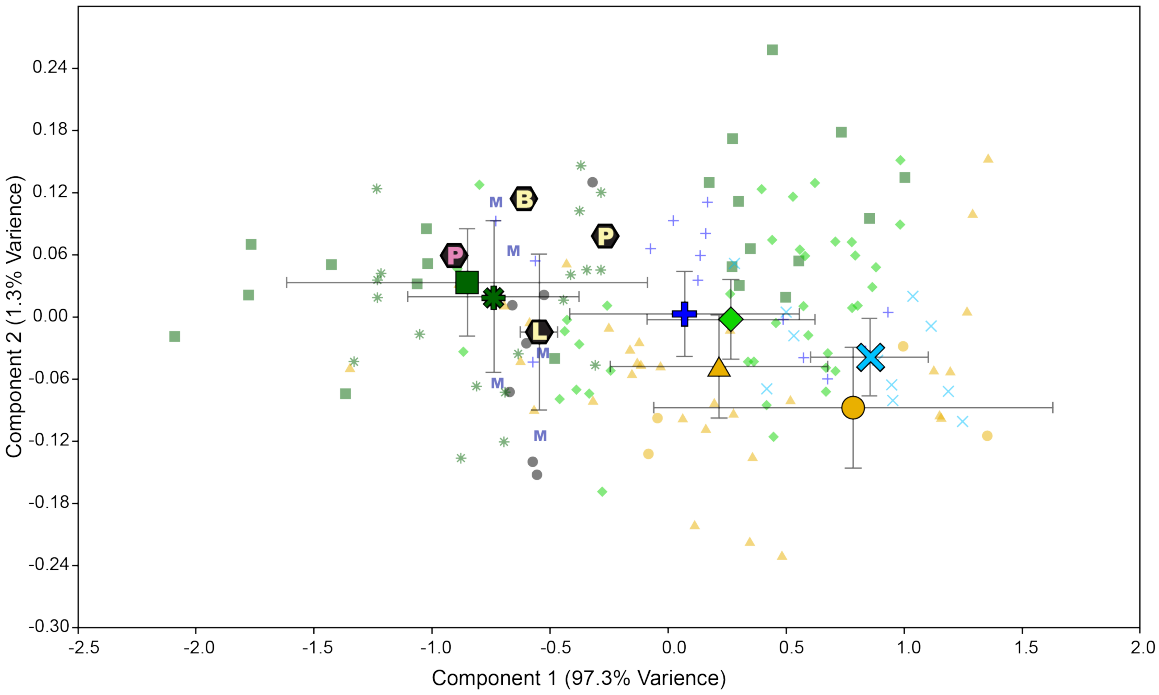

Figure 3. Components 1 and 2 of the distal humerus.

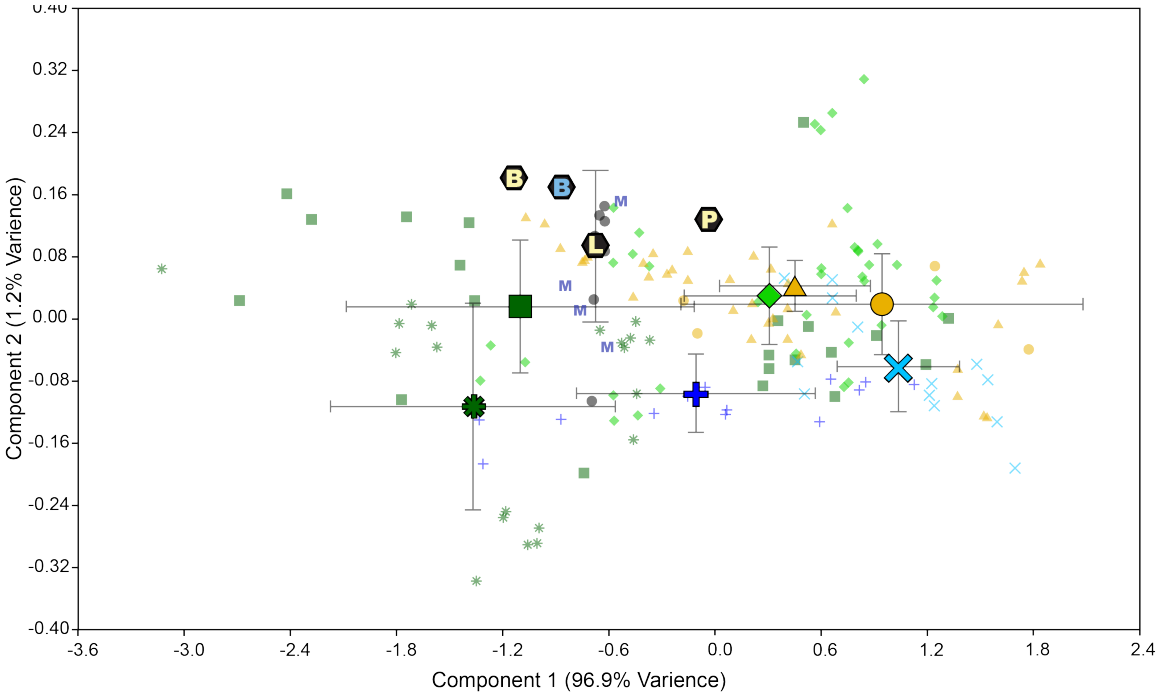

Figure 4. Components 1 and 2 of the radius.

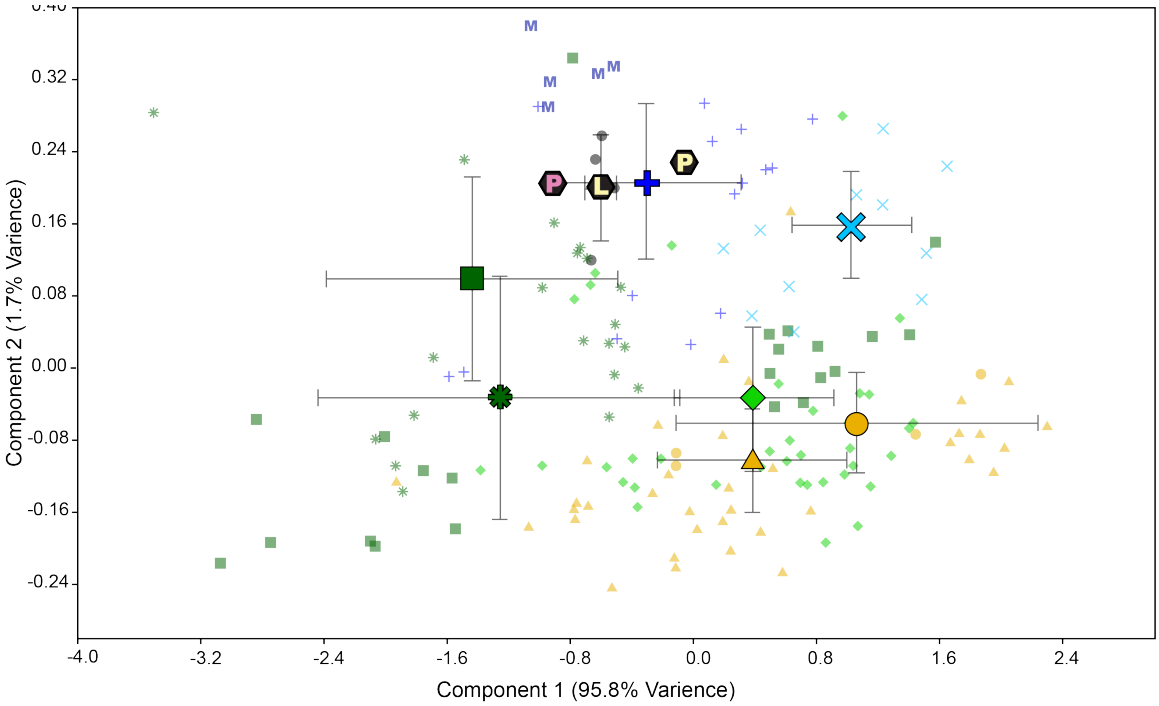

Figure 5. Components 1 and 2 of the femur.

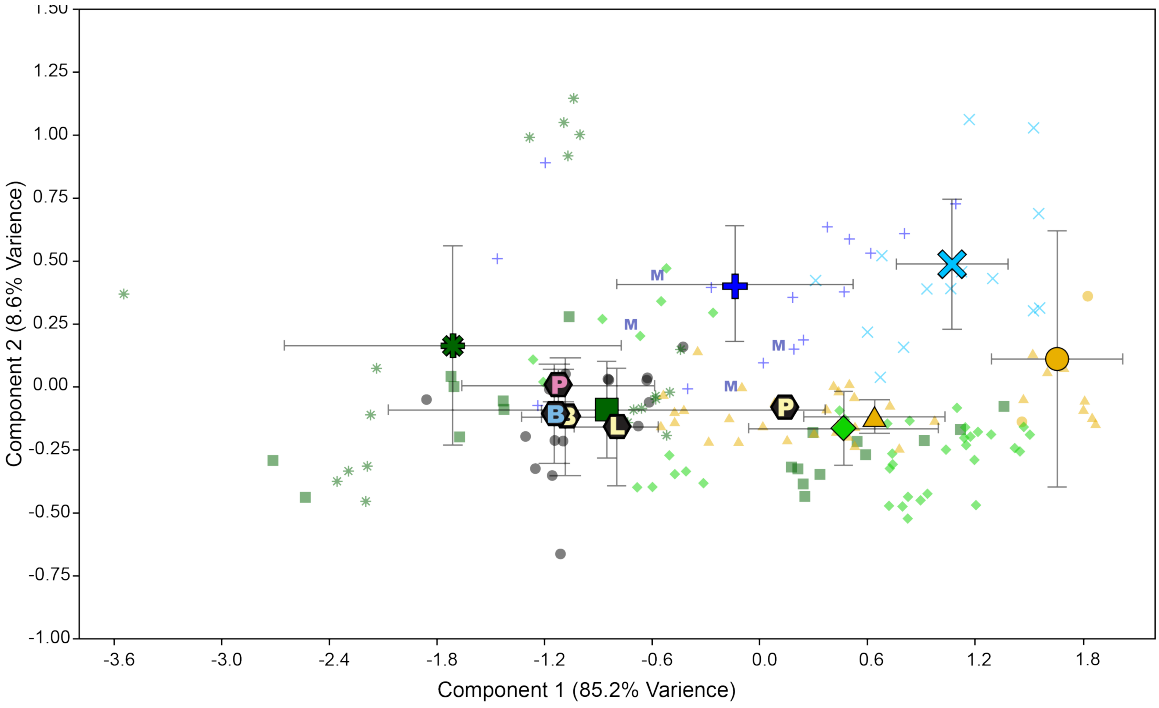

Figure 6. Components 1 and 2 of the metatarsal.

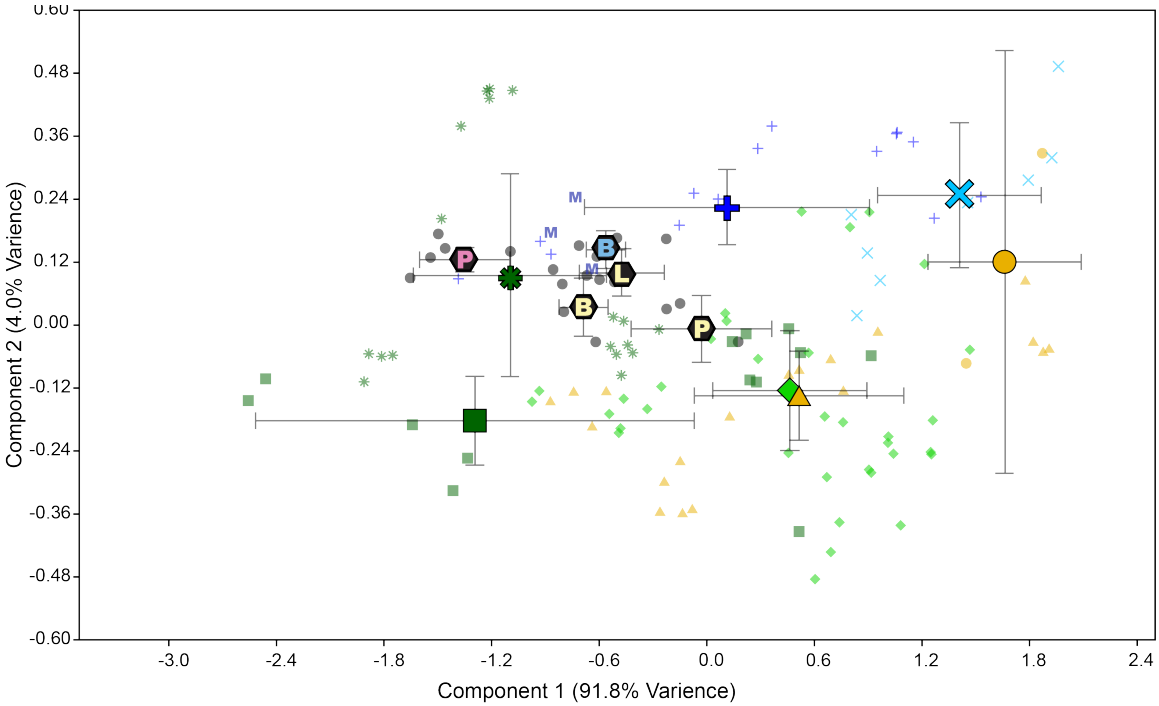

Figure 7. Components 1 and 2 of the forefoot proximal phalanges.

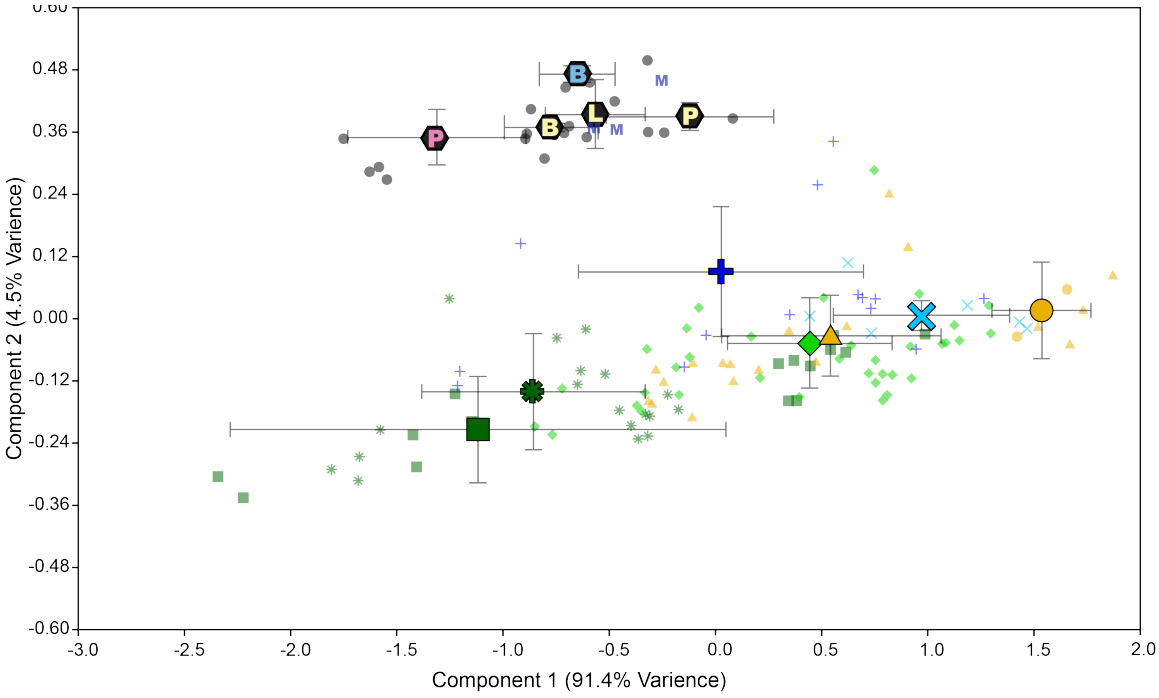

Figure 8. Components 1 and 2 of the hindfoot proximal phalanges.

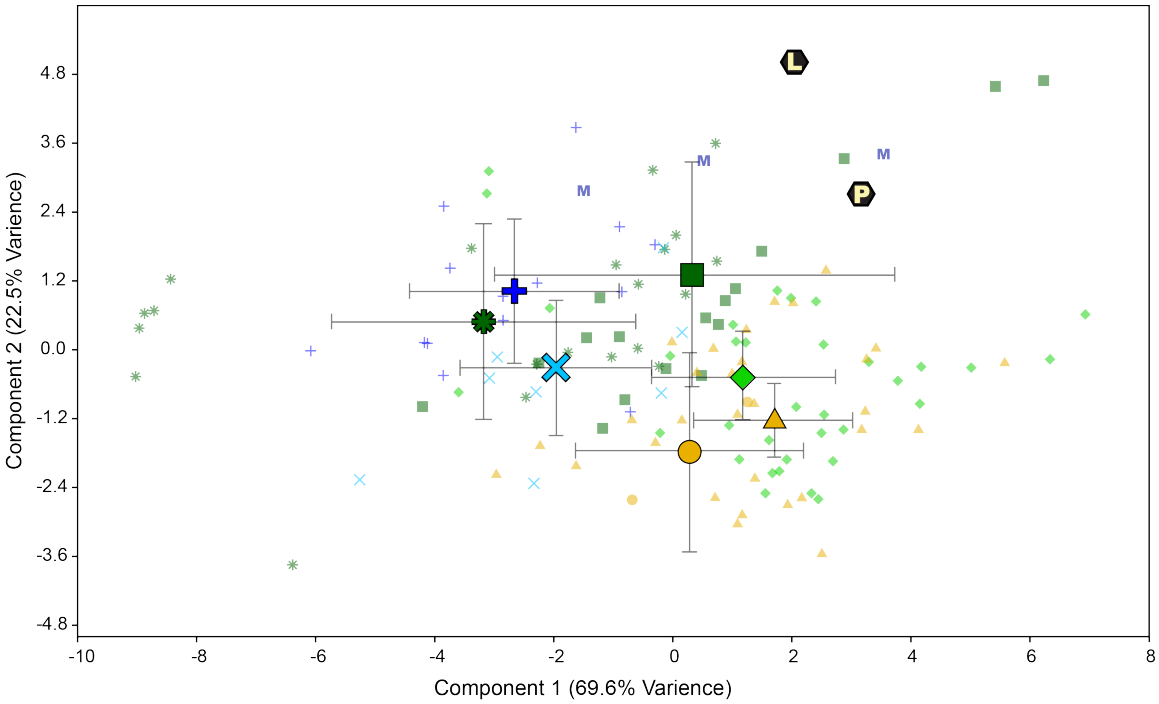

Figure 9. Components 1 and 2 of intermembral ratios.

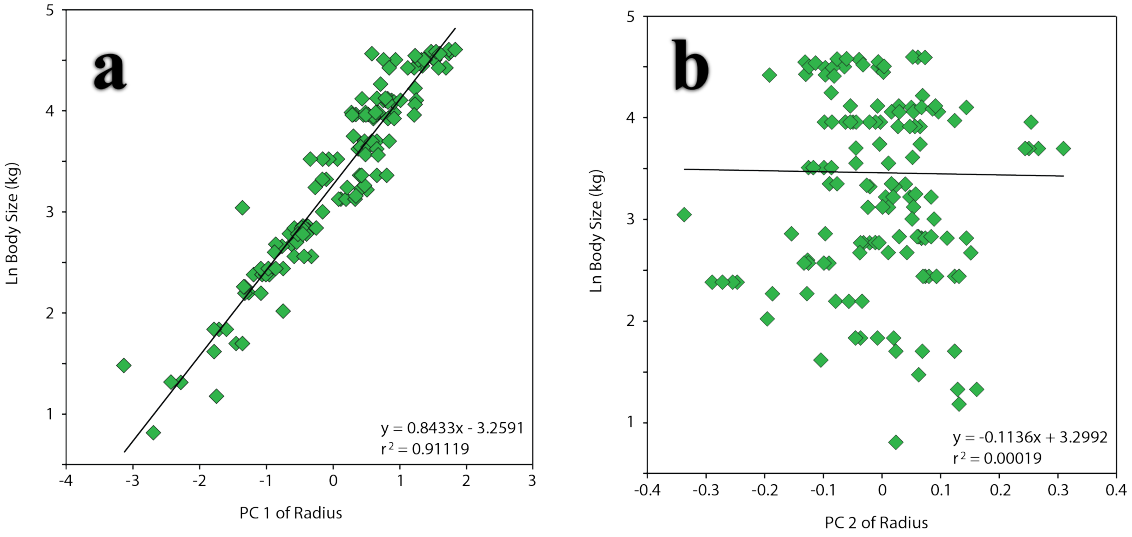

Figure 10. For each radius of extant specimens, the natural logarithim of species average body mass versus (a) principal component 1, and (b) principal component 2, using the same PCA data as Figure 4 and body size data as Table 1.

Figure 11. A photograph of the original UNSM 125572 specimen preserved in matrix in its field jacket. Photograph by Jason Head.

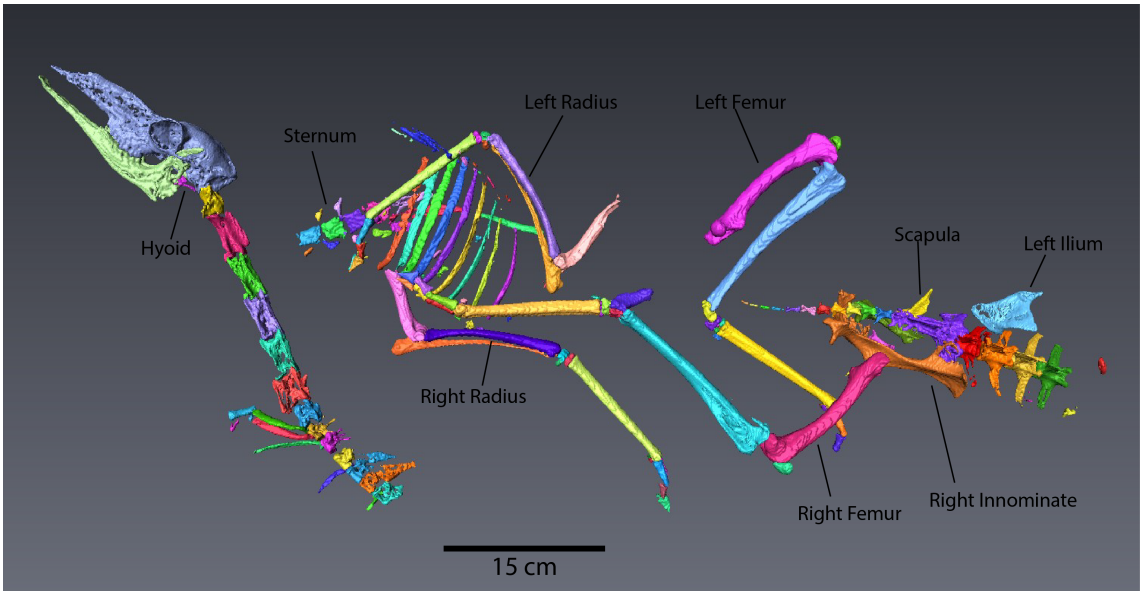

Figure 12. Digital rendering of the CT scanned L. wellsi skeleton, UNSM 125572, from Ashfall Fossil Beds State Historical Park, NE. Image captured in Avizo 8.0.

Figure 13. Left view of UNSM 125572 skull in matrix. Photograph by Jason Head.

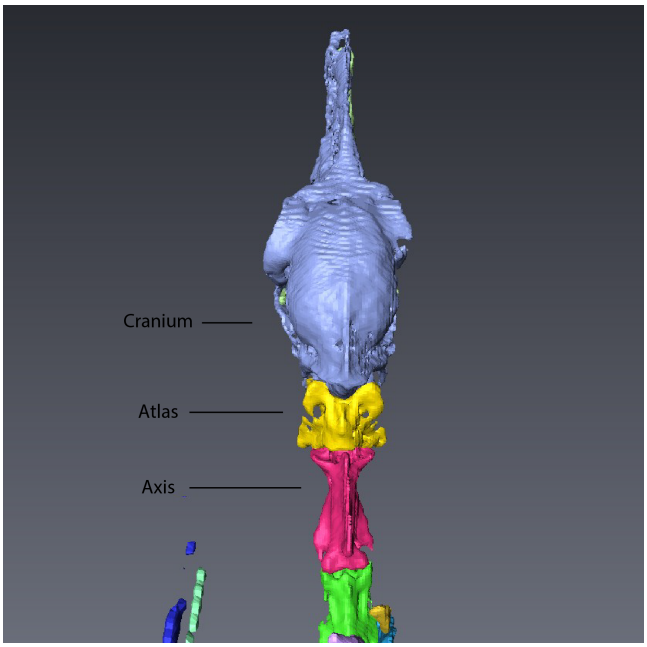

Figure 14. Dorsal posterior view of UNSM 125572 cranium.

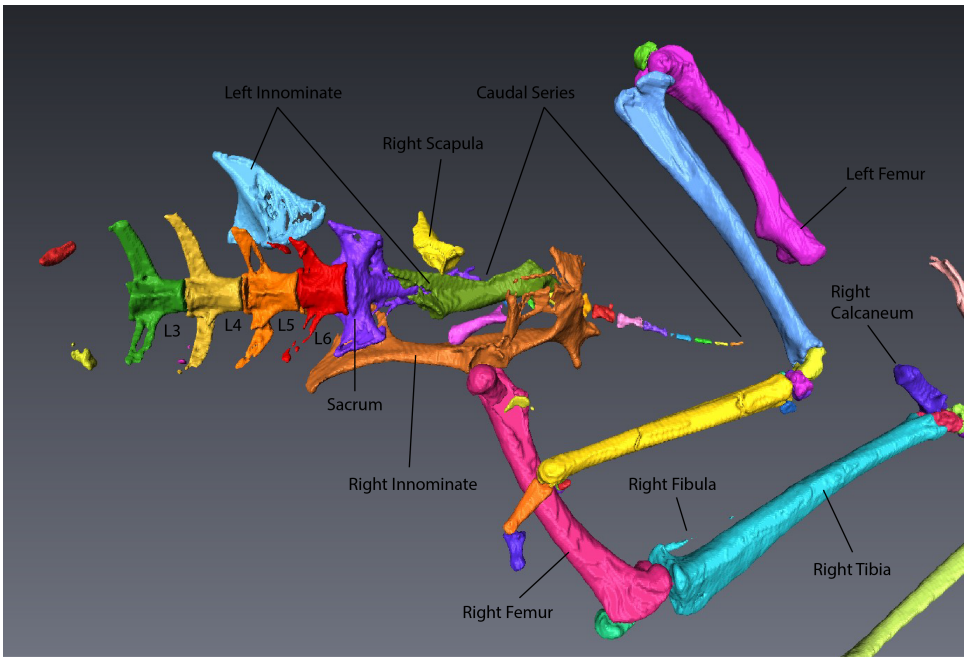

Figure 15. Ventral view of UNSM 125572 lumbar vertebrae and sacrum.

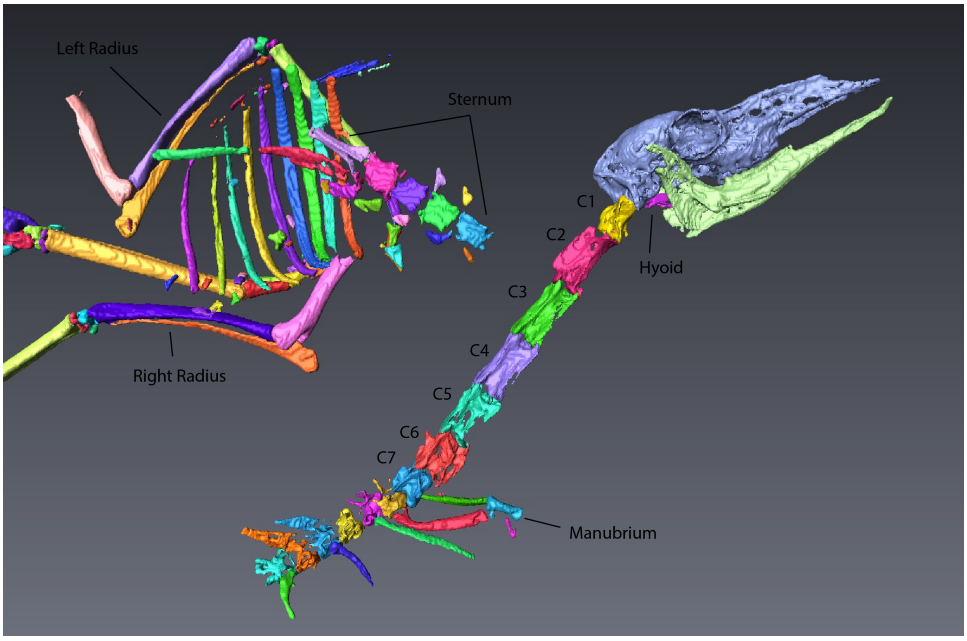

Figure 16. Right side of UNSM 125572 head and neck.

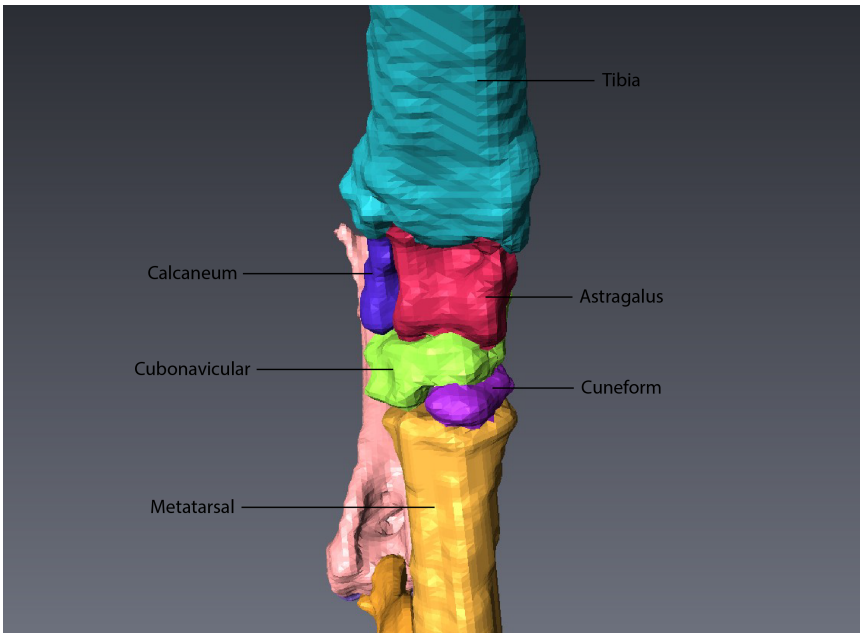

Figure 17. Dorsal anterior view of UNSM 125572 right ankle.

APPENDICES

APPENDIX A: MEASUREMENTS

Linear measurements of bones—humerus (H), radius (R), femur (F), metatarsal (MT), proximal phalanx (Pa), and calcaneum (C)—used in principal components analyses. Codes defined and described in Table 2. Modified from Kovarovic (2004).

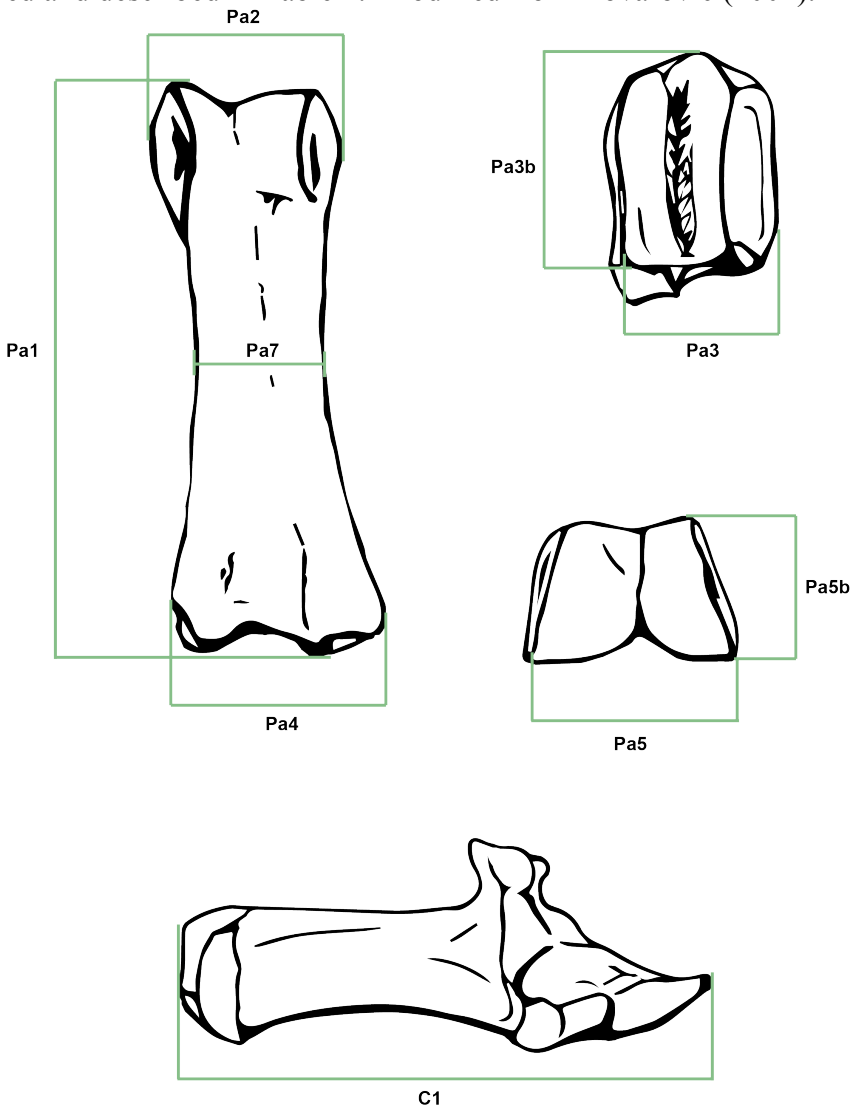

Not shown: Pa6 (anterior-posterior mid-shaft diameter)

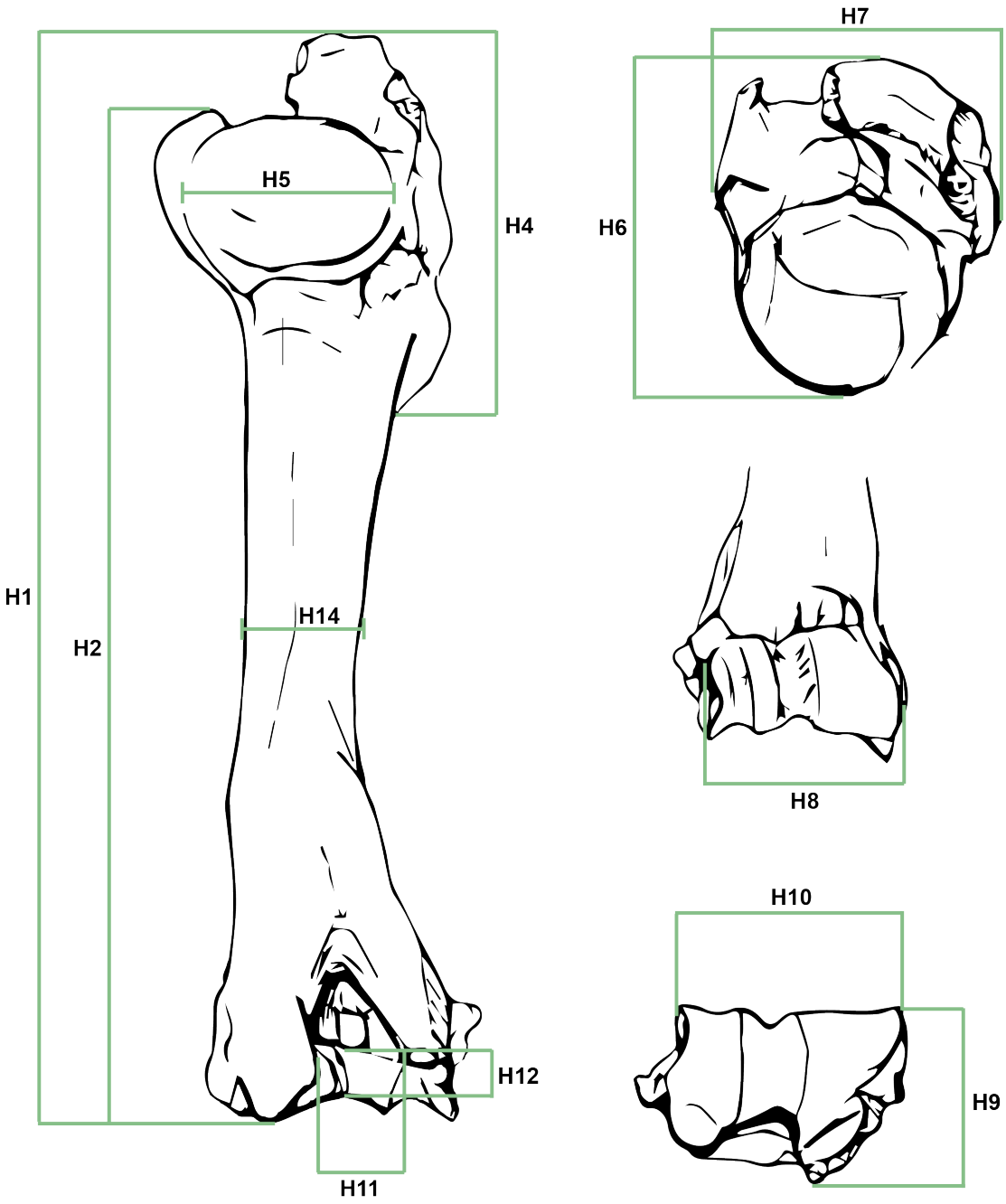

Not shown: H13 (anterior-posterior mid-shaft diameter)

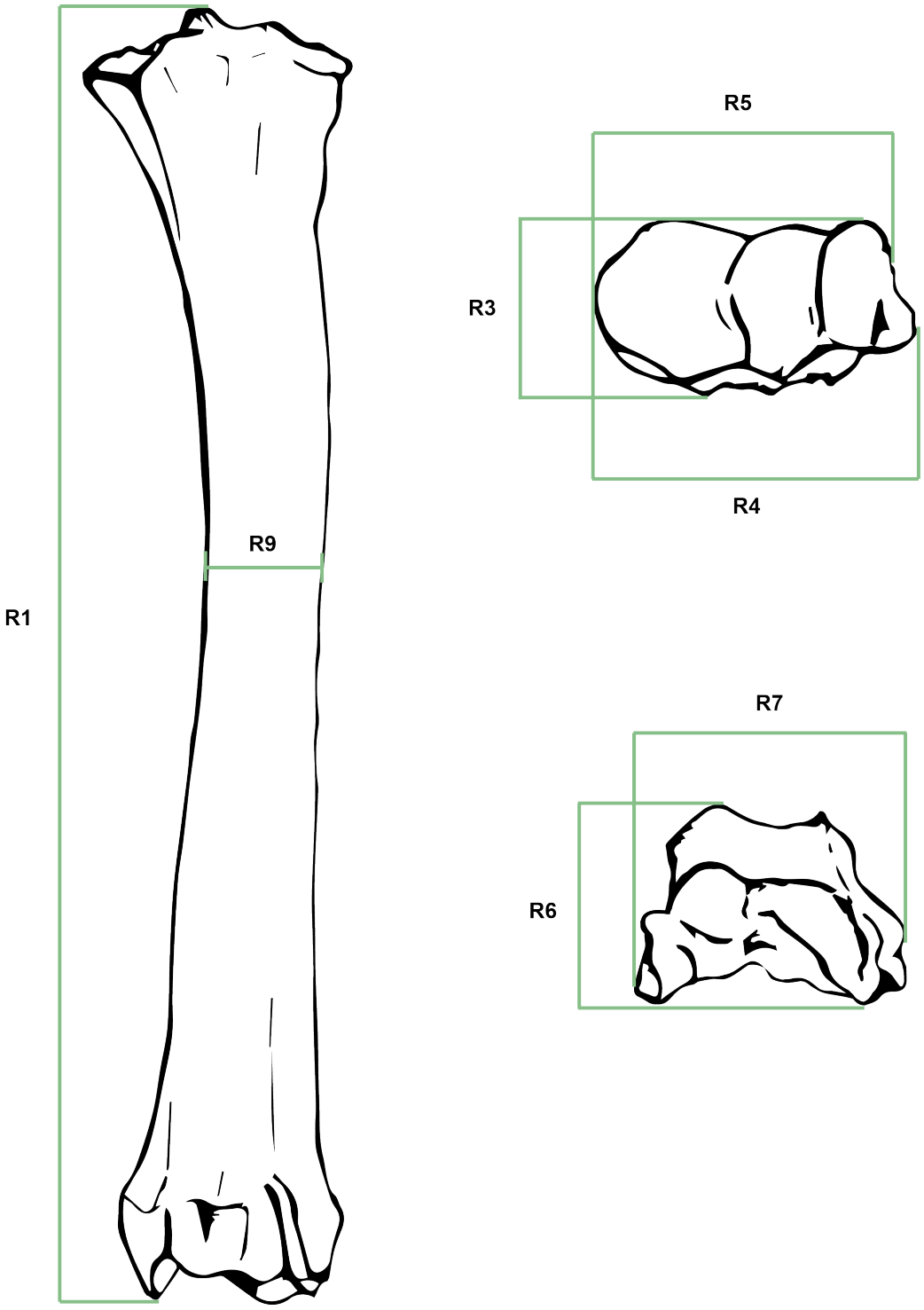

Not shown: R8 (anterior-posterior mid-shaft diameter)

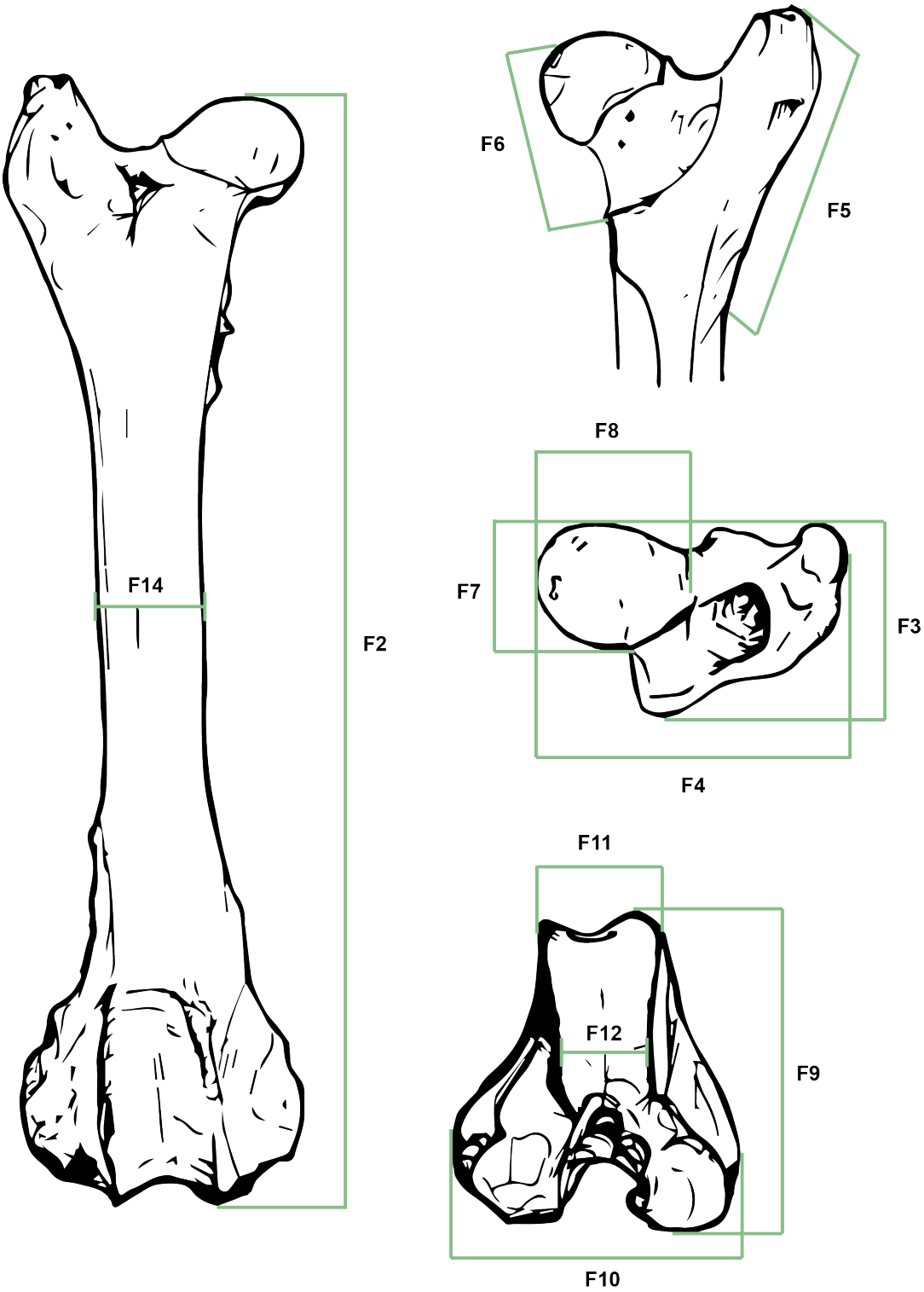

Not shown: F13 (anterior-posterior mid-shaft diameter)

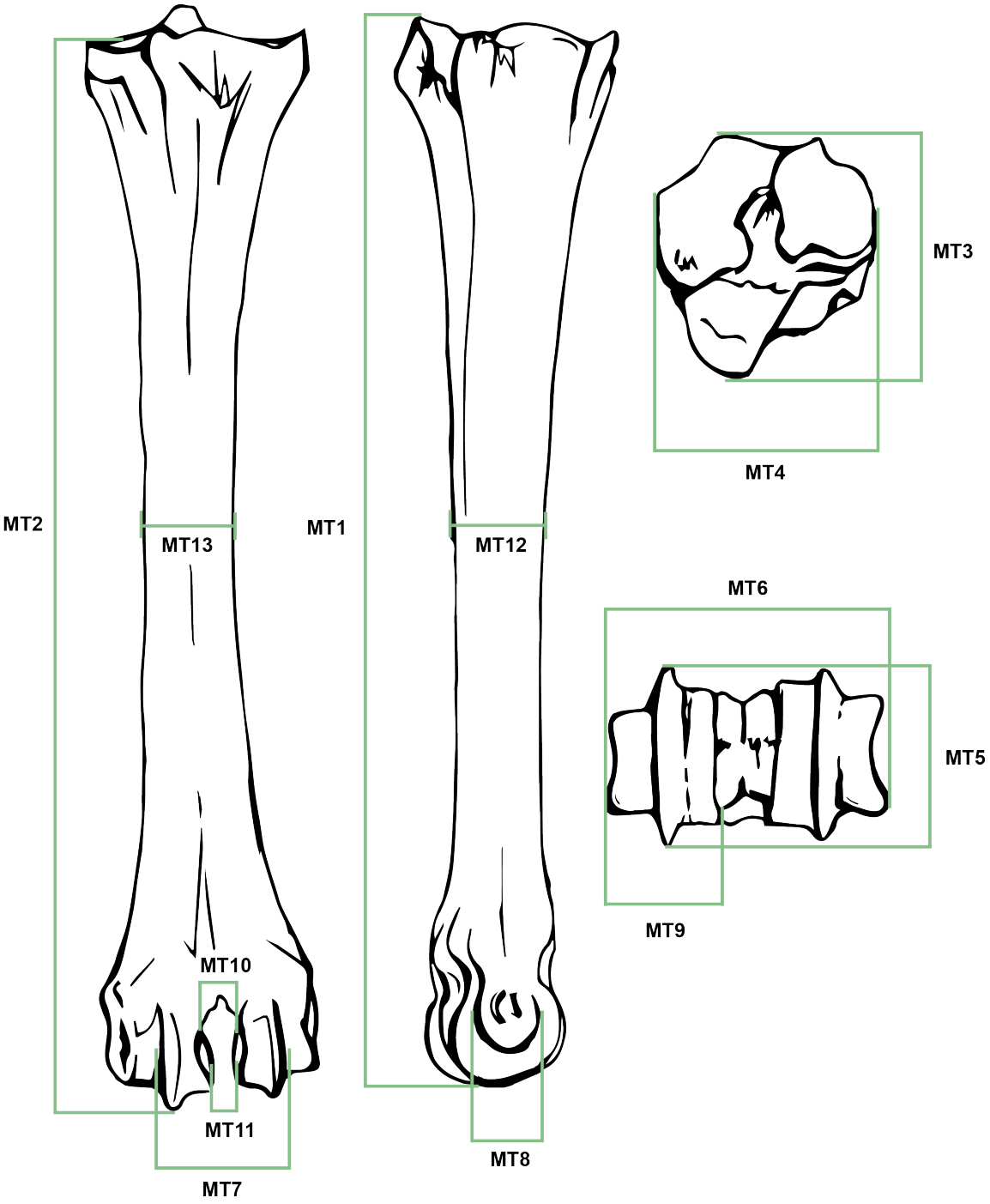
MT2
MT13
MT10
MT11
MT7
MT1
MT12
MT8
MT3
MT4
MT6
MT5
MT9

APPENDIX B: MODERN SPECIMENS

Modern sample of artiodactyls measured by Kris Kovarovic (KK) or Katheryn Chen (KC). Specimens come from the American Museum of Natural History (AMNH), University of Nebraska State Museum (UNSM), Smithsonian Institution National Museum of Natural History (USNM), the Natural History Museum in London, Powell-Cotton Museum (PC), and Museum of Vertebrate Zoology (MVZ). The sample includes wild-caught adult artiodactyls, except where indicated as zoo specimens. Average weight for species of is derived from the literature: Kovarovic and Andrews (2007), Nowak (1999), and University of Michigan's Animal Diversity Web (http://animaldiversity.org).

Collector	Collection	Number	Species	Avg. Weight	Sex	Zoo
KK	AMNH	113812	*Addax nasomaculatus*	97.5	?	
KK	NHM	1967.11.8.1.	*Aepyceros melampus*	60	female	
KK	NHM	69.1142	*Aepyceros melampus*	60	female	
KK	NHM	1960.11.10.2	*Aepyceros melampus*	60	female	
KK	NHM	1932.6.6.32	*Aepyceros melampus*	60	male	
KK	NHM	1960.11.10.5	*Aepyceros melampus*	60	male	
KK	NHM	1960.11.10.2	*Aepyceros melampus*	60	female	
KK	NHM	1968.6.20.1	*Aepyceros melampus*	60	female	
KC	UNSM	ZM 5104	*Antilocapra americana*	53	?	
KC	UNSM	ZM 694	*Antilocapra americana*	53	female	
KK	AMNH	35957	*Antilope cervicapra*	35	male	
KK	AMNH	54486	*Antilope cervicapra*	35	male	
KK	USNM	USNM 062092	*Capra sibirica*	82.5	female	
KK	USNM	USNM 062093	*Capra sibirica*	82.5	male	
KK	USNM	USNM 020409	*Capra sibirica*	82.5	male	
KC	UNSM	ZM 15509	*Cephalophus dorsalis*	21	?	
KK	NHM	1950.9.23.1	*Cephalophus leucogaster*	17.5	male	
KK	PC	MERFIELD 891	*Cephalophus leucogaster*	17.5	female	
KK	AMNH	34736	*Cephalophus monticola*	6.25	male	
KK	NHM	1936.10.28.28	*Cephalophus monticola*	6.25	male	
KK	NHM	1936.10.28.29	*Cephalophus monticola*	6.25	male	
KK	NHM	1936.10.28.30	*Cephalophus monticola*	6.25	female	
KK	NHM	1936.10.28.31	*Cephalophus monticola*	6.25	female	
KK	AMNH	52943	*Cephalophus nigrifrons*	16	male	
KK	AMNH	52930	*Cephalophus nigrifrons*	16	female	
KK	AMNH	52940	*Cephalophus nigrifrons*	16	female	
KK	PC	MERFIELD 244	*Cephalophus nigrifrons*	16	male	
KK	PC	MERFIELD 342	*Cephalophus nigrifrons*	16	male	

KK	PC	MERFIELD 649	*Cephalophus nigrifrons*	16	male	
KC	UNSM	ZM-18673	*Dama dama*	70	female	
KK	NHM	70.345	*Damaliscus dorcas*	67.5	male	
KK	AMNH	88406	*Damaliscus hunteri*	99	male	
KK	AMNH	88408	*Damaliscus hunteri*	99	female	
KK	NHM	1938.7.11.1	*Damaliscus hunteri*	99	male	
KC	UNSM	ZM 30972	*Elaphodus cephalophus*	33.5	male	zoo
KC	UNSM	ZM 30973	*Elaphodus cephalophus*	33.5	female	zoo
KK	AMNH	114551	*Elaphodus cephalophus*	33.5	female	
KK	AMNH	115638	*Elaphodus cephalophus*	33.5	male	
KK	AMNH	84462	*Elaphodus cephalophus*	33.5	male	
KK	AMNH	84463	*Elaphodus cephalophus*	33.5	male	
KK	NHM	1939.2563	*Gazella cuvieri*	25	male	
KK	PC	ALGERIA 4	*Gazella cuvieri*	25	female	
KK	NHM	1936.9.5.2	*Gazella granti*	57.5	male	
KK	NHM	1935.12.14.2	*Gazella granti*	57.5	male	
KK	NHM	1936.3.28.10	*Gazella granti*	57.5	male	
KK	NHM	1936.9.5.3	*Gazella granti*	57.5	female	
KK	USNM	USNM 252685	*Gazella rufifrons*	25	male	
KK	USNM	USNM 252686	*Gazella rufifrons*	25	male	
KK	USNM	USNM 240693	*Gazella soemmerringi*	42	male	
KK	USNM	USNM 240691	*Gazella soemmerringi*	42	male	
KK	NHM	1936.12.13.3	*Gazella spekei*	20	male	
KK	NHM	1896.10.6.1	*Gazella spekei*	20	?	
KK	NHM	1897.1.14.6	*Gazella subgutturosa*	25.5	male	
KK	USNM	USNM 062088	*Gazella subgutturosa*	25.5	male	
KK	USNM	USNM 163048	*Gazella thomsonii*	22.5	male	
KK	USNM	USNM 162005	*Gazella thomsonii*	22.5	female	
KK	USNM	USNM 172903	*Gazella thomsonii*	22.5	male	
KK	USNM	USNM 163053	*Gazella thomsonii*	22.5	male	
KK	PC	MERFIELD 197	*Hyemoschus aquaticus*	10.85	female	
KK	PC	MERFIELD 403	*Hyemoschus aquaticus*	10.85	male	
KK	PC	MERFIELD 395	*Hyemoschus aquaticus*	10.85	male	
KK	PC	MERFIELD 577	*Hyemoschus aquaticus*	10.85	male	
KK	PC	CONGO 318	*Hyemoschus aquaticus*	10.85	female	
KK	USNM	USNM 252689	*Kobus kob*	90.5	male	
KK	USNM	USNM 163194	*Kobus kob*	90.5	male	
KK	USNM	USNM 163195	*Kobus kob*	90.5	male	
KK	USNM	USNM 163345	*Kobus kob*	90.5	female	
KK	USNM	USNM 164499	*Kobus kob*	90.5	female	

KK	NHM	69.1147	*Kobus leche*	95	male	
KK	AMNH	81170	*Litocranius walleri*	40	male	
KK	AMNH	88409	*Litocranius walleri*	40	male	
KK	AMNH	187829	*Litocranius walleri*	40	female	
KC	MVZ	122419	*Litocranius walleri*	40	?	
KK	NHM	1936.3.28.3	*Litocranius walleri*	40	male	
KK	NHM	1962.7.6.17	*Litocranius walleri*	40	male	
KK	NHM	1962.10.18.1	*Madoqua guentheri*	4.6	female	
KK	NHM	1936.5.28.2	*Madoqua kirki*	5.5	male	
KK	NHM	1932.6.6.49	*Madoqua kirki*	5.5	female	
KK	NHM	1932.6.6.51	*Madoqua kirki*	5.5	female	
KK	NHM	1932.6.6.46	*Madoqua kirki*	5.5	female	
KK	NHM	1869.2.2.10	*Madoqua saltiana*	3.25	female	
KC	AMNH	M-46405	*Moschus moschiferus*	14.5	male	
KC	AMNH	M-17951	*Moschus moschiferus*	14.5	male	
KC	AMNH	M-57078	*Moschus moschiferus*	14.5	male	
KC	AMNH	M-89032	*Moschus moschiferus*	14.5	female	
KC	AMNH	M-110500	*Moschus moschiferus*	14.5	female	
KC	UNSM	ZM 13423	*Muntiacus reevsi*	13.5	male	zoo
KK	AMNH	165683	*Naemorhedus crispus*	82.5	female	
KK	USNM	USNM 013829/A20934	*Naemorhedus crispus*	82.5	male	
KK	USNM	USNM 259023	*Naemorhedus goral*	28.5	female	
KK	USNM	USNM 259398	*Naemorhedus goral*	28.5	male	
KK	USNM	USNM 259399	*Naemorhedus goral*	28.5	female	
KK	USNM	USNM 311229	*Naemorhedus swinhoei*	95	female	
KK	NHM	1937.8.4.26	*Neotragus batesi*	3.75	male	
KK	NHM	1937.8.4.27	*Neotragus batesi*	3.75	female	
KK	NHM	1962.12.14.5	*Neotragus moschatus*	5	male	
KK	USNM	USNM 429835	*Neotragus pygmaeus*	2.25	male	
KK	USNM	USNM 567252	*Odocoileus virginianus*	90	male	
KK	USNM	USNM 566616	*Odocoileus virginianus*	90	male	
KK	USNM	USNM 256055	*Odocoileus virginianus*	90	female	
KK	USNM	USNM 396283	*Odocoileus virginianus*	90	female	
KK	USNM	USNM 174617	*Oreamnos americanus*	93	female	
KK	USNM	USNM A20752	*Oreamnos americanus*	93	?	
KK	AMNH	82074	*Oreotragus oreotragus*	13	female	
KK	AMNH	27827	*Oreotragus oreotragus*	13	male	
KK	AMNH	80553	*Oreotragus oreotragus*	13	male	
KK	NHM	1936.5.28.4	*Oreotragus oreotragus*	13	female	

KK	AMNH	82070	*Ourebia ourebi*	17	male	
KK	AMNH	34764	*Ourebia ourebi*	17	male	
KK	AMNH	53317	*Ourebia ourebi*	17	female	
KK	PC	JUBALAND 101	*Ourebia ourebi*	17	male	
KK	PC	JUBALAND 40	*Ourebia ourebi*	17	male	
KK	AMNH	122673	*Ovis canadensis*	98	male	
KK	AMNH	164125	*Ovis canadensis*	98	male	
KK	AMNH	54616	*Ovis vignei*	61.5	male	
KK	AMNH	54615	*Ovis vignei*	61.5	female	
KK	AMNH	119526	*Ovis vignei*	61.5	male	
KC	UNSM	ZM 15538	*Philantomba maxwellii*	7.5	male	zoo
KK	USNM	USNM 084084	*Procapra picticaudata*	27.5	female	
KK	USNM	USNM 084085	*Procapra picticaudata*	27.5	male	
KK	USNM	USNM 240681	*Pseudois nayaur*	52.5	female	
KK	USNM	USNM 259712	*Pseudois nayaur*	52.5	male	
KK	USNM	USNM 282141	*Pudu mephistophiles*	9.6	male	
KK	USNM	USNM 309045	*Pudu mephistophiles*	9.6	female	
KC	MVZ	158479	*Pudu puda*	12	female	
KK	AMNH	216389	*Raphicerus campestris*	11.5	female	
KK	AMNH	80538	*Raphicerus campestris*	11.5	male	
KK	AMNH	233045	*Raphicerus campestris*	11.5	male	
KK	NHM	76.579	*Raphicerus campestris*	11.5	male	
KK	NHM	76.581	*Raphicerus campestris*	11.5	male	
KK	NHM	1936.5.28.3	*Raphicerus campestris*	11.5	male	
KK	USNM	USNM 367433	*Raphicerus sharpei*	9	female	
KK	USNM	USNM 367434	*Raphicerus sharpei*	9	male	
KK	USNM	USNM 367445	*Raphicerus sharpei*	9	male	
KK	NHM	1936.3.30.9	*Redunca fulvorufula*	28.5	male	
KK	USNM	USNM 161992	*Redunca fulvorufula*	28.5	female	
KK	USNM	USNM 161994	*Redunca fulvorufula*	28.5	female	
KK	NHM	1962.12.14.7	*Redunca redunca*	50	female	
KK	NHM	1960.11.10.1	*Redunca redunca*	50	female	
KK	USNM	USNM 163188	*Redunca redunca*	50	male	
KK	USNM	USNM 163190	*Redunca redunca*	50	male	
KK	AMNH	90234	*Rupicapra rupicapra*	37	male	
KK	AMNH	90235	*Rupicapra rupicapra*	37	male	
KK	NHM	1966.7.28.1	*Sylvicapra grimmia*	16.75	female	
KK	NHM	1966.8.18.1	*Sylvicapra grimmia*	16.75	male	
KK	NHM	1966.9.22.1	*Sylvicapra grimmia*	16.75	female	
KK	NHM	1966.9.26.1	*Sylvicapra grimmia*	16.75	male	

KK	NHM	1966.8.5.1	*Sylvicapra grimmia*	16.75	male
KK	NHM	1936.3.30.7	*Sylvicapra grimmia*	16.75	male
KK	AMNH	53244	*Tragelaphus scriptus*	52	male
KK	AMNH	216371	*Tragelaphus scriptus*	52	female
KK	AMNH	187806	*Tragelaphus scriptus*	52	female
KK	AMNH	53245	*Tragelaphus scriptus*	52	female
KK	AMNH	36404	*Tragelaphus scriptus*	52	male
KK	AMNH	34757	*Tragelaphus scriptus*	52	male
KK	AMNH	34753	*Tragelaphus scriptus*	52	female
KK	NHM	1966.5.20.1	*Tragelaphus scriptus*	52	female
KK	NHM	1966.5.20.2	*Tragelaphus scriptus*	52	female
KK	NHM	1966.6.7.1	*Tragelaphus scriptus*	52	male
KK	NHM	71.2115	*Tragelaphus scriptus*	52	female
KK	USNM	USNM 164558	*Tragelaphus spekii*	85	male
KC	AMNH	M-113768	*Tragulus javanicus*	4.35	female

APPENDIX C: FOSSIL SPECIMENS

Fossil blastomerycines specimens from the American Museum of Natural History Fossil Mammal Collections (AMNH FM), the AMNH Frick Collections (AMNH F:AM), and the University of Nebraska State Museum (UNSM). The sample includes humeri, radai, femora, metatarsals, and proximal phalanges from adults, based on fusion of epiphyses.

Collection/ Number	Species	NALMA	County	State
AMNH FM 13015	cf. *Pseudoblastomeryx advena*	Hemingfordian	Shannon	SD
AMNH FM 13224	cf. *Problastomeryx primus*	Hemingfordian	Niobrara	WY
AMNH FM 13822	cf. *Problastomeryx primus*	Hemingfordian	Shannon	SD
AMNH FM 13823	cf. *Pseudoblastomeryx advena*	Hemingfordian	Shannon	SD
AMNH F:AM 144677	cf. *Longirostromeryx clarendonensis*	Clarendonian	Donley	TX
AMNH F:AM 144678	cf. *Blastomeryx gemmifer*	Clarendonian	Donley	TX
AMNH F:AM 144679	cf. *Blastomeryx gemmifer*	E. Barstovian	San Jacinto	TX
AMNH F:AM 144680	cf. *Blastomeryx gemmifer*	E. Barstovian	San Jacinto	TX
AMNH F:AM 144681	cf. *Blastomeryx gemmifer*	E. Barstovian	San Jacinto	TX
AMNH F:AM 117117	cf. *Blastomeryx gemmifer*	E. Barstovian	San Jacinto	TX
AMNH F:AM 31953	*Blastomeryx gemmifer*	Barstovian	Brown	NE
AMNH F:AM 54682	*Longirostromeryx* sp.	Clarendonian	Todd	SD
AMNH F:AM 54684	*Longirostromeryx* sp.	Clarendonian	Todd	SD
AMNH F:AM 54688	*Longirostromeryx* sp.	Clarendonian	Todd	SD
AMNH F:AM 54701	*Longirostromeryx* sp.	Clarendonian	Brown	NE
AMNH F:AM 54703	*Longirostromeryx* sp.	Clarendonian	Brown	NE
AMNH F:AM 54706	*Longirostromeryx* sp.	Clarendonian	Brown	NE
AMNH F:AM 54708	*Longirostromeryx* sp.	Clarendonian	Brown	NE
AMNH F:AM 54716	cf. *Blastomeryx gemmifer*	E. Clarendonian	Sheridan	NE
AMNH F:AM 54720	cf. *Blastomeryx gemmifer*	E. Clarendonian	Sheridan	NE
AMNH F:AM 54722	cf. *Blastomeryx gemmifer*	E. Clarendonian	Sheridan	NE
AMNH F:AM 54724	cf. *Blastomeryx gemmifer*	E. Clarendonian	Sheridan	NE
AMNH F:AM 54726	*Longirostromeryx clarendonensis*	Clarendonian	Donley	TX
AMNH F:AM 54729	*Longirostromeryx clarendonensis*	Clarendonian	Donley	TX
AMNH F:AM 54733	cf. *Blastomeryx gemmifer*	Clarendonian	Donley	TX
AMNH F:AM 54734	cf. *Blastomeryx gemmifer*	Clarendonian	Donley	TX
AMNH F:AM 144682	cf. *Blastomeryx gemmifer*	E. Clarendonian	Sheridan	NE
AMNH F:AM 144683	cf. *Problastomeryx primus*	L. Hemingfordian	Dawes	NE
AMNH F:AM 31360	*Parablastomeryx gregorii*	Clarendonian	Cherry	NE
AMNH F:AM 31729	*Longirostromeryx wellsi*	Clarendonian	Rio Arriba	NM
AMNH F:AM 31901	*Blastomeryx gemmifer*	L. Hemingfordian	Sioux	NE
UNSM 125572	*Longirostromeryx wellsi*	Clarendonian	Antelope	NE

UNSM 27831	*Longirostromeryx wellsi*	Clarendonian	Antelope	NE
UNSM 133126	*Longirostromeryx wellsi*	Clarendonian	Antelope	NE
UNSM 133125	cf. *Blastomeryx gemmifer*	M. Barstovian	Brown County	NE
UNSM 133127	*Longirostromeryx wellsi*	Clarendonian	Antelope	NE
UNSM 133128	*Longirostromeryx wellsi*	Clarendonian	Antelope	NE

APPENDIX D: FOSSIL MEASUREMENTS

Thirteen linear measurements of the humerus (see Table 2 and Figure 1), in millimeters, of fossil specimens.

Collection number	Species	H1	H2	H4	H5	H6	H7	H8
UNSM 27831	*L. wellsi* (Cl.)		113.3		8.8	27.9		19.1
AMNH F:AM 31360	*P. gregorii* (Cl.)	152.4	144.5	41.1	25.3	35.2	29.8	21.7
AMNH F:AM 54682	*L. sp.* (Cl.)	120.3	112.1	42.0	21.3	30.3	25.7	17.9
AMNH F:AM 54706	*L. sp.* (Cl.)	118.3	110.0		22.6	30.4	19.9	18.6
		H8	**H9**	**H10**	**H11**	**H12**	**H13**	**H14**
UNSM 27831	*L. wellsi* (Cl.)	19.1	18.0	18.2	8.1	8.2	12.4	8.8
AMNH F:AM 31360	*P. gregorii* (Cl.)	21.7	24.0	21.9	7.6	8.2	13.4	11.6
AMNH F:AM 54682	*L. sp.* (Cl.)	17.9	17.2	19.4	7.1	7.3	13.4	9.3
AMNH F:AM 54706	*L. sp.* (Cl.)	18.6	18.2	20.3	6.6	7.8	13.6	9.9

Five linear measurements of the distal humerus (see Table 2 and Figure 1), in millimeters, of fossil specimens.

Collection number	Species	H8	H9	H10	H11	H12
UNSM 27831	*L. wellsi* (Cl.)	19.1	18.0	18.2	8.1	8.2
AMNH F:AM 31360	*P. gregorii* (Cl.)	21.7	24.0	21.9	7.6	8.2
AMNH F:AM 54682	*L. sp.* (Cl.)	17.9	17.2	19.4	7.1	7.3
F:AM 54706	*L. sp.* (Cl.)	18.6	18.2	20.3	6.6	7.8
AMNH F:AM 54726	*L. clarendonensis* (Cl.)	18.5	17.8	19.2	8.5	6.9
UNSM 125572	*L. sp.* (Cl.)	19.3	17.2	18.6	7.2	6.6
AMNH F:AM 54726B	*L. clarendonensis* (Cl.)	17.1	16.8	18.4	8.4	8.0
AMNH F:AM 54722	*B. gemmifer* (Cl.)	18.8	17.3	20.9	6.4	7.7
AMNH F:AM 54701A	*L. sp.* (Cl.)	18.1	18.4	20.9	8.3	6.7
AMNH F:AM 54701B	*L. sp.* (Cl.)	19.2	20.2	21.9	8.1	9.6
AMNH F:AM 144683	*Pr. primus* (H.)	16.2	15.9	16.6	6.3	6.8

Nine linear measurements of the radius (see Table 2 and Figure 2), in millimeters, of fossil specimens.

Collection number	Species	R1	R3	R4	R5	R6	R7	R8	R9
UNSM 27831	*L. wellsi* (Cl.)	135.5	11.0	18.7	18.4	14.0	18.5	6.5	12.2

AMNH F:AM 31360	*P. gregorii* (Cl.)	152.0	14.1	22.3	21.3	22.5	19.0	9.6	14.6
AMNH F:AM 31729	*L. wellsi* (Cl.)	113.3	9.4			12.7	15.3	6.4	11.5
AMNH F:AM 54684	*L. sp.* (Cl.)	132.0	10.5	19.7	18.3	13.9	17.8	7.3	12.7
UNSM 125572	*L. sp.* (Cl.)	126.3	10.3	18.6	17.0	13.0	17.3	13.8	7.8
AMNH F:AM 54684c	*L. sp.* (Cl.)	129.8	11.3	18.4	18.0	12.7	17.3	7.0	12.5
AMNH F:AM 54684d	*L. sp.* (Cl.)	132.6	10.7	18.9	18.2	13.2	18.0	7.0	12.3
UNSM 133126	*L. wellsi* (Cl.)	137.0	11.6	18.2	17.9	13.9	18.0	7.2	12.5
UNSM 133127	*L. wellsi* (Cl.)	135.6	11.3	19.1	18.1	13.8	18.2	6.9	12.7
AMNH F:AM 144681	*B. gemmifer* (B.)	129.9	10.3	16.3	16.0	12.1	16.9	7.2	11.6
AMNH F:AM 54716	*B. gemmifer* (Cl.)	119.4	9.2	15.1	15.0	11.4	15.0	5.9	10.8

Thirteen linear measurements of the femur (see Table 2 and Figure 3), in millimeters, of fossil specimens.

Collection number	**Species**	**F2**	**F3**	**F4**	**F5**	**F6**	**F7**	**F8**
AMNH F:AM 31360	*Parablastomeryx gregorii* (Cl.)	185.7	24.1	39.1	40.6	36.6	18.4	23.0
AMNH F:AM 54703	*Longirostromeryx sp.* (Cl.)	150.9	21.1	37.0	30.1	35.7	16.0	20.2
AMNH F:AM 54708	*Longirostromeryx sp.* (Cl.)	143.5	24.2	33.2		29.3	14.4	18.0
UNSM 125572	*Longirostromeryx sp.* (Cl.)	142.4	24.2	32.0	34.9	27.3	15.2	18.3
AMNH F:AM 54703A	*Longirostromeryx sp.* (Cl.)	138.9	20.9	32.9		28.7	14.5	17.3
AMNH FM 13822	*Problastomeryx primus* (H.)	147.6	18.0	32.2	33.7	28.3	13.6	15.8
			F9	**F10**	**F11**	**F12**	**F13**	**F14**
AMNH F:AM 31360	*Parablastomeryx gregorii* (Cl.)		41.7	33.6	15.8	14.4	14.0	13.8
AMNH F:AM 54703	*Longirostromeryx sp.* (Cl.)		34.6	28.9	14.1	13.9	12.9	13.0
AMNH F:AM 54708	*Longirostromeryx sp.* (Cl.)		33.7	28.0	14.4	12.8	13.0	11.8
UNSM 125572	*Longirostromeryx sp.* (Cl.)		35.8	27.2	15.5	11.1	14.8	11.7
AMNH F:AM 54703A	*Longirostromeryx sp.* (Cl.)		34.8	26.6	14.7	13.2	11.6	12.5
AMNH FM 13822	*Problastomeryx primus* (H.)		32.5	26.7	12.1	11.7	12.2	11.6

Thirteen linear measurements of the metatarsal (see Table 2 and Figure 4), in millimeters, of fossil specimens.

Collection Number	**Species**	**MT1**	**MT2**	**MT3**	**MT4**	**MT5**	**MT6**	**MT7**
AMNH FM 31953	*B. gemmifer* (B.)	122.0	120.7	15.0	13.2	10.1	15.0	9.0
AMNH F:AM 31360	*P. gregorii* (Cl.)	177.9	177.3	20.8	19.0	15.1	21.9	13.7
AMNH F:AM 31729	*L. blicki* (Cl.)	123.3	121.0	15.5	14.4	11.1	18.0	10.7

AMNH F:AM 54688	*L. sp.* (Cl.)	133.1	131.3	16.0	16.2	12.1	17.0	8.4
AMNH F:AM 54729	*L. clarendonensis* (Cl.)	122.7	122.1	14.8	14.5	10.9	15.3	8.5
AMNH F:AM 54733	*B. gemmifer* (Cl.)	116.9	114.7	14.8	14.1	10.6	15.0	8.8
UNSM 125572	*L. sp.* (Cl.)	137.3	135.8	16.5	15.7	10.9	17.8	10.6
AMNH F:AM 54688a	*L. sp.* (Cl.)	139.5	137.3	16.8	16.3	12.3	17.2	9.8
AMNH F:AM 54688c	*L. sp.* (Cl.)	138.4	137.1	16.1	15.6	12.3	17.1	9.9
AMNH F:AM 144677	*L. clarendonensis* (Cl.)	127.2	126.7	15.8	15.4	12.0	6.8	9.3
AMNH F:AM 144680	*B. gemmifer* (Cl.)	128.2	126.0	14.4	14.2	10.8	17.3	9.5
AMNH F:AM 54724	*B. gemmifer* (Cl.)	130.3	127.6	17.8	16.8	11.3	18.2	11.4
AMNH F:AM 54720a	*B. gemmifer* (Cl.)	123.7	121.4	14.0	13.8	10.3	15.4	9.1
AMNH F:AM 54720b	*B. gemmifer* (Cl.)	126.6	125.1	15.1	14.5	11.5	6.8	9.2
AMNH F:AM 54720c	*B. gemmifer* (Cl.)	121.3	119.8	14.1	13.3	10.4	15.1	8.5
AMNH FM 13224	*Pr. primus* (H.)	129.4	128.0	14.4	14.5	10.5	18.0	10.5
AMNH FM 13822	*Pr. primus* (H.)	138.9	137.0	15.3	15.5	11.1	18.7	12.6
AMNH FM 13823	*Ps. advena* (H.)	92.0	90.4	12.0	11.4	8.7	14.0	8.3
AMNH F:AM 31901	*B. gemmifer* (H.)	124.5	123.9	14.1	12.2	9.4	15.8	9.6
UNSM 133125	*B. gemmifer* (B.)	132.9	132.5	14.2	13.0	9.1	15.7	9.0

		MT8	**MT9**	**MT10**	**MT11**	**MT12**	**MT13**
AMNH FM 31953	*B. gemmifer* (B.)	6.5	5.4	1.9	1.9	8.7	8.9
AMNH F:AM 31360	*P. gregorii* (Cl.)	9.2	9.5	2.8	2.2	13.3	11.0
AMNH F:AM 31729	*L. blicki* (Cl.)	7.2	7.8	1.8	1.7	10.6	9.3
AMNH F:AM 54688	*L. sp.* (Cl.)	7.8	7.7	1.7	0.5	10.3	10.5
AMNH F:AM 54729	*L. clarendonensis* (Cl.)	7.0	7.0	1.9	1.2	9.5	8.8
AMNH F:AM 54733	*B. gemmifer* (Cl.)	6.8	6.5	1.8	1.9	9.4	9.7
UNSM 125572	*L. sp.* (Cl.)	8.3	7.9	3.5	2.2	11.1	10.4
AMNH F:AM 54688a	*L. sp.* (Cl.)	7.8	7.6	2.1	1.9	10.9	9.6
AMNH F:AM 54688c	*L. sp.* (Cl.)	8.2	7.6	2.3	1.5	10.7	10.2
AMNH F:AM 144677	*L. clarendonensis* (Cl.)	7.2	7.8	1.6	1.4	10.3	10.7
AMNH F:AM 144680	*B. gemmifer* (Cl.)	6.8	8.0	1.5	1.2	9.3	9.2
AMNH F:AM 54724	*B. gemmifer* (Cl.)	7.2	7.7	1.9	1.9	11.5	10.2
AMNH F:AM 54720a	*B. gemmifer* (Cl.)	6.6	6.1	1.9	1.4	9.3	9.0
AMNH F:AM 54720b	*B. gemmifer* (Cl.)	7.2	7.8	1.8	1.2	8.6	11.5
AMNH F:AM 54720c	*B. gemmifer* (Cl.)	6.8	6.5	1.4	1.4	8.6	8.6
AMNH FM 13224	*Pr. primus* (H.)	6.9	7.7	2.0	1.8	10.4	9.3
AMNH FM 13822	*Pr. primus* (H.)	7.2	8.5	2.2	1.6	10.4	10.2
AMNH FM 13823	*Ps. advena* (H.)	5.5	6.2	1.3	1.0	7.9	7.8
AMNH F:AM 31901	*B. gemmifer* (H.)	6.0	6.6	1.9	1.8	9.3	8.4
UNSM 133125	*B. gemmifer* (B.)	6.4	6.3	1.7	1.8	8.7	9.3

Nine linear measurements of the proximal phalanx (see Table 2 and Figure 5), in millimeters, of fossil specimens.

Collection Number	Species	Pa1	Pa2	Pa3	Pa3b	Pa4	Pa5	Pa5b	Pa6	Pa7
AMNH F:AM 31360	*P. gregorii* (Cl.)	40.4	8.6	9.9	12.3	11.1	8.4	8.0	9.4	7.9
AMNH F:AM 31360	*P. gregorii* (Cl.)	33.9	8.0	9.1	10.4	9.7	7.5	7.1	7.5	7.2
AMNH F:AM 31729	*L. wellsi* (Cl.)	27.4	6.6	8.8	8.9	9.3	6.5	6.1	7.5	6.1
AMNH F:AM 31729	*L. wellsi* (Cl.)	26.3	6.9	8.0	9.0	8.5	6.6	5.9	7.2	6.2
UNSM 125572	*L. sp.* (Cl.)	29.9	8.1	9.0	11.4	10.7	6.8	6.6	8.0	7.6
UNSM 125572	*L. sp.* (Cl.)	26.6	7.9	7.0	8.6	7.6	7.0	5.5	6.3	7.3
AMNH F:AM 54734c	*B. gemmifer* (Cl.)	28.0	7.3	7.8	10.2	8.4	6.3	6.5	7.1	5.5
F:AM 54734d	*B. gemmifer* (Cl.)	24.8	6.8	7.4	9.7	8.1	6.4	6.1	6.6	5.2
AMNH F:AM 144678	*B. gemmifer* (Cl.)	24.9	6.5	7.9	8.9	8.3	6.4	6.0	6.3	5.6
UNSM 133128	*L. sp.* (Cl.)	31.9	7.9	8.6	11.6	10.0	7.6	7.5	8.3	7.5
AMNH F:AM 117117	*B. gemmifer* (B.)	26.3	7.0	8.2	9.8	9.0	6.7	5.7	7.4	6.1
AMNH F:AM 144679	*B. gemmifer* (B.)	26.3	6.9	9.1	10.2	9.4	6.9	6.2	7.4	6.5
AMNH F:AM 144682	*B. gemmifer* (Cl.)	25.1	6.8	8.2	10.5	8.8	6.8	6.8	8.1	6.3
AMNH FM 13015	*Ps. advena* (H.)	18.6	5.2	6.1	6.4	6.6	5.2	4.4	5.3	4.7
AMNH FM 13015	*Ps. advena* (H.)	18.6	5.4	6.3	6.2	6.9	5.2	4.4	5.4	4.8
AMNH FM 13015	*Ps. advena* (H.)	18.9	5.7	6.1	6.4	6.8	5.3	4.6	5.4	4.8
AMNH FM 13224	*Pr. primus* (H.)	22.3	6.2	7.1	7.1	8.0	6.0	5.1	5.9	5.2
AMNH FM 13822	*Pr. primus* (H.)	26.0	6.6	7.8	7.1	8.4	6.6	5.6	6.4	5.8
AMNH FM 13823	*Ps. advena* (H.)	18.6	5.2	5.9	5.8	6.2	5.1	4.4	4.8	4.4

Key ratios of limb elements in fossil and modern specimens (see Table 3).

Collection number		Species	H2/ H14	R1/ R9	F2/ F14	MT1/ MT13	MT1/ F2	C1/ MT1	R1/ H2
AMNH	F:AM 31360	*Parablastomeryx gregorii*	12.43	10.44	13.47	16.19	0.96	0.15	1.05
UNSM	125572/27831	*Longirostromeryx wellsi*	13.13	16.20	12.17	13.15	0.96	0.34	1.12
UNSM	ZM 15509	*Cephalophus dorsalis*	7.56	6.50	8.47	7.62	0.69	0.37	1.04
NHM	1950.9.23.1	*Cephalophus leucogaster*	9.70	8.03	10.95	11.14	0.81	0.38	1.00
PC	MERFIELD 891	*Cephalophus leucogaster*	9.86	8.59	11.53	11.12	0.81	0.48	1.01
AMNH	34736	*Cephalophus monticola*	13.10	10.50	13.43	13.61	0.80	0.61	0.92

NHM	1936.10.28.28	*Cephalophus monticola*	11.99	9.69	12.38	13.21	0.88	0.46	0.99
NHM	1936.10.28.29	*Cephalophus monticola*	11.87	9.86	11.84	12.98	0.90	0.48	1.00
NHM	1936.10.28.30	*Cephalophus monticola*	11.56	9.62	11.78	12.20	0.85	0.36	0.99
NHM	1936.10.28.31	*Cephalophus monticola*	11.07	9.44	12.02	13.47	0.84	0.52	1.01
AMNH	52930	*Cephalophus nigrifrons*	10.02	8.91	11.58	11.56	0.89	0.38	1.07
AMNH	52940	*Cephalophus nigrifrons*	10.13	8.73	11.42	13.24	0.89	0.24	1.08
AMNH	52943	*Cephalophus nigrifrons*	11.09	9.49	12.13	12.60	0.85	0.26	1.06
PC	MERFIELD 244	*Cephalophus nigrifrons*	10.98	10.17	13.08	13.71	0.91	0.25	1.03
PC	MERFIELD 342	*Cephalophus nigrifrons*	10.22	9.07	11.09	12.31	0.86	0.27	1.08
PC	MERFIELD 649	*Cephalophus nigrifrons*	10.04	9.06	11.93	12.73	0.85	0.26	1.05
PC	CONGO 318	*Hyemoschus aquaticus*	10.98	7.23	10.79	4.85	0.51	0.67	0.79
PC	MERFIELD 197	*Hyemoschus aquaticus*	10.92	7.55	10.49	4.60	0.51	0.80	0.80
PC	MERFIELD 395	*Hyemoschus aquaticus*	11.10	7.28	9.75	4.64	0.49	0.76	0.79
PC	MERFIELD 403	*Hyemoschus aquaticus*	10.02	7.32	9.82	4.55	0.50	0.71	0.80
PC	MERFIELD 577	*Hyemoschus aquaticus*	11.67	7.27	10.79	5.15	0.50	0.75	0.83
MVZ	158479	*Pudu puda*	11.01	9.73	12.66	9.55	0.64	0.58	0.81
AMNH	M-113768	*Tragulus javanicus*	13.49	11.12	10.74	12.46	0.80	0.77	0.92
AMNH	113812	*Addax nasomaculatus*	7.24	10.15	10.27	12.31	0.86	0.20	1.29
NHM	70.345	*Damaliscus dorcas*	8.74	11.23	10.97	13.97	0.99	0.19	1.39
NHM	1932.6.6.46	*Madoqua kirkii*	12.64	11.82	13.23	15.44	0.92	0.38	1.12
NHM	1932.6.6.49	*Madoqua kirkii*	11.14	10.27	11.10	13.95	0.98	0.84	1.10
NHM	1932.6.6.51	*Madoqua kirkii*	11.63	10.73	11.95	14.40	0.95	0.82	1.14
NHM	1937.8.4.26	*Neotragus batesi*	13.83	13.03	13.53	17.72	1.10	0.38	1.06
NHM	1937.8.4.27	*Neotragus batesi*	14.44	12.65	13.16	18.74	1.06	0.39	1.03
UNSM	ZM 15538	*Philantomba maxwellii*	9.34	7.47	11.22	9.48	0.68	0.35	0.96
NHM	71.2115	*Tragelaphus scriptus*	9.81	9.13	11.53	13.85	0.86	0.17	1.14
AMNH	34757	*Tragelaphus scriptus*	10.14	8.25	12.64	12.04	0.84	0.16	1.10
AMNH	36404	*Tragelaphus scriptus*	9.76	8.59	11.82	11.13	0.77	0.12	1.07
AMNH	53244	*Tragelaphus*	9.53	7.88	10.54	12.57	0.87	0.24	1.09

		scriptus							
AMNH	53245	*Tragelaphus scriptus*	10.63	9.06	11.17	12.45	0.88	0.40	1.08
AMNH	187806	*Tragelaphus scriptus*	9.91	11.87	11.16	13.25	0.87	0.43	1.52
AMNH	216371	*Tragelaphus scriptus*	10.64	9.05	12.36	13.93	0.86	0.47	1.12
NHM	1966.5.20.1	*Tragelaphus scriptus*	10.54	8.81	10.49	13.41	0.86	0.51	1.05
NHM	1966.5.20.2	*Tragelaphus scriptus*	11.63	9.16	11.67	14.47	0.88	0.42	1.09
NHM	1966.6.7.1	*Tragelaphus scriptus*	9.39	8.14	11.83	12.80	0.86	0.38	1.09
USNM	USNM 164558	*Tragelaphus spekii*	10.74	9.52	12.03	11.91	0.79	0.30	1.00
NHM	69.1142	*Aepyceros melampus*	8.91	10.11	11.47	15.67	1.09	0.29	1.42
NHM	1932.6.6.32	*Aepyceros melampus*	8.18	9.05	10.33	15.04	1.07	0.27	1.40
NHM	1960.11.10.2	*Aepyceros melampus*	8.31	9.82	10.26	14.92	1.07	0.32	1.41
NHM	1960.11.10.2	*Aepyceros melampus*	8.34	9.92	10.22	15.01	1.08	0.40	1.40
NHM	1960.11.10.5	*Aepyceros melampus*	8.59	9.52	10.61	15.25	1.07	0.12	1.40
NHM	1967.11.8.1.	*Aepyceros melampus*	8.86	9.78	11.34	16.13	1.13	0.34	1.39
NHM	1968.6.20.1	*Aepyceros melampus*	8.30	10.31	11.71	15.53	1.15	0.37	1.44
UNSM	ZM-18673	*Dama dama*	9.01	9.20	11.12	14.33	0.96	0.41	1.14
NHM	1939.2563	*Gazella cuvieri*	9.19	9.68	11.46	15.34	1.03	0.41	1.24
PC	ALGERIA 4	*Gazella cuvieri*	9.92	9.81	12.09	16.56	1.09	0.44	1.25
NHM	1935.12.14.2	*Gazella granti*	7.77	9.00	11.18	15.94	1.08	0.31	1.37
NHM	1936.3.28.10	*Gazella granti*	8.82	10.59	12.13	17.18	1.09	0.31	1.34
NHM	1936.9.5.2	*Gazella granti*	7.93	8.94	11.13	15.85	1.04	0.31	1.36
NHM	1936.9.5.3	*Gazella granti*	8.42	10.16	10.52	15.86	1.11	0.29	1.37
AMNH	81170	*Litocranius walleri*	9.38	11.37	11.91	16.95	1.25	0.23	1.50
AMNH	88409	*Litocranius walleri*	9.39	12.18	11.38	17.60	1.24	0.32	1.50
AMNH	187829	*Litocranius walleri*	10.01	8.95	12.04	17.36	1.28	0.35	1.09
NHM	1936.3.28.3	*Litocranius walleri*	9.54	12.03	11.96	19.02	1.27	0.30	1.46
NHM	1962.7.6.17	*Litocranius walleri*	10.62	12.52	11.45	19.53	1.27	0.34	1.53
USNM	256055	*Odocoileus virginianus*	9.08	8.92	10.84	15.14	1.03	0.35	1.18
USNM	396283	*Odocoileus virginianus*	9.83	9.51	12.70	14.27	0.99	0.29	1.10
USNM	566616	*Odocoileus virginianus*	9.96	9.44	12.82	15.84	0.99	0.28	1.12
USNM	567252	*Odocoileus virginianus*	8.99	8.36	11.25	13.38	0.95	0.42	1.17

AMNH	27827	*Oreotragus oreotragus*	12.33	10.13	13.01	9.72	0.72	0.67	0.99
AMNH	80553	*Oreotragus oreotragus*	9.49	8.59	10.72	9.79	0.70	0.77	1.02
NHM	1936.5.28.4	*Oreotragus oreotragus*	11.98	10.02	12.85	9.73	0.69	0.81	1.00
USNM	367433	*Raphicerus sharpei*	10.78	9.01	11.73	11.22	0.80	0.65	1.06
NHM	1960.11.10.1	*Redunca redunca*	8.55	8.68	11.17	14.66	0.97	0.24	1.28
USNM	163190	*Redunca redunca*	9.55	9.17	12.65	13.21	0.90	0.19	1.22
NHM	1936.3.30.7	*Sylvicapra grimmia*	10.99	10.26	11.87	15.06	0.98	0.26	1.17
NHM	1966.7.28.1	*Sylvicapra grimmia*	9.98	10.48	12.26	13.92	0.98	0.48	1.24
NHM	1966.8.18.1	*Sylvicapra grimmia*	10.21	9.68	11.84	14.44	1.01	0.50	1.24
NHM	1966.9.22.1	*Sylvicapra grimmia*	10.53	11.11	12.01	15.20	1.06	0.50	1.29
NHM	1966.9.26.1	*Sylvicapra grimmia*	11.04	10.37	11.91	14.77	1.02	0.32	1.27
AMNH	84462	*Elaphodus cephalophus*	10.42	9.04	13.42	12.38	0.79	0.41	1.00
AMNH	84463	*Elaphodus cephalophus*	10.72	8.51	13.23	11.07	0.73	0.44	0.95
AMNH	114551	*Elaphodus cephalophus*	10.30	8.77	12.14	10.43	0.76	0.38	0.96
AMNH	115638	*Elaphodus cephalophus*	10.83	7.70	13.01	10.75	0.76	0.40	0.90
UNSM	ZM 30972	*Elaphodus cephalophus*	11.38	9.93	12.86	12.72	0.79	0.35	0.95
UNSM	ZM 30973	*Elaphodus cephalophus*	11.30	9.26	14.14	12.24	0.75	0.39	0.95
AMNH	M-110500	*Moschus moschiferus*	12.71	9.35	12.63	11.68	0.78	0.46	0.91
AMNH	M-46405	*Moschus moschiferus*	12.50	11.35	14.27	16.23	0.97	0.35	1.04
AMNH	M-57078	*Moschus moschiferus*	13.33	10.16	12.53	13.56	0.85	0.52	0.93
UNSM	ZM 13423	*Muntiacus reevsi*	9.86	8.25	10.35	12.96	0.87	0.41	0.98
AMNH	165683	*Naemorhedus crispus*	9.59	9.67	11.44	8.77	0.65	0.49	1.03
USNM	013829/A20934	*Naemorhedus crispus*	10.75	9.56	12.46	9.22	0.67	0.47	1.02
USNM	259023	*Naemorhedus goral*	10.00	8.31	11.81	9.26	0.68	0.48	0.98
USNM	259398	*Naemorhedus goral*	9.56	8.10	11.62	9.62	0.69	0.48	1.02
USNM	311229	*Naemorhedus swinhoei*	9.72	7.97	11.76	7.31	0.62	0.52	0.94
USNM	282141	*Pudu mephistophiles*	11.70	9.35	13.23	9.16	0.65	0.48	0.78
USNM	309045	*Pudu mephistophiles*	13.49	10.23	12.87	11.27	0.68	0.45	0.79
USNM	020409	*Capra sibirica*	8.15	7.31	10.40	8.44	0.63	0.50	1.04
USNM	062092	*Capra sibirica*	9.67	9.10	11.57	10.24	0.70	0.47	1.12
AMNH	122673	*Ovis canadensis*	9.17	9.00	11.42	10.96	0.79	0.42	1.14

AMNH	164125	*Ovis canadensis*	7.81	8.68	10.60	11.05	0.79	0.41	1.22
AMNH	54616	*Ovis vignei*	9.32	9.79	11.01	12.94	0.90	0.36	1.28
AMNH	119526	*Ovis vignei*	10.43	9.77	11.45	13.31	0.89	0.35	1.23
USNM	259712	*Pseudois nayaur*	9.36	8.68	11.62	10.24	0.67	0.44	1.10
AMNH	90234	*Rupicapra rupicapra*	11.03	11.32	12.27	12.43	0.82	0.40	1.13
AMNH	35957	*Antilope cervicapra*	9.77	10.73	11.76	16.23	1.02	0.35	1.26
AMNH	54486	*Antilope cervicapra*	8.37	9.41	10.25	14.74	1.03	0.34	1.34
AMNH	88406	*Damaliscus hunteri*	7.45	9.96	10.03	14.33	1.03	0.36	1.53
AMNH	88408	*Damaliscus hunteri*	7.29	9.71	10.17	14.32	1.03	0.36	1.52
NHM	1938.7.11.1	*Damaliscus hunteri*	7.77	10.10	9.85	13.82	1.02	0.37	1.53
USNM	252685	*Gazella rufifrons*	8.78	10.09	11.36	16.36	1.10	0.33	1.35
USNM	252686	*Gazella rufifrons*	9.18	10.60	10.91	16.28	1.08	0.34	1.36
NHM	1936.12.13.3	*Gazella spekei*	8.95	10.93	10.59	17.13	1.13	0.33	1.36
NHM	1897.1.14.6	*Gazella subgutturosa*	9.87	11.37	11.56	18.48	1.14	0.31	1.30
USNM	163048	*Gazella thomsonii*	7.24	9.06	9.99	16.05	1.05	0.34	1.35
USNM	163053	*Gazella thomsonii*	8.02	9.29	10.11	15.37	1.07	0.33	1.34
USNM	172903	*Gazella thomsonii*	7.58	10.28	10.46	15.26	1.04	0.35	1.38
USNM	163195	*Kobus kob*	8.05	7.75	11.15	10.67	0.78	0.45	1.17
USNM	164499	*Kobus kob*	8.67	8.23	10.93	11.31	0.80	0.44	1.16
USNM	252689	*Kobus kob*	8.05	8.47	11.29	11.83	0.83	0.43	1.22
NHM	69.1147	*Kobus leche*	9.22	9.10	10.61	12.67	0.86	0.41	1.15
AMNH	34764	*Ourebia ourebi*	10.03	9.91	10.60	13.56	0.96	0.37	1.27
AMNH	53317	*Ourebia ourebi*	8.95	9.64	11.43	14.31	0.96	0.34	1.30
AMNH	82070	*Ourebia ourebi*	10.34	10.96	11.07	14.07	0.96	0.38	1.29
PC	JUBALAND 101	*Ourebia ourebi*	8.39	9.61	10.99	12.87	0.97	0.36	1.30
PC	JUBALAND 40	*Ourebia ourebi*	9.16	10.58	10.74	14.33	0.98	0.37	1.32
NHM	76.579	*Raphicerus campestris*	10.87	10.73	11.52	14.63	0.99	0.34	1.22
NHM	76.581	*Raphicerus campestris*	9.91	10.76	10.77	14.07	0.99	0.34	1.27
AMNH	80538	*Raphicerus campestris*	10.76	10.70	11.80	14.94	1.11	0.33	1.27
AMNH	216389	*Raphicerus campestris*	10.37	10.86	10.99	16.41	1.01	0.34	1.29
AMNH	233045	*Raphicerus campestris*	11.56	11.37	11.17	15.36	1.00	0.35	1.26
NHM	1936.5.28.3	*Raphicerus campestris*	9.63	10.71	10.82	13.90	0.99	0.34	1.28
NHM	1936.3.30.9	*Redunca fulvorufula*	9.02	8.82	11.48	13.59	0.93	0.37	1.23
USNM	161992	*Redunca fulvorufula*	9.70	9.65	12.52	13.83	0.94	0.36	1.27
USNM	161994	*Redunca fulvorufula*	9.94	9.96	11.83	13.03	0.90	0.37	1.23

APPENDIX E: PCA RESULTS FOR MODERN ARTIODACTYLS

A summary of the PCA on the humerus that was derived from transformed data of modern taxa.

PC	Eigenvalue	% variance
1	1.94634	97.905
2	0.0158012	0.79483
3	0.00748427	0.37647
4	0.00437443	0.22004
5	0.00357768	0.17996
6	0.00311995	0.15694
7	0.00280248	0.14097
8	0.00139947	0.070396
9	0.00110929	0.055799
10	0.000979203	0.049256
11	0.000618029	0.031088
12	0.000320697	0.016132
13	7.13E-05	0.0035886

Loadings of the PCA on the humerus that was derived from transformed data of modern taxa.

	PC 1	PC 2	PC 3	PC 4	PC 5	PC 6	PC 7	PC 8	PC 9	PC 10	PC 11	PC 12	PC 13
Ln H1	0.2328	0.5278	0.0841	0.0892	-0.1900	0.1427	0.0786	0.0921	-0.0210	0.1323	-0.0600	0.0210	-0.7477
Ln H2	0.2260	0.5892	0.1031	0.0916	-0.2046	0.1958	0.0433	0.0559	0.0235	0.2223	-0.0849	0.0894	0.6576
Ln H4	0.2824	0.2608	-0.4574	0.0809	0.2487	-0.5019	-0.4900	0.1077	0.2117	-0.1097	-0.0778	-0.0897	0.0113
Ln H5	0.2862	-0.2828	-0.1323	0.1252	-0.2071	-0.3708	0.3136	-0.0414	0.2222	0.6210	0.2666	0.1353	-0.0147
Ln H6	0.2844	0.0481	-0.1212	-0.1485	-0.2642	0.0242	0.1608	0.1171	0.0378	-0.5739	0.6438	0.1511	0.0442
Ln H7	0.3003	-0.1647	-0.2330	-0.0249	-0.1712	-0.1277	0.4770	0.1618	-0.1534	-0.2937	-0.6452	0.0235	0.0421
Ln H8	0.2941	-0.0298	0.0783	0.2059	-0.0333	0.0618	0.0982	-0.4381	0.0119	-0.0896	0.0787	-0.8012	0.0356
Ln H9	0.3031	-0.2119	0.3191	-0.4398	-0.4060	-0.1356	-0.4771	0.1435	-0.3191	0.1250	-0.0703	-0.1186	0.0064
Ln H10	0.2832	-0.0640	0.1678	0.2309	0.0372	-0.0425	-0.1816	-0.6789	-0.1385	-0.1584	-0.1051	0.5300	-0.0317
Ln H11	0.2616	-0.3205	0.0085	0.6461	0.0842	0.3501	-0.2254	0.4472	-0.1601	0.0091	0.0651	0.0296	0.0118
Ln H12	0.2516	0.0513	0.6569	-0.0556	0.5341	-0.2946	0.2300	0.2339	0.0979	-0.0916	0.0345	0.0117	0.0215
Ln H13	0.2889	0.0311	-0.3441	-0.3545	0.4999	0.2632	0.1155	-0.0763	-0.4978	0.2494	0.1515	0.0153	0.0032
Ln H14	0.2972	-0.2018	-0.0228	-0.3217	0.0927	0.4821	-0.1130	-0.0361	0.6897	0.0189	-0.1751	0.0602	-0.0390

A summary of the PCA on the radius that was derived from transformed data of modern taxa.

PC	Eigenvalue	% variance
1	1.40375	98.378
2	0.0114033	0.79917
3	0.00450458	0.31569
4	0.0030065	0.2107
5	0.00194133	0.13605
6	0.00102222	0.071639
7	0.000862152	0.060421
8	0.000409684	0.028712

Loadings of the PCA on the radius that was derived from transformed data of modern taxa.

	PC 1	PC 2	PC 3	PC 4	PC 5	PC 6	PC 7	PC 8
Ln R1	0.32873	0.89716	-0.090429	0.1999	-0.16581	0.080811	0.06553	0.024331
Ln R3	0.34829	0.027141	0.019204	-0.1749	0.81888	0.37226	-0.017763	0.19378
Ln R4	0.3724	-0.16344	-0.37036	0.045922	-0.064849	0.18739	-0.41973	-0.6927
Ln R5	0.36456	-0.18471	-0.4267	-0.12511	-0.28099	-0.10525	-0.33301	0.65903
Ln R6	0.35165	0.072525	0.22529	-0.25787	0.19979	-0.82581	-0.075352	-0.16206
Ln R7	0.36607	-0.20238	-0.24619	-0.21765	-0.16661	0.044902	0.82189	-0.10851
Ln R8	0.34484	-0.081846	0.7111	-0.29336	-0.3848	0.34153	-0.13322	0.014191
Ln R9	0.34994	-0.28395	0.2349	0.84366	0.055197	-0.089856	0.096935	0.097254

A summary of the PCA on the femur that was derived from transformed data of modern taxa.

PC	Eigenvalue	% variance
1	1.80198	97.053
2	0.0273253	1.4717
3	0.00890071	0.47938
4	0.00392725	0.21152
5	0.00339906	0.18307
6	0.00331439	0.17851
7	0.00248892	0.13405
8	0.00144821	0.077999
9	0.00121922	0.065666
10	0.000899708	0.048457
11	0.000760158	0.040941
12	0.000656719	0.03537
13	0.00038478	0.020724

Loadings of the PCA on the femur that was derived from transformed data of modern taxa.

	PC 1	PC 2	PC 3	PC 4	PC 5	PC 6	PC 7	PC 8	PC 9	PC 10	PC 11	PC 12	PC 13
Ln F2	0.2456	0.0834	0.4870	0.0259	0.3635	0.0247	0.5563	-0.2082	-0.0073	0.3168	-0.0487	0.3174	0.0761
Ln F3	0.2439	0.5610	-0.6944	-0.1221	0.1432	0.0806	0.2581	0.0307	0.0933	0.0981	-0.0421	0.0590	-0.1029
Ln F4	0.3076	-0.1622	-0.0560	0.2239	0.1652	0.1215	-0.2389	-0.1330	-0.4283	0.2242	-0.4891	-0.1974	-0.4439
Ln F5	0.2950	0.0219	-0.1115	0.0943	-0.3387	0.2330	-0.2150	-0.6380	-0.0620	-0.0952	-0.0331	0.2395	0.4444
Ln F6	0.2644	0.2572	0.2844	0.0564	-0.4623	0.3976	0.2857	0.3732	-0.2303	-0.3200	-0.0724	-0.1589	-0.0359
Ln F7	0.2681	0.1268	0.1774	-0.2071	0.0444	0.2879	-0.3449	0.1197	0.2152	0.5337	0.2924	-0.4127	0.1808
Ln F8	0.2920	-0.2664	-0.0126	-0.6126	-0.1157	-0.0368	-0.1746	0.3256	0.0443	0.0393	-0.2684	0.4914	-0.0100
Ln F9	0.2917	-0.2049	-0.1137	-0.3203	0.2780	-0.2656	0.1669	-0.0377	-0.4667	-0.2726	0.2122	-0.3704	0.3255
Ln F10	0.2782	0.0811	0.1970	-0.1820	0.1736	0.0506	-0.1661	-0.2995	0.2720	-0.4620	0.3198	0.0168	-0.5515
Ln F11	0.3047	-0.5792	-0.2492	0.1901	-0.3188	-0.0326	0.3950	-0.0153	0.3290	0.1605	0.1857	-0.1361	-0.1659
Ln F12	0.2722	-0.1184	-0.0391	0.4150	0.4438	0.1330	-0.1481	0.3185	0.3658	-0.3340	-0.2110	0.0264	0.3310
Ln F13	0.2706	0.2998	0.1918	0.0574	-0.2600	-0.7167	-0.0645	-0.0487	0.2457	0.0134	-0.3122	-0.2202	0.0507
Ln F14	0.2624	0.1018	-0.0236	0.3959	-0.0521	-0.2756	-0.2282	0.2758	-0.3294	0.1290	0.5187	0.3966	-0.0721

A summary of the PCA on the metatarsal that was derived from transformed data of modern taxa.

PC	**Eigenvalue**	**% variance**
1	1.56109	88.929
2	0.123447	7.0323
3	0.0327467	1.8654
4	0.0172135	0.98058
5	0.0107696	0.6135
6	0.00360038	0.2051
7	0.00251172	0.14308
8	0.00189026	0.10768
9	0.00100427	0.057209
10	0.00058799	0.033495
11	0.000307505	0.017517
12	0.000239444	0.01364
13	2.73E-05	0.0015558

Loadings of the PCA on the metatarsal that was derived from transformed data of modern taxa.

	PC 1	PC 2	PC 3	PC 4	PC 5	PC 6	PC 7	PC 8	PC 9	PC 10	PC 11	PC 12	PC 13

Ln MT1	0.2627	-0.4886	0.3054	0.0363	0.1574	-0.0936	0.1239	-0.0924	0.0488	0.0313	-0.0625	0.0452	0.7286
Ln MT2	0.2595	-0.5219	0.3167	0.0595	0.1962	-0.0207	0.1255	-0.1879	0.0355	0.0680	0.1586	-0.0457	-0.6583
Ln MT3	0.2751	-0.1243	-0.1154	0.2335	-0.0630	0.3455	-0.1752	0.2725	0.3541	0.0477	-0.6821	-0.0972	-0.1018
Ln MT4	0.2647	0.0686	-0.2707	0.1015	-0.0065	0.2544	-0.1823	-0.1619	0.2190	0.6182	0.3796	0.3716	0.0718
Ln MT5	0.2795	-0.0213	-0.0691	0.0297	-0.1003	-0.3580	-0.1709	0.5013	0.4548	-0.3061	0.4359	-0.0809	0.0058
Ln MT6	0.2862	0.2167	-0.0039	0.1085	0.0085	0.1208	-0.2072	-0.3693	-0.0369	0.0064	0.1582	-0.7923	0.1054
Ln MT7	0.2951	0.2748	0.2526	0.2559	0.0620	-0.5421	-0.3027	0.1302	-0.3856	0.2908	-0.2231	0.1186	-0.0690
Ln MT8	0.3288	-0.2140	-0.3842	-0.6211	-0.3586	-0.2693	-0.0878	-0.2177	-0.1179	0.0017	-0.1997	0.0156	-0.0501
Ln MT9	0.2872	0.1994	0.0654	0.1787	0.0009	0.1337	-0.1955	-0.4349	0.0183	-0.6308	-0.0220	0.4443	-0.0146
Ln MT10	0.2538	0.2625	0.0314	-0.5251	0.7131	0.1845	0.0009	0.2097	-0.0199	-0.0353	-0.0342	0.0220	-0.0078
Ln MT11	0.2591	0.3451	0.5520	-0.2366	-0.4888	0.2008	0.3739	0.0906	0.1109	0.1086	0.0166	0.0353	-0.0151
Ln MT12	0.2959	-0.1730	-0.2027	0.1629	-0.1376	0.3693	0.1126	0.3880	-0.6558	-0.1442	0.2114	0.0029	0.0294
Ln MT13	0.2475	0.2058	-0.3907	0.2761	0.1539	-0.2626	0.7367	-0.1087	0.0956	-0.0025	-0.1012	-0.0225	-0.0209

A summary of the PCA on the distal humerus that was derived from transformed data of modern taxa.

PC	**Eigenvalue**	**% variance**
1	0.865987	98.703
2	0.00524723	0.59807
3	0.00364654	0.41562
4	0.00196072	0.22348
5	0.000522071	0.059505

Loadings of the PCA on the distal humerus that was derived from transformed data of modern taxa.

	PC 1	PC 2	PC 3	PC 4	PC 5
Ln H8	0.47078	-0.081552	0.17399	-0.52884	-0.67954
Ln H9	0.48099	0.075071	-0.85449	0.17819	-0.033245
Ln H10	0.45452	-0.052169	0.12076	-0.48912	0.73271
Ln H11	0.41639	-0.66273	0.29038	0.55036	0.014054
Ln H12	0.40872	0.73877	0.37506	0.38268	-0.0072857

A summary of the PCA on both forefoot and hindfoot proximal phalanges that was derived from transformed data of modern taxa.

PC	**Eigenvalue**	**% variance**
1	2.26929	94.353
2	0.0608343	2.5294
3	0.0290808	1.2091

4	0.0183158	0.76153
5	0.0110889	0.46105
6	0.00507666	0.21108
7	0.00290626	0.12084
8	0.00248175	0.10319
9	0.00176223	0.07327
10	0.000952534	0.039605
11	0.000820626	0.03412
12	0.000598973	0.024904
13	0.000507389	0.021096
14	0.000434716	0.018075
15	0.000417559	0.017361
16	0.000312221	0.012982
17	0.000121643	0.0050577
18	0.000108894	0.0045276

Loadings of the PCA on both forefoot and hindfoot proximal phalanges that was derived from transformed data of modern taxa.

	PC 1	PC 2	PC 3	PC 4	PC 5	PC 6	PC 7	PC 8	PC 9
Ln Pa1f	0.2592	0.5931	0.0225	-0.1560	0.2465	-0.1284	-0.3991	-0.4014	-0.0881
Ln Pa2f	0.2589	-0.2047	-0.0021	-0.2622	-0.2073	-0.1951	-0.1393	0.0896	0.0576
Ln Pa3f	0.2528	-0.2347	0.1773	-0.3305	-0.0762	-0.1437	-0.2133	0.1599	0.0236
Ln Pa3fb	0.2431	0.0986	0.4585	-0.2041	-0.1551	0.0997	0.2824	-0.3285	0.4500
Ln Pa4f	0.2470	-0.2345	-0.0655	-0.1629	0.2137	0.3886	-0.0405	-0.0246	-0.1727
Ln Pa5f	0.2516	-0.1714	-0.2894	-0.2181	0.1080	0.2092	0.0916	0.0837	-0.0935
Ln Pa5fb	0.2527	0.2799	-0.3816	-0.1928	-0.1797	0.1444	0.0433	-0.0432	0.1196
Ln Pa6f	0.2444	0.0805	-0.0177	0.0664	-0.4879	0.2586	-0.2157	-0.0184	-0.4055
Ln Pa7f	0.2476	-0.2636	-0.1190	-0.1072	-0.1146	-0.2907	0.5236	-0.3132	-0.2463
Ln Pa1h	0.2234	0.3286	0.1026	-0.0147	0.3343	-0.2344	0.3180	0.4185	-0.4267
Ln Pa2h	0.2279	-0.1599	0.0187	0.1458	-0.0319	-0.3255	-0.3088	0.1112	0.0928
Ln Pa3h	0.2277	-0.1810	0.1910	0.0752	0.1409	-0.1454	-0.2694	0.2519	0.1490
Ln Pa3hb	0.2116	0.0737	0.5294	0.1264	0.0558	0.1191	0.1851	0.1059	-0.0870
Ln Pa4h	0.2199	-0.1539	0.0203	0.2446	0.4142	0.3785	0.0295	-0.1008	0.1787
Ln Pa5h	0.2250	-0.0907	-0.2184	0.1882	0.2193	0.1263	-0.0777	-0.0253	0.0950
Ln Pa5hb	0.2192	0.2811	-0.3059	0.0917	-0.1194	-0.0703	0.2291	0.4099	0.4857
Ln Pa6h	0.2040	0.0828	0.1114	0.5099	-0.3897	0.1990	-0.0005	0.0906	-0.1026
Ln Pa7h	0.2155	-0.1160	-0.1674	0.4714	0.0638	-0.3846	0.0292	-0.3745	0.0047

	PC 10	PC 11	PC 12	PC 13	PC 14	PC 15	PC 16	PC 17	PC 18
Ln Pa1f	-0.1582	-0.2881	0.0091	-0.1232	-0.0891	0.0715	0.1095	-0.0095	-0.0491
Ln Pa2f	0.2232	-0.2026	0.0685	0.1206	-0.1812	-0.4253	0.0025	-0.2622	-0.5639
Ln Pa3f	-0.1953	-0.2156	0.1648	0.2892	0.4958	0.0901	-0.0179	-0.1189	0.4225
Ln Pa3fb	0.2985	0.0448	-0.2501	-0.0531	0.0678	-0.0416	-0.1933	0.2195	0.0826
Ln Pa4f	0.1571	0.0241	-0.2900	0.3208	-0.0494	0.2053	0.5345	0.2597	-0.1205
Ln Pa5f	0.3001	-0.1462	0.1577	-0.7188	0.1058	0.0483	-0.0081	-0.0802	0.1529
Ln Pa5fb	-0.1173	0.5664	0.3739	0.1410	0.0880	-0.2679	0.0893	0.1394	0.0512
Ln Pa6f	-0.0235	0.2023	-0.3700	-0.0066	-0.0203	0.1994	-0.3403	-0.2801	0.0075
Ln Pa7f	-0.4680	-0.1026	-0.0046	-0.0277	-0.2460	0.0871	-0.0306	0.1167	0.0022
Ln Pa1h	0.1910	0.0546	-0.1815	0.1190	0.1110	-0.2511	-0.1719	0.1098	0.0535
Ln Pa2h	0.1893	0.1764	-0.0521	-0.0351	-0.5718	-0.0677	0.0944	0.1107	0.5039
Ln Pa3h	-0.3722	0.3137	-0.1324	-0.3542	0.1751	0.0941	-0.0772	0.3268	-0.3766
Ln Pa3hb	0.0184	0.1859	0.5002	-0.0193	-0.1943	0.3091	0.1942	-0.3404	-0.1042
Ln Pa4h	-0.3243	-0.0100	-0.1633	0.0394	-0.0593	-0.4429	-0.1128	-0.3776	0.1468
Ln Pa5h	0.1629	-0.1714	0.3189	0.3032	-0.1149	0.2920	-0.5921	0.2536	-0.1240
Ln Pa5hb	-0.1160	-0.2003	-0.2463	0.0472	-0.0597	0.3214	0.1549	-0.2170	-0.0320
Ln Pa6h	-0.0609	-0.4055	0.1598	-0.0709	0.1141	-0.2794	0.2049	0.3688	0.0338
Ln Pa7h	0.2997	0.1792	-0.0449	0.0388	0.4308	0.0759	0.1686	-0.2154	-0.0718

A summary of the PCA on key limb ratios, derived from measurements of modern taxa.

PC	**Eigenvalue**	**% variance**
1	9.78893	73.402
2	2.79432	20.953
3	0.503275	3.7738
4	0.243778	1.828
5	0.00332472	0.02493
6	0.00128729	0.0096527
7	0.00062415	0.0046802

Loadings of the PCA on key limb ratios, derived from measurements of modern taxa.

	PC 1	PC 2	PC 3	PC 4	PC 5	PC 6	PC 7	PC 8
H1/H14	0.0024461	0.88391	-0.16311	-0.43314	0.058766	0.02503	-0.017316	0.0099324
R1/R9	0.27699	0.31515	0.84862	0.31662	-0.038523	-0.041633	0.016309	-0.0086294
F1/F14	0.026552	0.32633	-0.44042	0.83543	0.026965	0.00030136	0.0095223	0.0082278
MT1/MT13	0.95816	-0.099761	-0.23482	-0.11435	-0.038448	-0.014156	-0.010119	0.044427
H2/F2	-0.008532	0.017084	0.011313	0.018047	-0.52275	0.81411	-0.23769	0.081492
MT1/F1	0.050542	-0.012269	0.0042789	-0.0046315	0.26877	0.4164	0.62693	-0.59882

C1/MT1	-0.024173	-0.00097587	0.012415	-0.0073758	0.0077369	0.11681	0.64317	0.75619
R1/H1	0.035788	-0.049969	0.061889	0.026678	0.80454	0.38423	-0.36882	0.24644

Raw *p* values of a Mann-Whitney U test on PC 1 (upper right corner) and PC 2 (lower left corner) of the humerus, derived from transformed data. Where $p < 0.05$, the test rejects the null hypothesis that those two groups sample the same distribution.

	Grassland	WB Grass	Light WB	Heavy WB	Forest	Montane Light	Montane Heavy
Grassland		0.3481	0.2049	0.08273	0.03689	0.8973	0.1715
WB Grass	0.516		0.6682	0.0409	0.02343	0.0678	0.7037
Light WB	0.3525	0.0378		0.02949	0.01693	0.03442	0.6605
Heavy WB	0.05248	0.002308	0.02347		0.5101	0.01692	0.1182
Forest	0.233	0.1547	0.2979	0.1643		0.008113	0.1044
Montane Light	0.02819	0.003175	0.01081	0.6514	0.2353		0.03832
Montane Heavy	0.04024	0.001139	0.009706	0.6854	0.1044	0.5203	

Raw *p* values of a Mann-Whitney U test on PC 1 (upper right corner) and PC 2 (lower left corner) of the radius, derived from transformed data. Where $p < 0.05$, the test rejects the null hypothesis that those two groups sample the same distribution.

	Grassland	WB Grass	Light WB	Heavy WB	Forest	Montane Light	Montane Heavy
Grassland		0.4195	0.8973	0.08273	0.02819	0.2049	0.1715
WB Grass	0.6865		0.08722	0.01859	0.001368	0.8768	0.3416
Light WB	0.9326	0.5558		0.01692	0.005075	0.09272	0.03832
Heavy WB	0.9187	0.9135	0.9646		0.8465	0.02949	0.09334
Forest	0.09329	0.02011	0.09272	0.1066		0.007875	0.05378
Montane Light	0.1556	0.03929	0.09272	0.2725	0.5752		0.3055
Montane Heavy	0.06825	0.004334	0.0168	0.09334	0.9431	0.432	

Raw *p* values of a Mann-Whitney U test on PC 1 (upper right corner) and PC 2 (lower left corner) of the femur, derived from transformed data. Where $p < 0.05$, the test rejects the null hypothesis that those two groups sample the same distribution.

	Grassland	WB Grass	Light WB	Heavy WB	Forest	Montane Light	Montane Heavy
Grassland		0.5012	0.2049	0.08273	0.02819	0.6985	0.1715
WB Grass	0.1785		0.6869	0.03902	0.005732	0.1479	0.2673
Light WB	0.9326	0.1003		0.0368	0.005677	0.07351	0.07101
Heavy WB	0.9187	0.2937	0.9646		0.8465	0.04539	0.2243
Forest	0.05281	0.004366	0.0197	0.08136		0.005075	0.1336

Montane Light	0.02819	0.002479	0.0197	0.04539	0.6889		0.01242
Montane Heavy	0.02265	0.0006557	0.005414	0.02403	0.5203	0.2246	

Raw *p* values of a Mann-Whitney U test on PC 1 (upper right corner) and PC 2 (lower left corner) of the metatarsal, derived from transformed data. Where $p < 0.05$, the test rejects the null hypothesis that those two groups sample the same distribution.

	Grassland	WB Grass	Light WB	Heavy WB	Forest	Montane Light	Montane Heavy
Grassland		0.1488	0.04126	0.06675	0.06675	0.1336	0.05704
WB Grass	0.4447		0.9259	0.05934	0.0007337	0.1248	0.113
Light WB	0.1071	0.2036		0.09272	0.004049	0.2123	0.1304
Heavy WB	0.6171	0.6931	0.4808		0.4712	0.04533	0.3531
Forest	0.8676	0.07218	0.09272	0.298		0.005075	0.03832
Montane Light	0.2433	0.0007337	0.004049	0.008239	0.1282		0.01242
Montane Heavy	0.3055	0.001526	0.002916	0.02681	0.284	0.9431	

Raw *p* values of a Mann-Whitney U test on PC 1 (upper right corner) and PC 3 (lower left corner) of the distal humerus, derived from transformed data. Where $p < 0.05$, the test rejects the null hypothesis that those two groups sample the same distribution.

	Grassland	WB Grass	Light WB	Heavy WB	Forest	Montane Light	Montane Heavy
Grassland		0.3481	0.2049	0.08273	0.02819	0.8973	0.1715
WB Grass	0.7182		0.7667	0.03387	0.007602	0.1466	0.7037
Light WB	0.6726	0.4887		0.0368	0.01081	0.04479	0.5914
Heavy WB	0.475	0.05873	0.04559		0.9485	0.01692	0.1182
Forest	0.8973	0.9626	0.5508	0.1752		0.005075	0.03832
Montane Light	0.09329	0.01001	0.01081	0.2725	0.06555		0.03832
Montane Heavy	0.1715	0.01266	0.009706	0.3253	0.07415	0.721	

Raw *p* values of a Mann-Whitney U test on PC 1 (upper right corner) and PC 2 (lower left corner) of the proximal phalanges, derived from transformed data. Where $p < 0.05$, the test rejects the null hypothesis that those two groups sample the same distribution.

	Grassland	WB Grass	Light WB	Heavy WB	Forest	Montane Light	Montane Heavy
Grassland		0.1949	0.04126	0.1052	0.08136	0.2472	0.05704
WB Grass	0.2888		0.7751	0.03724	0.007661	0.2472	0.4587
Light WB	0.2374	0.8383		0.01962	0.008458	0.1039	0.5914
Heavy WB	0.2472	0.9385	0.832		0.7133	0.03038	0.0726

Forest	0.5613	0.0113	0.02346	0.03734		0.01996	0.1044
Montane Light	0.817	0.006928	0.0403	0.03038	0.7133		0.1564
Montane Heavy	0.6605	0.001033	0.001516	0.01073	0.516	0.04722	

Raw *p* values of a Mann-Whitney U test on PC 1 (upper right corner) and PC 3 (lower left corner) of key ratios of the limbs, derived from data. Where $p < 0.05$, the test rejects the null hypothesis that those two groups sample the same distribution.

	Grassland	WB Grass	Light WB	Heavy WB	Forest	Montane Light	Montane Heavy
Grassland		0.3744	0.4521	0.8676	0.4047	0.2433	0.3055
WB Grass	0.03821		0.8053	0.451	0.007737	0.004179	0.006588
Light WB	0.04126	0.01243		0.7863	0.0197	0.01081	0.009706
Heavy WB	0.2433	0.3929	0.3566		0.2298	0.1735	0.1004
Forest	0.06675	0.3397	0.3566	0.8102		0.9362	0.6171
Montane Light	0.06675	0.5804	0.01081	0.2298	0.4712		0.9431
Montane Heavy	0.05704	0.05718	0.7327	0.2246	0.3531	0.05378	

Mean values and standard error of PC values by habitat group for modern taxa.

	Mean	**SE**		**Mean**	**SE**
PC 1		**Humerus**		**PC 2**	
F	-1.247654	0.2979005	F	-0.0374154	0.08961265
HWB	-1.364017	0.613545	HWB	0.09692325	0.04399777
LWB	0.321152	0.2914647	LWB	-0.02586637	0.01984161
WBG	0.1995792	0.3624031	WBG	-0.1031193	0.0257475
G	1.105177	0.6480401	G	-0.07476833	0.03556809
MTH	-0.008580286	0.3851345	MTH	0.09795014	0.03314737
MTL	1.38138	0.2190109	MTL	0.07440867	0.01894931
PC 1		**Distal Humerus**		**PC 3**	
F	-1.018713	0.3187417	F	-0.02076235	0.02234497
HWB	-0.8326675	0.3838654	HWB	0.02003013	0.01590336
LWB	0.257854	0.17959	LWB	-0.04427068	0.02109494
WBG	0.2074483	0.2295076	WBG	-0.02181773	0.007958695
G	0.7688073	0.4250887	G	-0.0134003	0.01880837
MTH	0.05653057	0.2448704	MTH	0.058582	0.02323311
MTL	0.8339017	0.127096	MTL	0.04983033	0.02086584
PC 1		**Radius**		**PC 2**	

F	-1.380495	0.4033494	F	-0.1050741	0.06505349
HWB	-1.112729	0.4969025	HWB	0.02941925	0.04553612
LWB	0.310639	0.2443028	LWB	0.0343793	0.028315
WBG	0.4429454	0.2137801	WBG	0.05206514	0.01739935
G	0.9460967	0.5700478	G	0.04247553	0.02946881
MTH	-0.1091414	0.3378941	MTH	-0.07196486	0.02422072
MTL	1.040988	0.1746387	MTL	-0.04153718	0.03077273
	PC 1	**Femur**		**PC 2**	
F	-1.391325	0.4737672	F	0.1082064	0.06442868
HWB	-1.215554	0.5908574	HWB	-0.04196475	0.06441139
LWB	0.44336	0.260159	LWB	-0.056329	0.04121883
WBG	0.4302532	0.3095176	WBG	-0.122745	0.02722624
G	1.112331	0.6022771	G	-0.08808	0.02332133
MTH	-0.255409	0.3103006	MTH	0.1917494	0.0429181
MTL	1.08276	0.1958965	MTL	0.1279058	0.02836237
	PC 1	**Metatarsal**		**PC 2**	
F	-1.834728	0.4696821	F	0.1161362	0.192542
HWB	-0.9801617	0.6090235	HWB	-0.1536222	0.09265412
LWB	0.335376	0.2652666	LWB	-0.2217024	0.07291327
WBG	0.5158428	0.1972205	WBG	-0.1860585	0.02387155
G	1.51675	0.18185	G	0.04039	0.23607
MTH	-0.2676657	0.329546	MTH	0.3317599	0.1148443
MTL	0.9449833	0.1542546	MTL	0.4095973	0.1293623
	PC 1	**Proximal Phalanges**		**PC 2**	
F	-1.661764	0.3733687	F	-0.1877464	0.1286219
HWB	-1.977432	0.8505726	HWB	0.16211	0.05700396
LWB	0.376876	0.2906449	LWB	0.1579053	0.06708721
WBG	0.4694144	0.3917702	WBG	0.1590529	0.0414974
G	1.99265	0.24695	G	-0.09723	0.22035
MTH	-0.1568587	0.5175333	MTH	-0.2726429	0.02799366
MTL	1.334437	0.3146379	MTL	-0.1543225	0.03105471
	PC 1	**Ratios**		**PC 3**	
F	-2.247124	1.3508	F	-0.0184	0.301297
HWB	0.97589	1.389077	HWB	0.02663967	0.3676767
LWB	1.586013	0.7518414	LWB	-0.4001682	0.127714
WBG	1.971396	0.6337262	WBG	0.1728204	0.1305894
G	0.576465	0.960735	G	1.5207	0.0196
MTH	-2.229249	0.9266507	MTH	-0.4584076	0.2739523
MTL	-2.577714	1.084106	MTL	0.3697625	0.225485

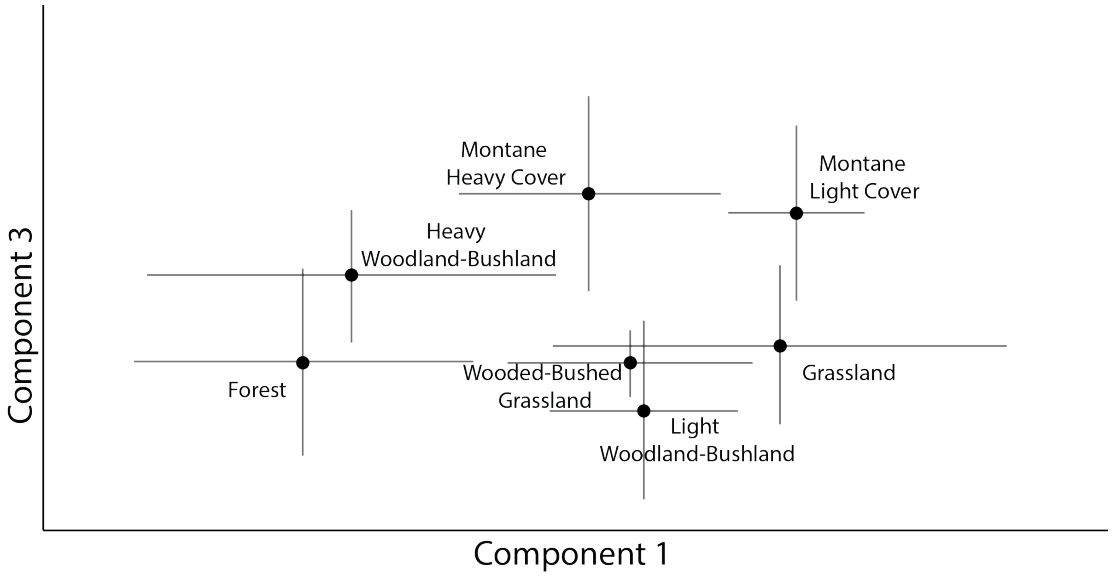

Centroids for PCs 1 and 3 of the distal humerus, in seven habitat groups. Error bars represent two standard errors.

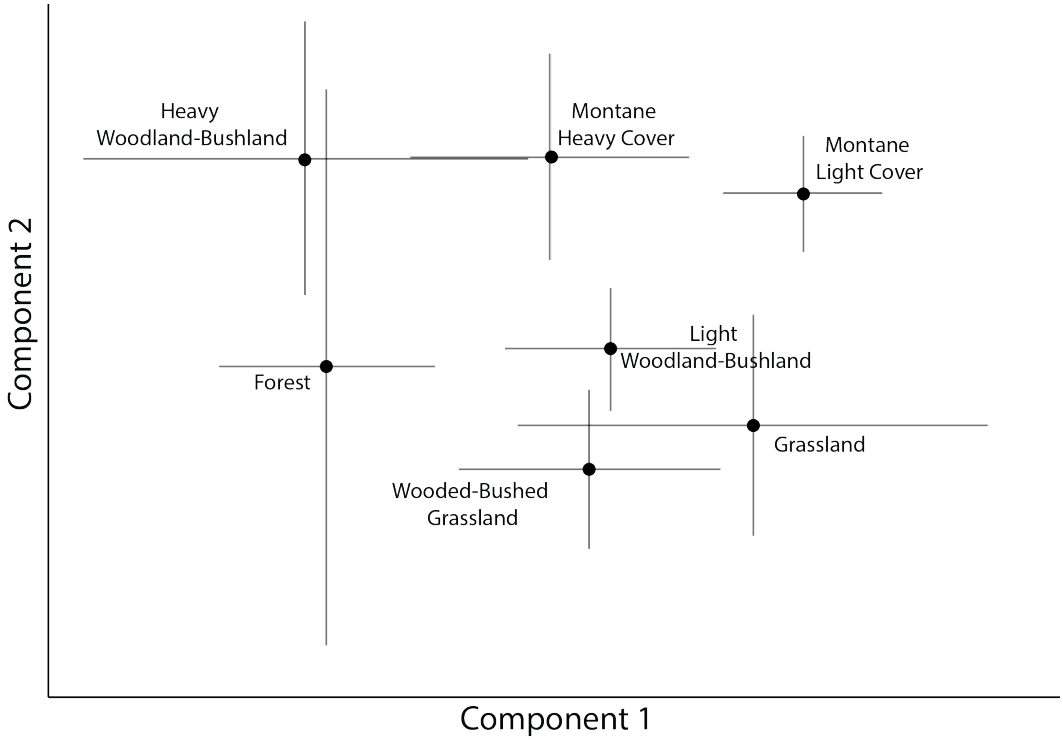

Centroids, or mean values, of PCs 1 and 2 of the humerus, in seven habitat groups. Error bars represent two standard errors.

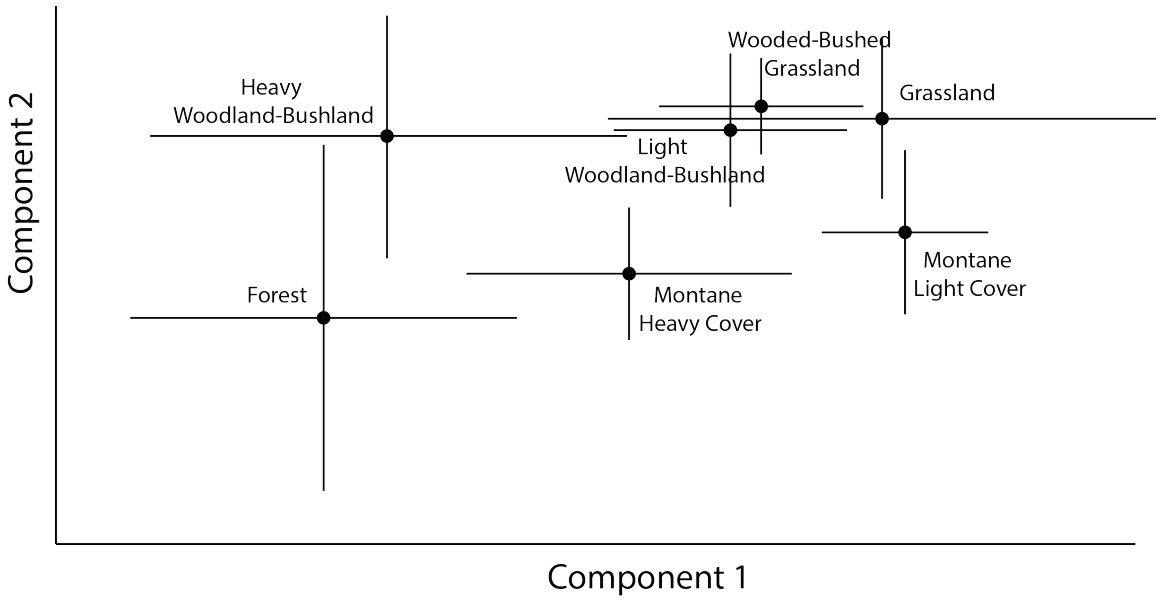

Centroids for PCs 1 and 2 of the radius, in seven habitat groups. Error bars represent two standard errors.

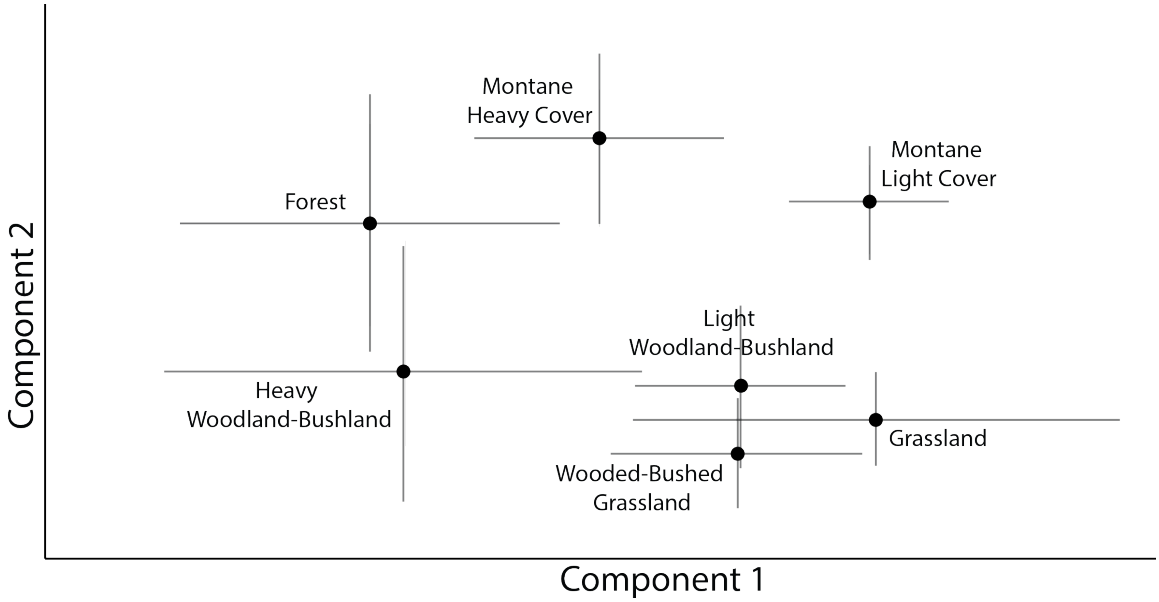

Centroids for PCs 1 and 2 of the femur, in seven habitat groups. Error bars represent two standard errors.

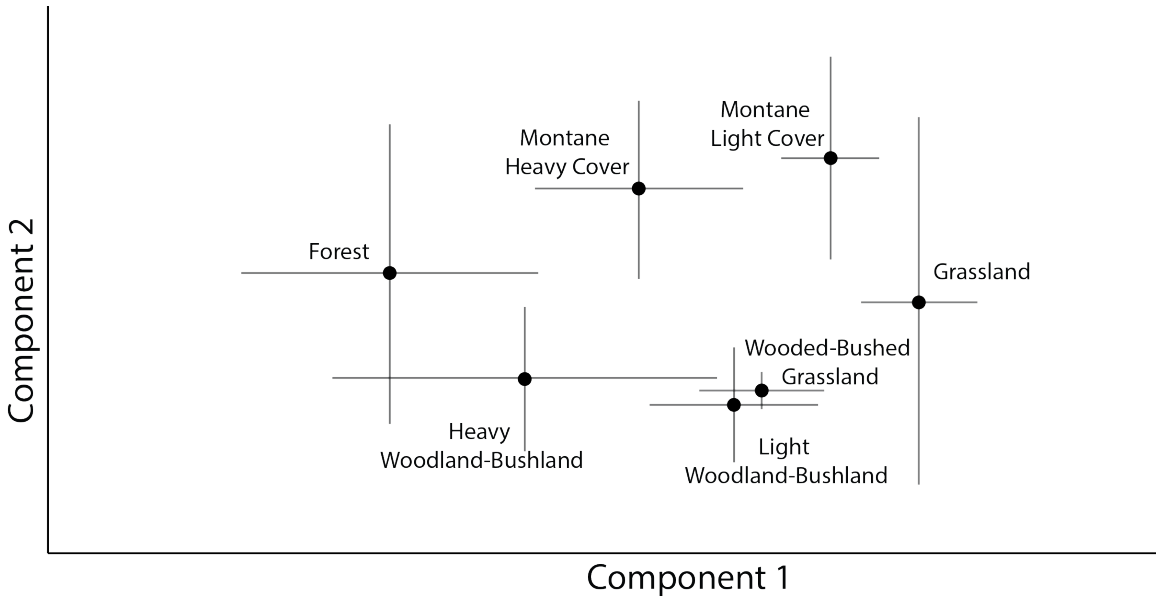

Centroids for PCs 1 and 2 of the metatarsal, in seven habitat groups. Error bars represent two standard errors.

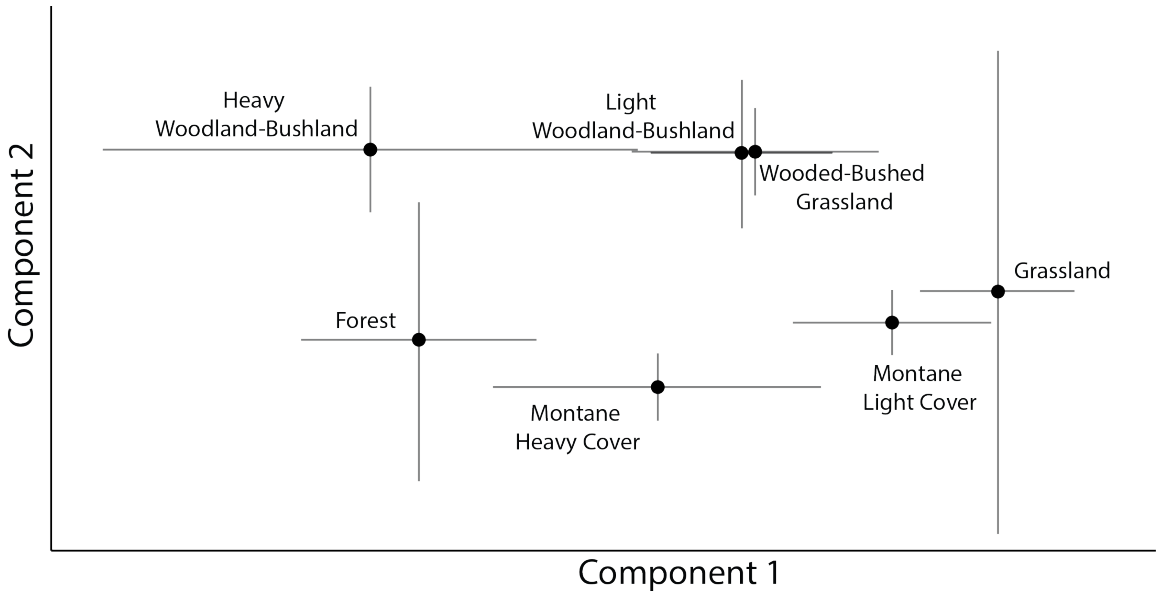

Centroids for PCs 1 and 2 of the proximal phalanges, in seven habitat groups. Error bars represent two standard errors.

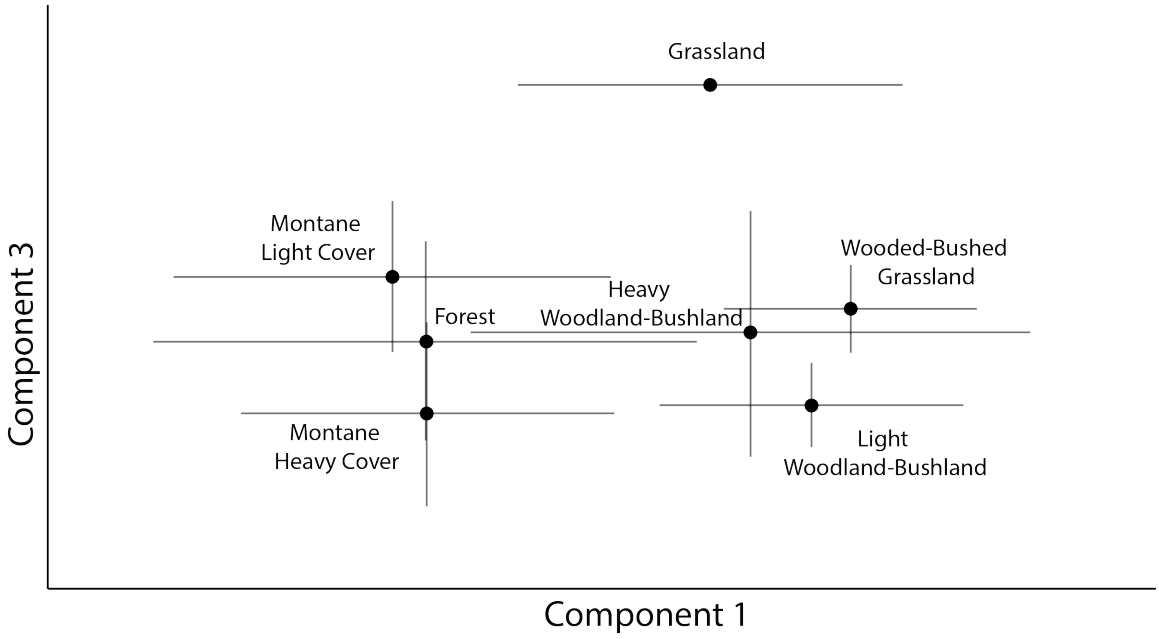

Centroids for PCs 1 and 3 of ratios for seven habitat groups. Error bars represent two standard errors.

APPENDIX F: PCA RESULTS FOR BLASTOMERYCINAE

A summary of the Humerus PCA from both fossil and modern specimens.

PC	Eigenvalue	% variance
1	1.42955	96.314
2	0.0154497	1.0409
3	0.00893263	0.60183
4	0.00736924	0.49649
5	0.00578822	0.38997
6	0.00509099	0.343
7	0.00364068	0.24529
8	0.00313321	0.2111
9	0.00200561	0.13513
10	0.00154168	0.10387
11	0.000990343	0.066723
12	0.000675007	0.045478
13	8.50E-05	0.0057234

Loadings of the Humerus PCA from both fossil and modern specimens.

	PC 1	PC 2	PC 3	PC 4	PC 5	PC 6	PC 7
Ln H1	0.22654	0.47557	0.17061	-0.053111	0.32972	-0.011711	0.057315
Ln H2	0.21745	0.51239	0.18625	-0.19579	0.38166	0.053831	0.059867
Ln H4	0.27543	0.39148	-0.49522	0.24475	-0.40313	0.3226	-0.35549
Ln H5	0.28963	-0.35183	-0.22327	-0.69424	0.053446	0.39219	0.12853
Ln H6	0.28579	0.019734	-0.058872	-0.1045	0.057119	-0.1721	-0.038517
Ln H7	0.30336	-0.11394	-0.18337	0.27553	0.1396	-0.33904	0.31632
Ln H8	0.29415	-0.036972	0.07278	0.047008	0.12653	0.10692	-0.090707
Ln H9	0.30189	-0.18097	0.27663	-0.11504	-0.063524	-0.42074	-0.66885
Ln H10	0.28298	-0.11644	0.077958	0.049861	0.038871	0.27605	-0.2139
Ln H11	0.26127	-0.36089	0.060189	0.554	0.36951	0.32689	0.057881
Ln H12	0.25564	0.045914	0.63908	0.057955	-0.58595	0.20103	0.32842
Ln H13	0.29271	0.11758	-0.31631	-0.025147	-0.20084	-0.26821	0.34626
Ln H14	0.30152	-0.16437	-0.063415	-0.036015	-0.1254	-0.33263	0.12747

	PC 8	PC 9	PC10	PC 11	PC 12	PC13
Ln H1	0.0057306	0.05921	0.085381	0.075992	-0.013914	0.74943
Ln H2	0.10239	0.094295	0.10672	0.072588	0.11718	-0.64439
Ln H4	-0.075526	0.11696	0.22623	-0.034026	-0.022322	-0.023413
Ln H5	-0.14901	0.18403	0.13076	0.092135	-0.021697	0.072081
Ln H6	-0.12089	0.061012	-0.30344	-0.86558	0.097685	0.002468

Ln H7	-0.64123	-0.13914	0.24791	0.15167	0.17478	-0.073517
Ln H8	-0.060015	-0.50105	-0.10179	-0.001858	-0.77209	-0.088257
Ln H9	-0.099516	0.29193	-0.039872	0.24573	-0.022325	-0.018108
Ln H10	0.11713	-0.57017	-0.26908	0.14048	0.58393	0.049114
Ln H11	0.21888	0.43838	-0.0409	-0.025898	-0.038969	-0.01604
Ln H12	-0.13277	0.091171	0.031098	-0.044093	0.0013168	-0.0172
Ln H13	0.25958	0.14748	-0.60532	0.32678	-0.071435	-0.014311
Ln H14	0.61289	-0.18265	0.55326	-0.1325	0.028288	0.025945

A summary of the Distal Humerus PCA from both fossil and modern specimens.

PC	Eigenvalue	% variance
1	0.556913	97.269
2	0.00717731	1.2536
3	0.00457071	0.79831
4	0.00295439	0.51601
5	0.000931943	0.16277

Loadings of the Distal Humerus PCA from both fossil and modern specimens.

	PC 1	PC 2	PC 3	PC 4	PC 5
Ln H8	0.46768	-0.069619	-0.15723	-0.50759	-0.70289
Ln H9	0.48095	0.11742	-0.66344	0.55847	0.053486
Ln H10	0.45285	-0.098131	-0.075536	-0.52694	0.70846
Ln H11	0.41919	-0.66501	0.4945	0.36939	-0.03259
Ln H12	0.4113	0.72767	0.53375	0.12784	-0.010122

A summary of the Radius PCA from both fossil and modern specimens.

PC	Eigenvalue	% variance
1	1.00306	96.895
2	0.0119233	1.1518
3	0.008073	0.77985
4	0.00483432	0.46699
5	0.00304165	0.29382
6	0.0020215	0.19528
7	0.00177522	0.17149
8	0.000475721	0.045954

Loadings of the Radius PCA from both fossil and modern specimens.

	PC 1	PC 2	PC 3	PC 4	PC 5	PC 6	PC 7	PC 8
Ln R1	0.32808	0.90216	-0.015069	-0.14119	-0.21095	0.090752	-0.062767	0.04052
Ln R3	0.34369	0.028017	-0.030296	0.14997	0.52889	0.34967	0.66646	0.10734
Ln R4	0.37671	-0.18526	-0.21202	-0.39853	-0.23156	-0.21525	0.29615	-0.65752
Ln R5	0.36622	-0.25579	-0.2298	-0.41172	-0.16757	-0.1665	0.0080405	0.72268
Ln R6	0.35253	0.064314	0.073511	0.069297	0.61893	-0.57755	-0.37227	-0.078432
Ln R7	0.36043	-0.2232	-0.078581	-0.096716	0.10285	0.67003	-0.56614	-0.15722
Ln R8	0.3405	-0.15363	0.88279	0.07887	-0.26323	-0.016096	0.065231	0.033251
Ln R9	0.35789	-0.089584	-0.33195	0.7803	-0.36212	-0.11261	-0.027648	0.016316

A summary of the Femur PCA from both fossil and modern specimens.

PC	Eigenvalue	% variance
1	1.26949	95.816
2	0.0226009	1.7058
3	0.00858447	0.64792
4	0.00489428	0.3694
5	0.00436663	0.32958
6	0.00312798	0.23609
7	0.0030033	0.22668
8	0.0021737	0.16406
9	0.0018728	0.14135
10	0.00156542	0.11815
11	0.00124166	0.093715
12	0.0010992	0.082963
13	0.000907712	0.06851

Loadings of the Femur PCA from both fossil and modern specimens.

	PC 1	PC 2	PC 3	PC 4	PC 5	PC 6	PC 7
Ln F2	0.24026	0.16963	0.20397	0.16971	0.36825	0.35673	-0.36899
Ln F3	0.23978	0.55445	-0.6556	-0.32991	0.074857	0.13332	0.19451
Ln F4	0.30725	-0.1579	-0.10886	0.19431	-0.13937	-0.13853	0.16702
Ln F5	0.29725	0.038566	-0.19705	-0.022886	-0.18096	-0.2613	-0.35068
Ln F6	0.25763	0.2903	0.1218	0.17059	0.28103	-0.51836	-0.30998
Ln F7	0.26136	0.12267	0.13708	0.081435	0.27682	-0.10687	0.29835
Ln F8	0.294	-0.26419	0.16238	-0.26604	0.28178	-0.36911	0.39582
Ln F9	0.29349	-0.24473	0.098897	-0.24794	0.12691	0.37418	0.24756
Ln F10	0.27445	0.085463	0.22821	0.12847	0.15294	0.33024	-0.023735

Ln F11	0.31553	-0.55304	-0.28101	-0.27214	-0.0052468	0.052109	-0.46028
Ln F12	0.27262	-0.11672	-0.26604	0.6626	-0.15937	0.21316	0.16406
Ln F13	0.27403	0.28237	0.43346	-0.33376	-0.50214	0.15689	-0.095084
Ln F14	0.26545	0.043253	0.13571	0.12285	-0.50452	-0.17118	0.15397

	PC 8	PC 9	PC 10	PC 11	PC 12	PC 13
Ln F2	0.29971	-0.13781	-0.43646	-0.048051	0.27216	0.26152
Ln F3	0.12929	0.076117	-0.011677	-0.0026032	0.07999	-0.078619
Ln F4	0.04207	-0.18337	-0.51573	-0.47898	-0.31068	-0.37045
Ln F5	-0.52188	-0.54833	0.013245	0.12793	0.14683	0.18884
Ln F6	0.11267	0.24234	0.39872	-0.34006	-0.12162	-0.02859
Ln F7	-0.060732	-0.030162	-0.12676	0.51517	-0.60066	0.2594
Ln F8	-0.10977	0.17862	-0.17047	0.053235	0.54621	-0.010803
Ln F9	0.0047682	-0.29056	0.44965	-0.42077	-0.13548	0.28859
Ln F10	-0.18889	-0.10657	0.25246	0.25972	0.085779	-0.72814
Ln F11	0.21291	0.2921	0.014846	0.23505	-0.18738	-0.075614
Ln F12	-0.2219	0.39493	0.11278	-0.0037477	0.17252	0.23829
Ln F13	-0.24183	0.3901	-0.15907	-0.097343	-0.082957	0.088178
Ln F14	0.63414	-0.24519	0.18692	0.24245	0.17336	0.023805

A summary of the Metatarsal PCA from both fossil and modern specimens.

PC	Eigenvalue	% variance
1	1.19977	85.16
2	0.121357	8.6139
3	0.0343083	2.4352
4	0.0191085	1.3563
5	0.0109422	0.77668
6	0.00947654	0.67264
7	0.00542377	0.38498
8	0.00283206	0.20102
9	0.0019489	0.13833
10	0.00175172	0.12434
11	0.00106387	0.075513
12	0.000817448	0.058022
13	4.93E-05	0.0035014

Loadings of the Metatarsal PCA from both fossil and modern specimens.

	PC 1	PC 2	PC 3	PC 4	PC 5	PC 6	PC 7
Ln MT1	0.26122	-0.46757	0.27947	0.050175	0.21571	0.10596	-0.04148
Ln MT2	0.25786	-0.5002	0.30088	0.056259	0.26033	0.13948	-0.00057287

Ln MT3	0.27724	-0.12357	-0.12205	0.13136	-0.083144	0.039583	0.12536
Ln MT4	0.26624	0.0398	-0.26648	0.010059	-0.093351	0.017293	0.041293
Ln MT5	0.28376	-0.02976	-0.11716	0.0315	-0.17695	-0.012936	-0.28825
Ln MT6	0.28878	0.21666	-0.061765	0.033731	0.46072	-0.7034	0.3328
Ln MT7	0.29172	0.27714	-0.001946	0.24733	0.24356	0.10138	-0.41769
Ln MT8	0.32549	-0.22386	-0.10599	-0.34698	-0.58047	-0.37219	-0.16043
Ln MT9	0.28441	0.17209	-0.12403	0.10005	0.13585	0.0057333	-0.51661
Ln MT10	0.26189	0.25095	0.12644	-0.8246	0.22736	0.29931	0.089358
Ln MT11	0.26249	0.43398	0.69311	0.23661	-0.38735	0.045015	0.184
Ln MT12	0.29679	-0.18152	-0.12184	0.13808	-0.090771	0.04626	0.40678
Ln MT13	0.23688	0.16031	-0.43597	0.16805	-0.042577	0.4795	0.33558

	PC 8	PC 9	PC 10	PC 11	PC 12	PC 13
Ln MT1	0.14382	0.09973	0.074401	0.0070256	0.024541	0.73227
Ln MT2	0.14282	0.010091	0.15884	-0.0079751	0.047642	-0.67404
Ln MT3	-0.50209	0.3538	-0.064591	-0.018507	-0.68452	-0.034251
Ln MT4	-0.27845	0.19433	0.51751	-0.5192	0.43863	0.024709
Ln MT5	-0.038832	0.5081	-0.4648	0.33245	0.44478	-0.072447
Ln MT6	0.15009	0.11812	0.014343	0.10074	0.0068662	-0.0067147
Ln MT7	0.17711	-0.15988	-0.38187	-0.5557	-0.14489	-0.01741
Ln MT8	0.34712	-0.18424	0.044401	-0.10915	-0.20599	-0.018704
Ln MT9	-0.21175	-0.34407	0.40479	0.49741	-0.060674	0.023377
Ln MT10	-0.12069	0.0018993	-0.091007	0.0099608	-0.016293	0.002981
Ln MT11	0.010157	0.038292	0.12	0.058516	0.032599	-0.00031455
Ln MT12	-0.32408	-0.60825	-0.36253	0.046224	0.24402	0.03305
Ln MT13	0.53746	0.074603	0.12341	0.18843	-0.10148	0.0082399

A summary of the Forefoot Proximal Phalanx PCA from both fossil and modern specimens.

PC	Eigenvalue	% variance
1	1.0664	91.809
2	0.0458261	3.9453
3	0.0330108	2.842
4	0.00597078	0.51404
5	0.00323003	0.27808
6	0.00299478	0.25783
7	0.0023109	0.19895
8	0.00119239	0.10266
9	0.000611277	0.052626

Loadings of the Forefoot Proximal Phalanx PCA from both fossil and modern specimens.

	PC 1	PC 2	PC 3	PC 4	PC 5	PC 6	PC 7	PC 8	PC 9
Ln Pa1f	0.36363	-0.67907	0.23862	-0.37648	-0.26465	0.24255	-0.2809	0.010864	-0.0088642
Ln Pa2f	0.33789	0.22303	-0.041481	0.0044246	-0.31412	-0.40483	-0.19508	-0.4385	-0.58434
Ln Pa3f	0.31671	0.29263	0.26028	-0.067314	0.011047	-0.47649	-0.40629	0.39929	0.43602
Ln Pa3fb	0.3154	-0.041863	0.64492	0.17002	0.10542	-0.10946	0.62634	-0.18354	0.069696
Ln Pa4f	0.30951	0.31844	0.074714	-0.34029	0.51102	0.34851	-0.0039858	0.3068	-0.45242
Ln Pa5f	0.33227	0.19293	-0.34411	-0.36297	0.16826	0.13165	0.076033	-0.55277	0.49521
Ln Pa5fb	0.36839	-0.36661	-0.5582	0.064551	0.13081	-0.38164	0.36485	0.33719	-0.067547
Ln Pa6f	0.33061	-0.12925	-0.051792	0.73039	0.32603	0.2516	-0.37951	-0.15018	0.040864
Ln Pa7f	0.32034	0.33468	-0.13929	0.19907	-0.63812	0.43648	0.20671	0.28027	0.085688

A summary of the Hindfoot Proximal Phalanx PCA from both fossil and modern specimens.

PC	Eigenvalue	% variance
1	0.820952	91.369
2	0.0400016	4.452
3	0.0198901	2.2137
4	0.00675396	0.75169
5	0.00414159	0.46094
6	0.00333428	0.37109
7	0.00173953	0.1936
8	0.0011154	0.12414
9	0.00057344	0.063822

Loadings of the Hindfoot Proximal Phalanx PCA from both fossil and modern specimens.

	PC 1	PC 2	PC 3	PC 4	PC 5	PC 6	PC 7	PC 8	PC 9
Ln Pa1h	0.35207	-0.033445	-0.55379	-0.29832	0.52347	0.21537	-0.35169	-0.18099	0.049004
Ln Pa2h	0.33604	0.048773	0.22528	-0.14019	0.036732	-0.59211	-0.048971	-0.45335	-0.5044
Ln Pa3h	0.31346	0.35325	0.11484	-0.18988	-0.24394	-0.33194	-0.47803	0.43565	0.3738
Ln Pa3hb	0.29958	0.5608	-0.44575	0.11141	-0.14653	-0.061422	0.59905	0.0046392	0.022864
Ln Pa4h	0.31904	0.24176	0.30761	-0.14364	-0.20595	0.65944	-0.095887	0.11869	-0.47324
Ln Pa5h	0.34477	-0.18584	0.33518	-0.2548	-0.14381	0.18393	0.26318	-0.45058	0.58526
Ln Pa5hb	0.38299	-0.67216	-0.23857	-0.12099	-0.28212	-0.10625	0.20601	0.41055	-0.16759
Ln Pa6h	0.32881	-0.11123	-0.094219	0.81172	-0.20362	0.082984	-0.32348	-0.23246	0.068717
Ln Pa7h	0.31571	-0.0076043	0.39739	0.28949	0.67787	-0.046872	0.24698	0.36361	0.060225

A summary of the Ratios PCA from both fossil and modern specimens.

PC	Eigenvalue	% variance
1	9.54298	69.601
2	3.08321	22.487
3	0.714286	5.2096
4	0.353353	2.5771
5	0.0117825	0.085935
6	0.00382954	0.02793
7	0.00160085	0.011676

Loadings of the Ratios PCA from both fossil and modern specimens.

	PC 1	PC 2	PC 3	PC 4	PC 5	PC 6	PC 7
H2/H14	-0.015217	0.83139	-0.082072	-0.54104	-0.043579	0.084543	-0.0072296
R1/R9	0.31404	0.333	0.80536	0.37146	-0.0062117	-0.061871	0.0059995
F2/F14	0.055842	0.42351	-0.53133	0.72967	0.04601	0.023667	0.010762
MT1/MT13	0.94506	-0.11783	-0.24002	-0.17816	0.02034	-0.037474	-0.042573
MT1/F2	0.051046	-0.02288	0.0086384	-0.0096519	0.033456	0.27995	0.95771
C1/MT1	-0.024139	0.024707	0.027804	-0.053192	0.99621	-0.048874	-0.019424
R1/H2	0.041323	-0.059361	0.062278	0.047143	0.044429	0.952	-0.28354

Mean values and standard error of PC scores by group. Original PC scores listed in Appendix F. WB= Wooded-Bushed or Woodland-Bushland, L= *Longirostromeryx* spp., B= *Blastomeryx* spp., P= *Parablastomeryx gregorii*, Pr= *Problastomeryx primus,* Ps= *Pseudoblastomeryx advena*, Cl= Clarendonian, Ba= Barstovian, H= Hemingfordian.

	PC 1		**PC 2**	
	Mean	**SE**	**Mean**	**SE**
			Humerus	
Grassland	1.133	0.649	-0.074	0.032
WB Grass	0.227	0.362	-0.110	0.027
Light WB	0.342	0.291	-0.032	0.020
Heavy WB	-1.340	0.612	0.073	0.048
Forest	-1.221	0.297	-0.045	0.087
MT Light	1.405	0.219	0.084	0.014
MT Heavy	0.015	0.385	0.073	0.036
L (Cl)	-0.889	0.035	0.241	0.126
P (Cl)	-0.339	0	0.100	0
			Distal Humerus	

Grassland	0.761	0.425	-0.086	0.029
WB Grass	0.199	0.230	-0.048	0.024
Light WB	0.247	0.179	-0.002	0.019
Heavy WB	-0.842	0.383	0.033	0.025
Forest	-0.746	0.183	0.020	0.036
MT Light	0.824	0.127	-0.038	0.018
MT Heavy	0.048	0.245	0.003	0.020
L (Cl)	-0.562	0.039	-0.014	0.037
P (Cl)	-0.272	0	0.074	0
Pr (H)	-0.894	0	0.053	0
B (Cl)	-0.618	0	0.109	0
		Radius		
Grassland	0.959	0.570	0.011	0.031
WB Grass	0.454	0.214	0.034	0.016
Light WB	0.320	0.244	0.021	0.030
Heavy WB	-1.101	0.496	0.006	0.041
Forest	-1.367	0.403	-0.118	0.064
MT Light	1.048	0.175	-0.062	0.029
MT Heavy	-0.093	0.338	-0.094	0.025
L (Cl)	-0.660	0.012	0.077	0.029
P (Cl)	-0.035	0	0.123	0
B (Ba)	-0.866	0	0.155	0
B (Cl)	-1.138	0	0.167	0
		Femur		
Grassland	1.067	0.602	-0.060	0.028
WB Grass	0.380	0.310	-0.103	0.029
Light WB	0.394	0.261	-0.034	0.041
Heavy WB	-1.265	0.590	-0.034	0.068
Forest	-1.440	0.474	0.099	0.057
MT Light	1.031	0.195	0.161	0.030
MT Heavy	-0.309	0.310	0.208	0.043
L (Cl)	-0.602	0.033	0.203	0.030
P (Cl)	-0.066	0	0.228	0
Pr (H)	-0.924	0	0.207	0
		Metatarsal		
Grassland	1.646	0.183	0.111	0.249
WB Grass	0.640	0.198	-0.111	0.020

Light WB	0.455	0.265	-0.154	0.073
Heavy WB	-0.856	0.608	-0.082	0.094
Forest	-1.710	0.469	0.169	0.194
MT Light	1.068	0.156	0.480	0.126
MT Heavy	-0.146	0.330	0.406	0.112
L (Cl)	-0.803	0.116	-0.150	0.116
P (Cl)	0.140	0	-0.082	0
Pr/Ps (H)	-1.123	0.268	0.008	0.019
B (Ba)	-1.141	0.023	-0.101	0.060
B (Cl)	-1.088	0.121	-0.110	0.071
		Forefoot Proximal Phalanx		
Grassland	1.659	0.212	0.127	0.200
WB Grass	0.514	0.293	-0.126	0.043
Light WB	0.469	0.216	-0.118	0.057
Heavy WB	-1.279	0.613	-0.174	0.042
Forest	-1.099	0.272	0.102	0.095
MT Light	1.408	0.231	0.253	0.069
MT Heavy	0.104	0.398	0.233	0.036
L (Cl)	-0.471	0.118	0.108	0.023
P (Cl)	-0.024	0.200	-0.001	0.031
Pr/Ps (H)	-1.350	0.125	0.131	0.012
B (Ba)	-0.557	0.056	0.148	0.018
B (Cl)	-0.684	0.071	0.038	0.027
		Hindfoot Proximal Phalanx		
Grassland	1.538	0.118	0.011	0.045
WB Grass	0.545	0.260	-0.036	0.037
Light WB	0.450	0.193	-0.048	0.042
Heavy WB	-1.116	0.585	-0.211	0.049
Forest	-0.856	0.265	-0.139	0.054
MT Light	0.978	0.207	0.003	0.014
MT Heavy	0.026	0.336	0.085	0.061
L (Cl)	-0.563	0.117	0.378	0.032
P (Cl)	-0.117	0.199	0.373	0.013
Pr/Ps (H)	-1.309	0.210	0.336	0.026
B (Ba)	-0.649	0.057	0.451	0.005
B (Cl)	-0.775	0.071	0.353	0.003
		Ratios		
Grassland	0.286	0.968	-1.762	0.853

WB Grass	1.678	0.666	-1.222	0.313
Light WB	1.202	0.773	-0.449	0.376
Heavy WB	0.351	1.669	1.289	0.972
Forest	-3.127	1.267	0.491	0.842
MT Light	-1.936	0.806	-0.334	0.578
MT Heavy	-2.616	0.876	1.017	0.623
L (Cl)	2.023	0	5.014	0
P (Cl)	3.172	0	2.709	0